(12) INTERNATIONAL APPLICATION PUBLISHED UNDER THE PATENT COOPERATION TREATY (PCT)

(19) World Intellectual Property Organization
International Bureau

(43) International Publication Date
26 August 2021 (26.08.2021)

WIPO | PCT

(10) International Publication Number
WO 2021/166306 A1

(51) International Patent Classification:
C12N 15/09 (2006.01)

(21) International Application Number:
PCT/JP2020/035368

(22) International Filing Date:
14 September 2020 (14.09.2020)

(25) Filing Language: English

(26) Publication Language: English

(30) Priority Data:
62/978,312 19 February 2020 (19.02.2020) US

(71) Applicant: **KYOTO UNIVERSITY** [JP/JP]; 36-1, Yoshida-honmachi, Sakyo-ku, Kyoto-shi, Kyoto, 6068501 (JP).

(72) Inventors: **WOLTJEN, Knut**; c/o Kyoto University, 36-1, Yoshida-honmachi, Sakyo-ku, Kyoto-shi, Kyoto, 6068501 (JP). **MAURISSEN, Thomas Luc**; c/o Kyoto University, 36-1, Yoshida-honmachi, Sakyo-ku, Kyoto-shi, Kyoto, 6068501 (JP).

(74) Agent: **TANAI, Sumio** et al.; 1-9-2, Marunouchi, Chiyoda-ku, Tokyo, 1006620 (JP).

(81) Designated States *(unless otherwise indicated, for every kind of national protection available)*: AE, AG, AL, AM, AO, AT, AU, AZ, BA, BB, BG, BH, BN, BR, BW, BY, BZ, CA, CH, CL, CN, CO, CR, CU, CZ, DE, DJ, DK, DM, DO, DZ, EC, EE, EG, ES, FI, GB, GD, GE, GH, GM, GT, HN, HR, HU, ID, IL, IN, IR, IS, IT, JO, JP, KE, KG, KH, KN, KP, KR, KW, KZ, LA, LC, LK, LR, LS, LU, LY, MA, MD, ME, MG, MK, MN, MW, MX, MY, MZ, NA, NG, NI, NO, NZ, OM, PA, PE, PG, PH, PL, PT, QA, RO, RS, RU, RW, SA, SC, SD, SE, SG, SK, SL, ST, SV, SY, TH, TJ, TM, TN, TR, TT, TZ, UA, UG, US, UZ, VC, VN, WS, ZA, ZM, ZW.

(84) Designated States *(unless otherwise indicated, for every kind of regional protection available)*: ARIPO (BW, GH, GM, KE, LR, LS, MW, MZ, NA, RW, SD, SL, ST, SZ, TZ, UG, ZM, ZW), Eurasian (AM, AZ, BY, KG, KZ, RU, TJ, TM), European (AL, AT, BE, BG, CH, CY, CZ, DE, DK, EE, ES, FI, FR, GB, GR, HR, HU, IE, IS, IT, LT, LU, LV, MC, MK, MT, NL, NO, PL, PT, RO, RS, SE, SI, SK, SM, TR), OAPI (BF, BJ, CF, CG, CI, CM, GA, GN, GQ, GW, KM, ML, MR, NE, SN, TD, TG).

Declarations under Rule 4.17:
— *as to non-prejudicial disclosures or exceptions to lack of novelty (Rule 4.17(v))*

Published:
— *with international search report (Art. 21(3))*
— *with sequence listing part of description (Rule 5.2(a))*

(54) Title: PRODUCTION METHOD OF GENOME-EDITED CELLS AND KIT THEREFOR

(57) Abstract: A production method of genome-edited cells is provided. The method includes: synchronizing the cell cycle of the cells, treating the cells with an agent that modifies a DNA repair pathway, introducing a donor DNA into the cells, inducing a sequence-specific double-strand break in the genomic DNA of the cells in the presence of the donor DNA, so that the double-strand break is repaired according to all or part of the donor DNA sequence by homology directed repair or comparable pathway so that genome-edited cells are obtained.

WO 2021/166306 A1

DESCRIPTION

TITLE OF INVENTION

PRODUCTION METHOD OF GENOME-EDITED CELLS AND KIT THEREFOR

Technical Field

[0001]

The present invention relates to production method of genome-edited cells and kit therefore. More specifically, the present invention relates to production method of genome-edited cells, method of editing genome of cells, method of detecting gene editing on one or both allele and kit for genome editing. Priority is claimed on U.S. Provisional Patent Application No. 62/978,312 filed on February 19, 2020, the content of which is incorporated herein by reference.

Background Art

[0002]

Human induced pluripotent stem (iPS) cells are being widely employed to study human diseases, including inherited disorders, due to their ability to maintain a normal diploid karyotype through serial passages and differentiate into multiple derivative cell types. In general, genetic modeling consists of modifying a target site, either by deleting, inserting or replacing a specific DNA sequence. More specifically, precision gene editing aims to make modifications in the genome to correct or recreate pathogenic variants at single nucleotide resolution. The CRISPR-Cas9 system is the most used tool to generate targeted DNA double strand breaks (DSBs) in the genome, which are subsequently resolved by endogenous cellular DNA DSB repair pathways. Predominantly, nonhomologous end joining (NHEJ) results in insertion and deletion (indel) mutations,

while microhomology-mediated end joining (MMEJ) makes predictable deletions. NHEJ and MMEJ are referred to collectively as mutagenic end joining (MutEJ) as both repair outcomes can lead to a loss or gain of DNA sequence. In order to generate single-nucleotide changes or other designed modifications, the homology directed repair (HDR) pathway is leveraged in combination with a customized single or double stranded DNA repair template such as a PCR fragment, a donor plasmid, or single stranded donor oligonucleotide (ssODN).

Citation List

Non-Patent Literature

[0003]

Non-Patent Literature 1

Howden S. E., et al., A Cas9 Variant for Efficient Generation of Indel-Free Knockin or Gene-Corrected Human Pluripotent Stem Cells, Stem Cell Reports, 7 (3), 508-517, 2016.

Non-Patent Literature 2

Alewo Idoko-Akoh, et al., High fidelity CRISPR/Cas9 increases precise monoallelic and biallelic editing events in primordial germ cells, Sci Rep, 8 (1):15126, 2018.

Summary of Invention

Technical Problem

[0004]

However, recent approaches have met limited efficiency and applicability that are largely due to a lack of direct selection and the predominance of MutEJ outcomes

over precise repair (For example, refer to Non-Patent Literature 1 and 2.).

[0005]

The present invention aims to provide a technique for efficiently produce genome-edited cells, in which targeted DNA double strand breaks (DSBs) in the genome are repaired by homology-directed repair (HDR) or comparable pathway (alternative pathway).

Solution to Problem

[0006]

The present invention includes the following aspects:

[1] A production method of genome-edited cells, including: synchronizing the cell cycle of the cells, treating the cells with an agent that modifies a DNA repair pathway, introducing a donor DNA into the cells, and inducing a sequence-specific double-strand break in the genomic DNA of the cells in the presence of the donor DNA, so that the double-strand break is repaired according to all or part of the donor DNA sequence by homology directed repair or comparable pathway so that genome-edited cells are obtained.

[2] The production method according to [1], in which synchronizing the cell cycle of the cells includes incubating the cells at 25 to 35°C for 24 to 72 hours.

[3] The production method according to [1] or [2], in which synchronizing the cell cycle of the cells includes treating the cells with Cell Division Cycle 7 (CDC7) inhibitor.

[4] The production method according to any one of [1] to [3], in which the agent that modifies a DNA repair pathway includes a DNA-PK inhibitor or a DNA ligase IV inhibitor.

[5] The production method according to any one of [1] to [4], in which the agent that

modifies a DNA repair pathway includes a combination of a DNA-PK inhibitor and a DNA ligase IV inhibitor.

[6] The production method according to any one of [1] to [5], in which the sequence-specific double-strand break is induced by a ribonucleoprotein (RNP) complex comprising a Cas9 and a gRNA.

[7] The production method according to any one of [1] to [6], in which the donor DNA is a single-stranded donor oligonucleotide.

[8] The production method according to [7], in which the donor DNA has a nucleotide sequence that modifies a protospacer sequence or Protospacer Adjacent Motif (PAM) sequence.

[9] The production method according to any one of [1] to [8], in which the donor DNA has a mutation, and cells in which the mutation is introduced into one or both alleles are obtained.

[10] The production method according to any one of [1] to [9], in which the donor DNA comprises a combination of a plurality of kinds of donor DNAs corresponding to the same region on the genome.

[11] The production method according to [10], in which the donor DNA includes a combination of a first donor DNA and a second donor DNA, in which the first donor DNA has a mutation of interest, and the second donor DNA has a mutation that modifies a protospacer sequence or PAM sequence, and cells in which the mutation of interest is introduced into only one allele and protospacer sequence or PAM sequence of the other allele is modified are obtained.

[12] The production method according to any one of [1] to [11], in which the cells are induced pluripotent stem (iPS) cells.

[13] A method of editing genome of cells, including: synchronizing the cell cycle of the

cells, treating the cells with an agent that modifies a DNA repair pathway, introducing a donor DNA into the cells, and inducing a sequence-specific double-strand break in the genomic DNA of the cells in the presence of the donor DNA, so that the double-strand break is repaired according to all or part of the donor DNA sequence by homology directed repair or compatible pathway so that genome of the cells are edited.

[14] A method of detecting genome editing on one or both allele, including: introducing a donor DNA into a cell, in which the cell has genes encoding a fluorescent protein that emits a first fluorescence in both allele, and in which the donor DNA has a mutation that modifies the first fluorescence of the fluorescent protein into a second fluorescence; inducing a sequence-specific double-strand break in the genomic DNA of the cell in the presence of the donor DNA, so that the double-strand break is repaired according to all or part of the donor DNA sequence by homology directed repair or comparable pathway so that genome-edited cells are obtained; and analyzing the fluorescence of the genome-edited cells, and as a result, (i) if the first fluorescence is detected and the second fluorescence is not detected, it is indicated that (i-1) both alleles of the locus of the fluorescent protein did not change, or (i-2) one allele of the locus of the fluorescent protein did not change and an insertion or deletion mutation occurred in the other allele, (ii) if the first fluorescence is not detected and the second fluorescence is detected, it is indicated that (ii-1) both alleles of the fluorescent protein locus were repaired according to all or part of the donor DNA sequence by homology directed repair or comparable pathway, or (ii-2) one allele of the locus of the fluorescent protein was repaired according to all or part of the donor DNA sequence by homology directed repair or comparable pathway and an insertion or deletion mutation occurred in the other allele, (iii) if neither the first fluorescence nor the second fluorescence is detected, it is indicated that an insertion or deletion mutation occurred in both alleles of the locus of the fluorescent

protein, (iv) if both the first fluorescence and the second fluorescence are detected, it is indicated that one allele of the locus of the fluorescent protein was repaired according to all or part of the donor DNA sequence by homology directed repair or comparable pathway and the other allele did not change.

[15] The method according to [14], in which the fluorescent protein that emits the first fluorescence is a Green Fluorescent Protein (GFP), the fluorescent protein that emits the second fluorescence is a Blue Fluorescent Protein (BFP), and the donor DNA has a mutation in which the 66th tyrosine residue of GFP is replaced with a histidine residue to be modified into BFP.

[16] A kit for genome editing including a CDC7 inhibitor, a DNA-PK inhibitor, and a DNA ligase IV inhibitor.

[17] The kit for genome editing according to [16], further comprising a sequence-specific DNA-cleaving enzyme and a donor DNA.

[18] The kit for genome editing according to [17], in which the donor DNA has a mutation in which the 66th tyrosine residue of GFP is replaced with a histidine residue to be modified into BFP.

Advantageous Effects of Invention

[0007]

According to the present invention, a technique for efficiently produce genome-edited cells, in which targeted DNA double strand breaks (DSBs) in the genome are repaired by homology-directed repair (HDR) or comparable pathway is provided.

Brief Description of Drawings

[0008]

Fig. 1A to Fig. 1E shows visualization and quantification of DNA repair outcomes in a fluorescent DNA repair assay in human iPS cells. Fig.1A shows the sequence of the GFP reporter target site (Seq ID Nos: 60 and 61) and engineered modification to BFP. The sequence of gRNA GFPx199 (Seq ID No: 62), the GFP fluorophore residue p.Y66 (Seq ID No: 60) and BFP fluorophore residue p.H66 (Seq ID No: 64) are shown. Nucleotide changes are introduced in the ssODN sequence (Seq ID No: 63) and in the resulting BFP sequence product (Seq ID No: 64).

[0009]

Fig. 1B shows a schematic of the predicted outcomes from GFP editing in a heterozygous AAVS1-CAG::EGFP (GFP) iPS cell line, and their distribution in FACS.

[0010]

Fig. 1C shows a confocal microscopy images of the unedited heterozygous GFP iPS cell line (Control), and fluorescent conversion outcomes following cotransfection of Cas9 RNP and Y66H ssODN repair template (RNP+ssODN). Scalebars are 100 μm. Representative images of three independent experiments with similar results are shown.

[0011]

Fig. 1D shows representative FACS plots of unedited GFP iPS cells (top) and cells treated with Cas9 RNP and Y66H ssODN (bottom).

[0012]

Fig. 1E shows quantification of HDR, MutEJ or unmodified DNA repair outcomes by FACS analysis. Data are presented as the mean ± S.D. of three technical replicates of independent electroporations for each respective condition.

[0013]

Fig. 2A to Fig 2. F shows cold shock and cell-cycle synchronization with XL413 improve HDR efficiency in iPS cells. Fig. 2A shows Experimental timeline with no cold

shock [A], and cold shock for 24 h [B] or 48 h [C] following electroporation (EP) on day 0 (top). EdU/PI staining was performed after 48 h of culture, and FACS analysis on day 8. The resulting effect on DNA repair outcome frequency is shown (bottom).

[0014]

Fig. 2B shows ratio of HDR/MutEJ repair outcomes measured in Fig. 2A. Statistical significances were calculated with an unpaired two-tailed t-test, and p-values are indicated as **$p<0.01$, ***$p<0.001$. Cold shock significantly improved the HDR/MutEJ ratio.

[0015]

Fig. 2C shows representative FACS plots of EdU/PI staining (top) for quantification of cell-cycle phase (middle left) and mean EdU intensity of S-phase cells (middle right) 48 h after EP with no cold shock [A] or cold shock for 48 h [C] following EP. Schematic of the cell cycle showing cold shock arrest in G2/M phase (bottom).

[0016]

Fig. 2D shows experimental timeline (top) of XL413-induced cell-cycle arrest for 24 h post-EP, in the absence [A] or presence [C] of cold shock. EdU/PI staining was performed after 24 h of culture, and FACS analysis on day 8. Repair outcomes were quantified in the absence or presence of XL413 (bottom).

[0017]

Fig. 2E shown ratio of HDR/MutEJ repair outcomes measured in Fig. 2D. Statistical significances were calculated with an unpaired two-tailed t-test, and p-values are indicated as ***$p<0.001$. Cold shock and XL413 treatment significantly improved the HDR/MutEJ ratio.

[0018]

Fig. 2F shows representative FACS plots of EdU/PI staining (top) 24 h after EP

for untreated and XL413-treated cells under normal culture conditions [A], and quantification of cell-cycle phase (middle left) and mean EdU intensity of S-phase cells (middle right). Schematic of XL413-induced cellcycle arrest in the G1/early S phase (bottom). All data are presented as the mean ± S.D. of three technical replicates for each respective treatment.

[0019]

Fig. 3A to Fig. 3J shows combining DNA repair modulation and cell-cycle synchronization synergistically enhances HDR in iPS cells. Fig. 3A shows list of compounds tested with their function on molecular targets (left), and experimental timeline of compound pre- (4 h) and post-EP (48 h) treatment (right).

[0020]

Fig. 3B shows screening of compounds under cold shock condition [C], including untreated (-) and DMSO treated (DMSO) controls, showing the effect on DNA repair outcome frequency. Data are presented as the mean ± S.D. of three biological replicates.

[0021]

Fig. 3C shows ratio of HDR/MutEJ repair outcomes measured in Fig. 3B.

[0022]

Fig. 3D shows combination treatment of NU7441 and SCR7 under cold shock condition [C], and the effect on repair outcome frequency. Data are presented as the mean of two biological replicates, except N+ S is presented as the mean ± S.D. of four biological replicates.

[0023]

Fig. 3E shows ratio of HDR/MutEJ repair outcomes measured in Fig. 3D.

[0024]

Fig. 3F shows combination treatment of cell cycle inhibitor XL413 (XL) post-EP (24 h) and N+ S pre- (4 h) and post-EP (48 h) under normal culture conditions [A] or cold shock [C]. Data are presented as the mean ± S.D. of three technical replicates for each respective treatment.

[0025]

Fig. 3G shows ratio of HDR/MutEJ repair outcomes in heterozygous GFP iPS cells with combined treatment of XL413 (XL) for 24h after EP and NU7441+SCR7 (N+S) for 4h before and 48h after EP under normal culture conditions [A] or cold shock [C] for 48h after EP. Statistical significances were calculated with an unpaired two-tailed t-test, and p-values are indicated as **$p<0.01$, ***$p<0.001$. Individual and combined treatment significantly improved the HDR/MutEJ ratio compared to the untreated control (-).

[0026]

Fig. 3H shows statistical analysis of individual versus combined treatment to address synergistic editing. Statistical significances were calculated with an unpaired two-tailed t-test, and p-values are indicated as *$p<0.05$, **$p<0.01$, ***$p<0.001$. With NEPA21 electroporation, XL+N+S treatment was significantly higher than XL treatment alone, but not than N+S treatment alone. Cold shock and N+S combined treatment was significantly higher in comparison to cold shock treatment alone. Combining all conditions, cold shock with XL+N+S led to significant improvement compared to cold shock or XL treatment alone, but not compared to cold shock with N+S.

[0027]

Fig. 3I shows cell numbers recorded for samples in Fig. 3G on day 8, when harvesting cells for FACS analysis. We observed reduced cell numbers with each treatment, and additive reduction with combined treatment, which could be responsible

for the high variability and consequent low statistical significance observed in conditions with combined treatment. Possibly, the low viability resulting from combined treatment with NEPA21 electroporation, in particular with XL+N+S treatment led to higher replicate variability and statistical insignificance. This might happen through clonal drift in the case of low cell numbers.

[0028]

Fig. 3J shows representative FACS plots of cells treated with XL413 (XL) and N +S under normal [A] (left) and cold shock [C] (right) conditions, as tested in Fig. 3F.

[0029]

Fig. 4A to Fig. 4G shows homozygous fluorescent DNA repair assay to visualize and quantify allele-specific DNA repair outcomes during biallelic editing in iPS cells. Fig.4A shows schematic of the predicted outcomes from GFP editing in a homozygous AAVS1-CAG::EGFP (GFP) iPS cell line, and their distribution in FACS.

[0030]

Fig. 4B shows comparison of monoallelic and biallelic editing in heterozygous and homozygous GFP iPS cells, showing DNA repair outcome frequency. HDR* indicates double-positive BFP/GFP cells arising from heterozygous editing and HDR repair in homozygous GFP iPS cells.

[0031]

Fig. 4C shows ratio of HDR/MutEJ repair outcomes measured in Fig. 4B.

[0032]

Fig. 4D shows quantification of biallelic repair outcomes in homozygous GFP iPS cells obtained from FACS-gating on each possible DNA repair outcome represented in Fig. 4A.

[0033]

Fig. 4E shows effect of combined cold shock and drug treatment on repair outcome frequency in homozygous GFP iPS cells.

[0034]

Fig. 4F shows ratio of HDR/MutEJ repair outcomes measured in Fig. 4E.

[0035]

Fig. 4G shows biallelic repair outcomes in the absence (-) or presence (N + S) of combined drug treatment obtained from DNA repair outcomes represented in Fig. 4E. All data are presented as the mean ± S.D. of three technical replicates for each respective treatment.

[0036]

Fig. 5A to Fig. 5E shows generation of heterozygous mutations requires protection of one allele. Fig. 5A shows target sequence in the GFP reporter(Seq ID Nos: 65 and 66), and ssODN repair templates to create a missense Y66H mutation (ssODN M, Seq ID Nos: 68 and 69), a silent T65T blocking mutation (ssODN B, Seq ID Nos: 70 and 71) or no mutation (ssODN W, Seq ID Nos: 72 and 73). HDR repair of ssODN B T65T results in a protected GFP (pGFP) allele. Cells bearing unmodified or pGFP alleles are indistinguishable by FACS and are scored cumulatively as GFP.

[0037]

Fig. 5B shows GFP editing with ssODN M, B or W individually, or in M+ B and M+W combination, and effect on DNA repair outcome frequency under cold shock condition. HDR* indicates the frequency of heterozygous double-positive BFP/GFP or compound heterozygous double-positive BFP/pGFP repair outcomes. GFP positive cells include unmodified cells and HDR-mediated monoallelic pGFP/GFP, pGFP/indel (Δ), or biallelic pGFP/pGFP repair outcomes.

[0038]

Fig. 5C shows distribution of biallelic repair outcomes shown in Fig. 5B.

[0039]

Fig. 5D shows biallelic BFP/GFP repair outcome frequency measured in Fig. 5C.

[0040]

Fig. 5E shows representative FACS plots of BFP conversion only (ssODN M) or heterozygous compound BFP/pGFP mutations (ssODN M+ B). All data are presented as the mean ± S.D. of three technical replicates of independent electroporations for each respective condition.

[0041]

Fig. 6A to Fig. 6H shows synergistic gene editing at endogenous loci. Fig. 6A shows DNA repair outcomes of heterozygous (Hetero) GFP iPS cells generated in the 409B2 genetic background. Cells were targeted with Y66H-mutant ssODN M only (ssODN M), and treated individually or in combination with cell-cycle inhibitor XL413 (XL) post-EP (24 h) and N+ S pre- (4 h) and post-EP (48 h) under normal culture conditions (37 °C) or cold shock (32 °C for 48 h post-EP).

[0042]

Fig. 6B shows ratio of HDR/MutEJ repair outcomes in heterozygous GFP iPS cells with MaxCyte electroporation and the same treatment conditions than in Fig. 3G. Statistical significances were calculated with an unpaired two-tailed t-test, and p-values are indicated as *$p<0.05$, **$p<0.01$, ***$p<0.001$. With MaxCyte electroporation, for which cell viability was consistently high, both XL+N+S and cold shock with N+S synergistic conditions showed significantly higher HDR/MutEJ ratios compared to individual treatment. This confirms our observation of the existence of a synergistic effect when modulating the cell cycle and DNA repair simultaneously.

[0043]

Fig. 6C shows DNA repair outcomes and HDR/MutEJ ratios of homozygous (Homo) GFP iPS cells generated in the 409B2 genetic background. Cells were targeted with Y66H-mutant ssODN M only (ssODN M) and treated and quantified as described in a. HDR* indicates the frequency of heterozygous double-positive BFP/GFP.

[0044]

Fig. 6D shows ratio of HDR/MutEJ repair outcomes measured in Fig. 6C.

[0045]

Fig. 6E shows DNA repair outcomes and HDR/MutEJ ratios of homozygous (Homo) GFP iPS cells that were targeted with a combination of Y66H-mutant ssODN M and T65T silent blocking ssODN B (ssODN M+B), and treated and quantified as described in a. Here, HDR* includes heterozygous compound double-positive BFP/pGFP repair outcomes. GFP positive cells consist of unmodified cells and HDR-mediated monoallelic pGFP/GFP, pGFP/indel (Δ), or biallelic pGFP/pGFP repair outcomes.

[0046]

Fig. 6F shows ratio of HDR/MutEJ repair outcomes measured in Fig. 6E. Data are presented as the mean ± S.D. of three technical replicates for each respective treatment.

[0047]

Fig. 6G shows DNA repair outcome frequencies in 409B2 cells of single clones (n =32 or 31 as indicated), cultured either under normal conditions (-), with synergistic cell cycle inhibitor XL413 (XL) post-EP (24 h) and NU7441+ SCR7 (N + S) pre- (4 h) and post-EP (48 h) (XL + N + S) or with cold shock (32 °C for 48 h post-EP) and N + S (CS +N + S). HDR outcomes represent clones having undergone template-mediated modification on one or both alleles; MutEJ outcomes include all clones having a

mutagenic indel on either allele; and wild-type outcomes correspond to clones having both alleles unmodified. Each targeting is labelled with the target gene and desired missense mutation.

[0048]

Fig. 6H shows HDR/MutEJ ratios quantified in Fig. 6G, with the same number of single clones (n =32 or 31 as indicated).

[0049]

Fig. 7 shows summary of synergistic gene editing effects favoring HDR outcomes. Synchronization and release of cells into the HDR permissive S and G2 phases of the cell-cycle synergizes with DNA repair inhibition to improve HDR rates. Additional non-cell-cycle-dependent effects of cold shock may also play a role. Leveraging these mechanisms, homozygous mutations are generated at high efficiency, while heterozygous mutations may be generated without indels by using a combination of mutant and blocking ssODN templates.

[0050]

Fig. 8A to Fig. 8C shows Generation of GFP targeted clones. Fig. 8A shows Schematic of the AAVS1 locus before (top) and after targeting with a CAG-driven GFP cassette (bottom). The expected fragment sizes from *Sph*I digestion, as well as the positions of genomic or internal transgenic Southern blot probes (5' or GFP probe) are marked. Gray boxes correspond to *PPP1R12C* exons. HA-L/R, left/right homology arms; SA, splice acceptor; T2A, *Thosea asigna* virus 2A peptide; pA, bovine growth hormone or rabbit b-globin polyadenylation signals.

[0051]

Fig. 8B shows Southern blot analysis of *Sph*I-digested genomic DNA with a 5' genomic probe (left) or an internal GFP probe (right). Targeted alleles were detected by

the presence of a 3.5kbp (5' probe) or a 6.9kbp (GFP probe) product, while normal alleles conserved a 6.5kbp product detected with the 5' probe. Clones with aberrant banding due to donor backbone integration predicted and observed at 8.5kbp (5' probe) and 7.9kbp (GFP probe) are indicated with an asterisk (*). The heterozygous 073-1-3 (#3) and homozygous 073-1-2 (#2) clones were selected for further gene editing experiments. Southern blots are from one membrane and represent one incremental exposure.

[0052]

Fig. 8C shows schematic of the AAVS1 genotype (left), fluorescence microscopy images with brightfield (middle) and GFP fluorescence intensity by FACS (right) of the nontargeted 1383D6 parent iPS cell line (top), heterozygous (073-1-3; center) and homozygous (073-1-2; bottom) cell lines targeted with GFP. Scalebars are 500μm. Representative images of more than 3 independent experiments with similar results are shown.

[0053]

Fig. 9A to Fig. 9C shows characterization of the fluorescent DNA repair assay. Fig. 9A shows targeting of heterozygous GFP iPS cells with plasmid expressing Cas9 and GFPx199 and with ssODN (top middle), selection for 48h with Puromycin, and FACS sorting of HDR (BFP+; bottom left), MutEJ (double negative; bottom middle) and unmodified (GFP+; bottom right) DNA repair outcomes. FACS of lower panels was performed 1 week after sorting on expanded cells. The control shows untargeted heterozygous GFP iPS cells (top left).

[0054]

Fig. 9B shows Restriction Fragment Length Polymorphism (RFLP) assay of a *Nco*I restriction site introduced by ssODN-mediated targeting, for non-targeted (NT) control, heterozygous GFP (Hetero) control and sorted HDR, MutEJ and unmodified

outcomes obtained in Fig. 9A. Cleavage product quantification shows the percentage of HDR outcomes. RFLP analysis was performed once.

[0055]

Fig. 9C shows scheme (top left) and sequence (top right) of sorted heterozygous MutEJ cells, and TIDE analysis showing the resulting indel pattern (bottom).

[0056]

Fig. 10A to Fig. 10H shows effect of cell cycle synchronization on HDR efficiency. Fig. 10A shows experimental timeline with no cold shock [A], and cold shock for 24h [B] or 48h [C] following electroporation (EP), or cold shock for 24h before EP only [D], or for 24h [E] or 48h [F] following EP (top). The resulting effect on DNA repair outcome frequency is shown for conditions [D-F] (bottom).

[0057]

Fig. 10B shows ratio of HDR/MutEJ repair outcomes measured in Fig. 10A.

[0058]

Fig. 10C shows cell cycle synchronization in G2/M with Nocodazole does not affect HDR efficiency in iPS cells. Experimental timeline of Nocodazole treatment for 16h pre-EP, under normal culture [A] or cold shock [C] condition following EP on day 0 (top). EdU/PI staining was performed before EP, and FACS analysis on day 8. The resulting effect on DNA repair outcome frequency is shown (bottom).

[0059]

Fig. 10D shows ratio of HDR/MutEJ repair outcomes measured in Fig. 10C.

[0060]

Fig. 10E shows representative FACS plots of EdU/PI staining (top) before EP for untreated and Nocodazole-treated cells, and quantification of cell cycle phase (middle left) and mean EdU intensity of S-phase cells (middle right). Schematic of Nocodazole-

induced cell cycle arrest in the late G2/M phase (bottom).

[0061]

Fig. 10F shows cell cycle synchronization at the G1/S boundary with XL413 improves HDR efficiency in iPS cells. Experimental timeline of XL413 treatment for 24h pre- (Pre) or post-EP (Post) following EP, under normal culture [A] or cold shock [C] conditions (top). The resulting effect on DNA repair outcome frequency is shown (bottom).

[0062]

Fig. 10G Ratio of HDR/MutEJ repair outcomes measured in Fig. 10F.

[0063]

Fig. 10H relative cell number normalized to untreated control, obtained from Fig. 10F. XL413 Pre/Post treatment resulted in cell death and non-detectable (nd) repair outcomes in Fig. 10F and Fig. 10G. All data are presented as the mean ± S.D. of three technical replicates for each respective treatment.

[0064]

Fig. 11A to Fig. 11F shows heterozygous compound mutations prevent Cafs9 re-cleavage. Fig. 11A shows generation of a BFP/pGFP double-positive clone using Y66H mutant ssODN M (Seq ID Nos: 77 and 78) and T65T silent blocking ssODN B (Seq ID Nos: 79 and 80) in homozygous GFP iPS cells. Double-positive BFP/GFP cells were sorted on day 8 after targeting, and clones were picked and analyzed.

[0065]

Fig. 11B shows experimental timeline of a BFP/pGFP clone targeted with GFPx199 gRNA to measure Cas9-mediated re-cleavage activity of edited BFP and protected-GFP alleles under normal culture, and cold shock conditions, and combined NU7441+SCR7 (N+S) treatment (top). FACS plots of an untargeted BFP/pGFP clone

(Control) and re-targeting under normal culture [A], cold shock [C], and cold shock combined with N+S treatment (32°C +N+S) during FACS analysis on day 8 (bottom).

[0066]

Fig. 11C shows GFP editing with ssODN M, B or W individually, or in M+B and M+W combination, and effect on DNA repair outcome frequency under combined cold shock and N+S treatment. HDR* indicates the frequency of heterozygous double-positive BFP/GFP or compound heterozygous double-positive BFP/pGFP repair outcomes. GFP-positive cells include unmodified cells and HDRmediated monoallelic pGFP/GFP, pGFP/indel (Δ) or biallelic pGFP/pGFP repair outcomes.

[0067]

Fig. 11D shows distribution of biallelic repair outcomes shown in Fig. 11C.

[0068]

Fig. 11E shows biallelic BFP/GFP repair outcome frequency measured in Fig. 11D.

[0069]

Fig. 11F shows representative FACS plots of BFP conversion only (ssODN M) or heterozygous compound BFP/pGFP mutations (ssODN M+B). Data are presented as the mean ± S.D. of three technical replicates of independent electroporations for each respective condition.

[0070]

Fig. 12A to Fig. 12F shows generation of heterozygous mutations at endogenous loci. Fig. 12A shows target sequence and editing strategy at the *ATP1A1* locus to generate p.Q118R and p.N129D mutations. Shown are Sanger sequences of the *ATP1A1* locus before and after HDR editing.

[0071]

Fig. 12B shows experimental timeline for *ATP1A1* editing including cold shock, compound treatment and ouabain selection (top). Quantification of HDR colony formation with combined cold shock [C] and N+S drug treatment (bottom). Data are presented as the mean ± S.D. of four technical replicates for each respective treatment.

[0072]

Fig. 12C shows target sequence at the *KCNH2* locus and strategy to recreate a heterozygous p.N588K pathogenic mutation with an ssODN encoding a missense mutation (ssODN M) or a silent block (ssODN B) using combination of cold shock and N+S treatment. Shown are Sanger sequences of the *KCNH2* locus before and after HDR editing with mixed ssODN repair templates.

[0073]

Fig. 12D shows target sequence at the *PSMB8* locus and strategy to recreate a heterozygous p.G201V pathogenic mutation. Likewise, shown are Sanger sequences of the *PSMB8* locus before and after HDR editing with mixed ssODN repair templates.

[0074]

Fig. 12E shows quantification of the editing efficiency of compound heterozygous, homozygous and heterozygous mutations obtained from clonal analysis of editing with ssODN M (n=96) or ssODN M+B (n=92).

[0075]

Fig. 12F ssODN design and quantification is similar to Fig. 12E with ssODN M (n=91) or ssODN M+B (n=95).

[0076]

Fig. 13A to Fig. 13H shows increased editing efficiency with MaxCyte electroporation. Fig. 13A shows DNA repair outcome frequency using the MaxCyte electroporation instrument. Heterozygous (Hetero) and homozygous (Homo) GFP iPS

cells generated in the 1383D6 genetic background were targeted with Y66H mutant ssODN M only (ssODN M), and homozygous GFP iPS cells were targeted with a combination of Y66H mutant ssODN M and T65T silent blocking ssODN B (ssODN M+B) under normal culture (37°C) or cold shock (32°C for 48h post-EP) conditions, or cold shock combined with N+S treatment. HDR* indicates the frequency of heterozygous double-positive BFP/GFP and heterozygous compound double-positive BFP/pGFP repair outcomes. In the case of homozygous GFP iPS cells targeted with ssODN M+B, GFP-positive cells include unmodified cells and HDR-mediated monoallelic pGFP/GFP, pGFP/indel (Δ) or biallelic pGFP/pGFP repair outcomes.

[0077]

Fig. 13B shows ratio of HDR/MutEJ repair outcomes measured in Fig. 13A.

[0078]

Fig. 13C shows results of the same experiment as in Fig. 13A with heterozygous and homozygous GFP iPS cells generated in the 409B2 genetic background.

[0079]

Fig. 13D shows results of the same experiment as in Fig. 13B with heterozygous and homozygous GFP iPS cells generated in the 409B2 genetic background.

[0080]

Fig. 13E shows biallelic repair outcome frequencies obtained from Fig. 13A in homozygous GFP iPS cells targeted with ssODN M in the 1383D6 genetic background under normal culture or cold shock conditions, or cold shock combined with N+S treatment.

[0081]

Fig. 13F shows results of the same experiment as in Fig. 13E in homozygous GFP iPS cells targeted with ssODN M+B in the 1383D6 genetic background, and effect

on biallelic BFP/BFP and compound heterozygous BFP/pGFP efficiencies under normal culture or cold shock conditions, or cold shock combined with N+S treatment.

[0082]

Fig. 13G shows results of the same experiment as in Fig. 13E with homozygous GFP iPS cells generated in the 409B2 genetic background. All data are presented as the mean ± S.D. of three technical replicates for each respective treatment.

[0083]

Fig. 13H shows results of the same experiment as in Fig. 13F with homozygous GFP iPS cells generated in the 409B2 genetic background. All data are presented as the mean ± S.D. of three technical replicates for each respective treatment.

[0084]

Fig. 14A to Fig. 14D shows synergistic gene editing with MaxCyte electroporation. Fig. 14A shows biallelic repair outcome frequencies obtained from homozygous GFP iPS cells targeted with ssODN M during single or combination treatment with cell cycle inhibitor XL413 (XL) and N+S under normal culture conditions.

[0085]

Fig. 14B shows the result of the same experiment as in Fig. 14A but under cold shock conditions.

[0086]

Fig. 14C shows biallelic repair outcome frequencies obtained from homozygous GFP iPS cells targeted with ssODN M+B under normal culture conditions.

[0087]

Fig. 14D shows the result of the same experiment as in Fig. 14C but under cold shock conditions. All data are presented as the mean ± S.D. of three technical replicates

for each respective treatment.

[0088]

Fig. 15A to Fig. 15J shows sequence designs of endogenous loci targeted with synergistic gene editing and MaxCyte electroporation. Target sequence and editing strategy for all 10 targeting experiments including gRNA and ssODN template sequences, as well as the missense mutations being generated. Fig. 15A shows sequence designs for KCNE1 D85N gene editing.

[0089]

Fig. 15B shows sequence designs for KCNH2 N45D gene editing.

[0090]

Fig. 15C shows sequence designs for SCN5A A1428S gene editing.

[0091]

Fig. 15D shows sequence designs for KCNH2 N588D gene editing.

[0092]

Fig. 15E shows sequence designs for KCNH2 N588K gene editing.

[0093]

Fig. 15F shows sequence designs for APRT M136T gene editing.

[0094]

Fig. 15G shows sequence designs for HES7 R25W gene editing.

[0095]

Fig. 15H shows sequence designs for PSMB8 G201V gene editing.

[0096]

Fig. 15I shows sequence designs for KCNJ11 T293N gene editing.

[0097]

Fig. 15J shows sequence designs for KCNJ11 T294M gene editing.

Description of Embodiments

[0098]

[Production method of genome-edited cells]

In one embodiment, the present invention provides a production method of genome-edited cells, including: synchronizing the cell cycle of the cells, treating the cells with an agent that modifies a DNA repair pathway, introducing a donor DNA into the cells, and inducing a sequence-specific double-strand break in the genomic DNA of the cells in the presence of the donor DNA, so that the double-strand break is repaired according to all or part of the donor DNA sequence by homology directed repair or comparable pathway so that genome-edited cells are obtained.

[0099]

As described later in Examples, the inventors of this application have revealed that the production method of the present embodiment can improve the efficiency of homology directed repair or comparable pathway and perform accurate genome editing.

[0100]

The target cell for genome editing may be a human cell or a non-human animal cell. The non-human animal is not particularly limited, and examples thereof include mouse, rat, rabbit, pig, sheep, goat, cow, monkey and the like.

[0101]

The cells may be somatic cells or stem cells. Examples of stem cells include pluripotent stem cells and tissue stem cells. Examples of pluripotent stem cells include embryonic stem cells (ES cells) and induced pluripotent stem cells (iPS cells). Examples of tissue stem cells include hematopoietic stem cells, mesenchymal stem cells, neural

stem cells, muscle stem cells (satellite cells), skin stem cells, and the like. The cells may be cultured cells, cells that constitute an embryo, or cells that constitute an organism.

[0102]

In the production method of the present embodiment, the donor DNA may be any linear or circular double or single stranded DNA isolated, synthesized, or generated enzymatically. More specifically, a PCR fragment, a plasmid, a single-stranded oligonucleotide, a double-stranded oligonucleotide may be used as donor DNA. Among them, a single-stranded donor oligonucleotide (ssODN) is preferable. The length of the single-stranded donor oligonucleotide may be about several tens to several hundred bases, and may be about 100 bases.

[0103]

The step of inducing the sequence-specific double-strand break in the genomic DNA of the cell is preferably performed by introducing a sequence-specific DNA-cleaving enzyme into the cell. The sequence-specific DNA-cleaving enzyme will be described later.

[0104]

The donor DNA and the sequence-specific DNA-cleaving enzyme may be introduced into cells by a transfection reagent or an electroporation method.

[0105]

As the transfection reagent, for example, it is possible to use Lipofectamine 2000, Lipofectamine 3000, CRISPRMAX, and RNAMAX (all of which are from Thermo Fisher Scientific); FuGENE 6 and FuGENE HD (both are from Promega); and the like.

[0106]

The electroporation method can be performed using a device such as NEPA21

(Neppagene Co., Ltd.), MaxCyte STX (MaxCyte), Neon (Thermo Fisher Scientific), and 4D-Nucleofector (Lonza Co., Ltd.).

[0107]

The step of synchronizing the cell cycle of the cells preferably includes incubating the cells at 25 to 35°C, preferably about 32°C, for 24 to 72 hours, preferably about 48 hours (Hereinafter, this process may be referred to as "cold shock".).

[0108]

The cold shock is preferably performed immediately after the introduction of the donor DNA and the sequence-specific DNA-cleaving enzyme into the cell. The cold shock not only synchronizes the cell cycle, but also has the effect of improving the efficiency of homology directed repair or comparable pathway due to other unknown effects.

[0109]

The step of synchronizing the cell cycle of the cells preferably includes treating the cells with Cell Division Cycle 7 (CDC7) inhibitor. Examples of the CDC7 inhibitor include XL413 (CAS number: 1169558-38-6).

[0110]

XL413 is preferably added to the cell culture medium at a final concentration of 1 to 100μM, preferably about 33μM. It is preferable to add XL413 to the medium immediately after the introduction of the donor DNA and the sequence-specific DNA-cleaving enzyme into the cells. XL413 is preferably incubated with the cells for about 24 hours.

[0111]

The step of synchronizing the cell cycle of the cells is more preferably performed by using cold shock in combination with a CDC7 inhibitor.

[0112]

The agent that modifies a DNA repair pathway preferably includes a DNA-PK inhibitor or a DNA ligase IV inhibitor. It is more preferable that the agent that modifies a DNA repair pathway includes a combination of a DNA-PK inhibitor and a DNA ligase IV inhibitor.

[0113]

Examples of the DNA-PK inhibitor include NU7441 (CAS number: 503468-95-9). NU7441 is preferably added to the cell culture medium at a final concentration of 100 nM to 10μM, preferably about 2μM.

[0114]

Examples of the DNA ligase IV inhibitor include SCR7 (CAS number: 14892-97-8). SCR7 is preferably added to the cell culture medium at a final concentration of 100 nM to 10μM, preferably about 1μM.

[0115]

The agent that modifies a DNA repair pathway is preferably incubated with the cells from about 4 hours before the introduction of the donor DNA and the sequence-specific DNA-cleaving enzyme into the cells, to about 48 hours after the introduction.

[0116]

In general, sequence-specific DNA-cleaving enzymes used for inducing DSB to perform genome editing are roughly classified into RNA-induced nucleases and artificial nucleases. The sequence-specific DNA-cleaving enzyme may be an RNA-induced nuclease or an artificial nuclease.

[0117]

The sequence-specific DNA-cleaving enzyme is not particularly limited as long as it cleaves genomic DNA in a target sequence-specific manner to form a double-strand

break. A length of a target sequence recognized by the sequence-specific DNA-cleaving enzyme may be, for example, about 10 to 60 bases.

[0118]

Furthermore, the sequence-specific DNA-cleaving enzyme may be, for example, in a form in which a plurality of nickases are combined to cleave DNA. The nickase means an enzyme that forms a nick in a single strand of double-stranded DNA. For example, a double-strand break can be formed by forming nicks at both strands of double-stranded DNA at close locations on genomic DNA.

[0119]

The RNA-induced nuclease is an enzyme in which a short-chain RNA as a guide binds to a target sequence and recruits a nuclease having two DNA cleavage domains (nuclease domains) to induce sequence-specific cleavage. Examples of RNA-induced nucleases include CRISPR-Cas family proteins.

[0120]

Examples of CRISPR-Cas family protein include Cas9, Cas12 (Cpf1), Cas13 (C2c2), CasX, CasY and the like. The RNA-derived nuclease may be a homologue of a CRISPR-Cas family protein or a modified CRISPR-Cas family protein. For example, it may be a nickase-modified nuclease in which one of two existing wild-type nuclease domains is modified to be inactive. Alternatively, it may be Cas9-HF, HiFi-Cas9, eCas9, or the like having improved target specificity.

[0121]

Examples of Cas9 include those derived from *Pseudomonas aeruginosa*, *Staphylococcus aureus*, *Streptococcus thermophilus*, *Geobacillus stearothermophilus*, and the like. Examples of Cpf1 include those derived from *Acidaminococcus*,

Lachnospira, *Chlamydomonas*, *Francicella-Novicida*, and the like.

[0122]

The artificial nuclease is an artificial restriction enzyme having a DNA binding domain designed/produced to specifically bind to a target sequence and a nuclease domain (such as a DNA cleavage domain of FokI which is a restriction enzyme). Examples of artificial nucleases include Zinc finger nuclease (ZFN), Transcription activator-like effector nuclease (TALEN), meganucleases, and the like.

[0123]

In the production method of the present embodiment, the sequence-specific DNA-cleaving enzyme is preferably a ribonucleoprotein (RNP) complex containing Cas9 and gRNA.

[0124]

When CRISPR-Cas is used as the sequence-specific DNA-cleaving enzyme to be introduced into cells, the target base sequence is determined by gRNA. The gRNA may be introduced into the cell in the form of RNA, or may be introduced into the cell in the form of an expression vector and expressed in the cell.

[0125]

Examples of the method of preparing gRNA in the form of RNA include a method of preparing a construct in which a promoter such as T7 is added upstream of a nucleic acid fragment encoding gRNA, and synthesizing it by an in vitro transcription reaction, a method of chemical synthesis and the like. When chemically synthesizing gRNA, chemically modified RNA may be used.

[0126]

Examples of the expression vector include a plasmid vector or a viral vector that transcribes gRNA from Pol III promoter such as H1 promoter or U6 promoter. When gRNA

is expressed using an expression vector, gRNA may be expressed constitutively or may be expressed under the control of an expression-inducible promoter.

[0127]

The site-specific double-strand break site is determined by the Protospacer sequence of about 20 bases and the Protospacer Adjacent Motif (PAM) sequence of about 3 to 5 bases of gRNA that binds complementarily to the target sequence.

[0128]

The gRNA may be a complex of CRISPR RNA (crRNA) and trans-activated CRISPR RNA (tracrRNA), or may be a synthetic single gRNA (sgRNA) that is a combination of tracrRNA and crRNA.

[0129]

Induction of a site-specific double-strand break in the genomic DNA of a cell in the presence of donor DNA results in repair of the double-strand break by homology directed repair or comparable pathway according to all or part of the donor DNA sequence, or, it is repaired by a pathway involving insertion or deletion mutations. The comparable pathway of the homology directed repair may include such as single strand annealing (SSA) and Synthesis-Dependent Strand Annealing (SDSA).

[0130]

In the production method of the present embodiment, donor DNA may have a nucleotide sequence that modifies a protospacer sequence or Protospacer Adjacent Motif (PAM) sequence.

[0131]

When the double-strand break formed by the RNP complex containing Cas9 and gRNA was repaired by homology directed repair or comparable pathway according to all or part of the nucleotide sequence of the donor DNA having a mutation that modifies the

protospacer sequence or the Protospacer Adjacent Motif (PAM) sequence, it is possible to prevent the allele from recleavage by the RNP complex. That is, it is possible to prevent the target site from being cleaved by the RNP complex again and cause introduction of an insertion or deletion mutation at the re-repairing.

[0132]

In the production method of the present embodiment, donor DNA may have a mutation, and cells in which the mutation is introduced into one or both alleles may be obtained. The mutation may be a naturally occurring mutation or an engineered mutation. The naturally occurring mutation is a mutation which correspond to such as polymorphism or variant, in other words, a pre-existing variation detected in the human population which is benign, pathogenic or of unknown function. The engineered mutations is a mutation which is designed artificially.

[0133]

Donor DNA may contain a combination of a plurality of kinds of donor DNAs corresponding to the same region on the genome. For example, donor DNA includes a combination of a first donor DNA and a second donor DNA, in which the first donor DNA has a mutation of interest, and the second donor DNA has a mutation that modifies a protospacer sequence or PAM sequence, and cells in which the mutation of interest is introduced into only one allele and protospacer sequence or PAM sequence of the other allele is modified may be obtained.

[0134]

The first donor DNA has the mutation of interest. The mutation of interest is a mutation which is focused on, in other words, a mutation introducing it into cells is a purpose. Examples of the mutation of interest include a mutation that return disease-causing mutation to the wild type.

[0135]

When the sequence-specific double-strand break is repaired by homology directed repair or comparable pathway according to all or part of the nucleic acid sequence of the second donor DNA, the allele is protected from recleavage by the RNP complex.

[0136]

When the donor DNA contains a combination of the first donor DNA and the second donor DNA, production of a heterozygous mutant become easy because a mutation of interest is introduced into one allele by the first donor DNA and the other allele is protected by the second donor DNA.

[0137]

[Method of editing genome of cells]

In one embodiment, the present invention provides a method of editing genome of cells, including: synchronizing the cell cycle of the cells, treating the cells with an agent that modifies a DNA repair pathway, introducing a donor DNA into the cells, and inducing a sequence-specific double-strand break in the genomic DNA of the cells in the presence of the donor DNA, so that the double-strand break is repaired according to all or part of the donor DNA sequence by homology directed repair or compatible pathway so that genome of the cells are edited.

[0138]

As described later in Examples, the inventors of this application have revealed that the production method of the present embodiment can improve the efficiency of homology directed repair or comparable pathway and perform accurate genome editing.

[0139]

In the method of the present embodiment, the cell to be subjected to genome editing, the donor DNA, the step of synchronizing the cell cycle of the cell, the agent that

modifies the DNA repair pathway, the step of inducing a sequence-specific double-strand break in the genomic DNA of the cells in the presence of the donor DNA, etc. are the same as described above.

[0140]

[Method of detecting gene editing on one or both allele]

In one embodiment, the present invention provides a method of detecting gene editing on one or both allele, including: introducing a donor DNA into a cell, in which the cell has genes encoding a fluorescent protein that emits a first fluorescence in both allele, and in which the donor DNA has a mutation that modifies the first fluorescence of the fluorescent protein into a second fluorescence; inducing a sequence-specific double-strand break in the genomic DNA of the cell in the presence of the donor DNA, so that the double-strand break is repaired according to all or part of the donor DNA sequence by homology directed repair or comparable pathway so that genome-edited cells are obtained; and analyzing the fluorescence of the genome-edited cells, and as a result, (i) if the first fluorescence is detected and the second fluorescence is not detected, it is indicated that (i-1) both alleles of the locus of the fluorescent protein did not change, or (i-2) one allele of the locus of the fluorescent protein did not change and an insertion or deletion mutation occurred in the other allele, (ii) if the first fluorescence is not detected and the second fluorescence is detected, it is indicated that (ii-1) both alleles of the fluorescent protein locus were repaired according to all or part of the donor DNA sequence by homology directed repair or comparable pathway, or (ii-2) one allele of the locus of the fluorescent protein was repaired according to all or part of the donor DNA sequence by homology directed repair or comparable pathway and an insertion or deletion mutation occurred in the other allele, (iii) if neither the first fluorescence nor the second fluorescence is detected, it is indicated that an insertion or deletion mutation

occurred in both alleles of the locus of the fluorescent protein, (iv) if both the first fluorescence and the second fluorescence are detected, it is indicated that one allele of the locus of the fluorescent protein was repaired according to all or part of the donor DNA sequence by homology directed repair or comparable pathway and the other allele did not change.

[0141]

According to the method of the present embodiment, it become easy to visualize and quantitatively analyze whether or not the DNA repair in genome editing which target one allele or both alleles was performed by homology directed repair or comparable pathway, or insertion or deletion mutation occurred.

[0142]

For example, by performing the method of the present embodiment in the presence of a test substance, a substance that increases or decreases the efficiency of homology directed repair can be screened.

[0143]

In the method of the present embodiment, the fluorescent protein that emits the first fluorescence may be a Green Fluorescent Protein (GFP), the fluorescent protein that emits the second fluorescence may be a Blue Fluorescent Protein (BFP), and the donor DNA may have a mutation in which the 66th tyrosine residue of GFP is replaced with a histidine residue to be modified into BFP.

[0144]

In this case, by detecting whether the fluorescence emitted by the cells is the fluorescence of GFP or the fluorescence of BFP, it is possible to visualize and quantitatively analyze what kind of DNA repair was performed.

[0145]

Alternatively, the fluorescent protein that emits the first fluorescence may be a GFP, the fluorescent protein that emits the second fluorescence may be a Cyan Fluorescent Protein (CFP), and the donor DNA may have a mutation in which the 66th tyrosine residue of GFP is replaced with a tryptophan residue to be modified into CFP.

[0146]

In this case, by detecting whether the fluorescence emitted by the cells is the fluorescence of GFP or the fluorescence of CFP, it is possible to visualize and quantitatively analyze what kind of DNA repair was performed.

[0147]

[Kit for genome editing]

In one embodiment, the present invention provides a kit for genome editing including a CDC7 inhibitor, a DNA-PK inhibitor, and a DNA ligase IV inhibitor.

[0148]

The kit of the present embodiment can be suitably used for the production method of genome-edited cells and the method of editing genome of cells as described above. By using the kit of the present embodiment, the efficiency of homology directed repair or comparable pathway can be improved, and accurate genome editing can be performed.

[0149]

In the kit of the present embodiment, the CDC7 inhibitor, DNA-PK inhibitor, and DNA ligase IV inhibitor are the same as those described above.

[0150]

The kit of the present embodiment may further include a sequence-specific DNA-cleaving enzyme and a donor DNA. The sequence-specific DNA-cleaving enzyme and the donor DNA are the same as those described above.

[0151]

In the kit of the present embodiment, the donor DNA may have a mutation in which the 66th tyrosine residue of GFP is replaced with a histidine residue to be modified into BFP.

[0152]

In this case, by carrying out the above-described method of detecting the genome editing in one or both alleles of a cell having a gene encoding GFP in both alleles, it become easy to visualize and quantitatively analyze whether or not the DNA repair in genome editing which target one allele or both alleles was performed by homology directed repair or comparable pathway, or insertion or deletion mutation occurred.

Examples

[0153]

Next, the present invention will be described in more detail with reference to Examples, but the present invention is not limited to the following Examples.

[0154]

[Methods]

(Human iPS cell culture)

Human induced pluripotent stem (iPS) cell lines, namely 409B2 (RIKENBRC #HPS0076) and 1383D6 (RIKEN BRC #HPS1006) were maintained at 37 °C and 5% CO2 in commercially available StemFit AK02N medium (Ajinomoto, Cat. No. RCAK02N) on 0.5 mg/mL silk iMatrix-511, Recombinant Human Laminin-511 E8 Fragment (Nippi, Cat. No. 892021) coated tissue culture plates with daily medium

exchange. Cell passage was performed every 7 days during maintenance. Cells were first dissociated with Accumax (Innovative Cell Technologies, Cat. No. AM105-500) and 10 min incubation at 37 °C, then washed in StemFit AK02N medium supplemented with 10 μM ROCK inhibitor Y-27632 (Wako, Cat. No. 253-00513) and seeded onto iMatrix511-coated plates at a density of 1×10^3 cells/cm^2 in StemFit AK02N medium with ROCK inhibitor for 48 h after seeding, and then cultured without ROCK inhibitor. All the cell lines were routinely tested as negative for mycoplasma contamination.

[0155]

(AAVS1 targeting)

Cell lines targeted heterozygously or homozygously to the AAVS1 safe-harbor locus with a CAG-driven GFP cassette were established in two distinct human iPS cell genetic backgrounds, 409B2 and 1383D6. GFP heterozygous (317-A4) and homozygous (317-D6) clones generated in the 409B2 parental iPS cell line were previously reported43. GFP heterozygous (073-1-3) and homozygous (073-1-2) clones were generated in the 1383D6 parental iPS cell line as previously described43, employing the Neomycin (E182) donor vector and TALE nucleases. Genotyping was performed in targeted clones with Southern blotting using SphI digestion of genomic DNA, internal transgenic or genomic DIG-labelled probes (GFP or 5' probe), and chemiluminescent detection for 2.5 h.

[0156]

(iPS cell gene editing)

An equimolar amount of crRNA and tracrRNA sequences (IDT, Alt-R CRISPR-Cas9 crRNA and tracrRNA) was hybridized for 5 min at 95 °C to form functional crRNA:tracrRNA duplexes (gRNA). For each electroporation (EP), 30.5 pmol gRNA was mixed with 30.5 pmol Cas9 nuclease (IDT, Alt-R S.p. Cas9 Nuclease V3) (1:1

gRNA:Cas9 ratio) to form RNP complexes, and incubated for 30 min at room temperature (RT). Immediately before EP, 82 pmol ssODN repair templates (IDT, Ultramer DNA Oligonucleotides) was added to the preformed RNP complexes, or equal amounts of mixed ssODN repair templates totaling 82 pmol were added to the RNP when generating compound heterozygous mutants. gRNA and ssODN sequences are listed in Tables 1 to 4, respectively. Cells were harvested with Accumax, washed, counted and resuspended at a density of 5×10^5 cells/10 μL in Opti-MEM I reduced-serum medium (Life Technologies, Cat. No. 31985-062). 5×10^5 cells were added to the RNP and ssODN mixture and a total volume of 25 μl was electroporated in a Nepa Electroporation Cuvette 1mm gap (Nepa Gene, Cat. No. EC-001) using the NEPA21 Electroporator (Nepa Gene) instrument (Poring pulse: 125 V voltage, 2.5 ms pulse length, 50 ms pulse gap, 2 pulses, 10% pulse decay, +orientation; Transfer pulse: 20 V voltage, 50 ms pulse length, 50 ms pulse gap, 5 pulses, 40% pulse decay, ±orientation). Electroporated cells were then transferred to an iMatrix511-coated plate in StemFit AK02N medium supplemented with ROCK inhibitor and incubated at 37 °C, or at 32 °C for 48 h for cold shock treatment and then incubated at 37 °C. Medium exchange was performed after 48 h with StemFit AK02N without ROCK inhibitor, and cells were maintained normally until FACS analysis on day 8. When editing endogenous loci in 409B2 iPS cells, RNP complexes were formed using 61 pmol gRNA and 61 pmol Cas9 (maintaining 1:1 gRNA:Cas9 ratio), an equal amount of 82 pmol ssODN repair templates was added to the RNP before EP, or alternatively 41 pmol of either mixed ssODN repair templates when generating compound heterozygous mutants. Then, 1×10^6 cells were added to the RNP and ssODN mixture and a total volume of 40 μl was electroporated in a Nepa Electroporation Cuvette 1mm gap on the NEPA21 Electroporator under the same electroporation conditions as outlined above.

[0157]

[Table 1]

gRNA

Gene	Target	Name	Sequence	Seq ID No:
EGFP	c.196T>C	GFPx199	GCTGAAGCACTGCACGCCGT	3
ATP1A1	RD	ATP1A1x356	GTTCCTCTTCTGTAGCAGCT	4
KCNH2	c.1764C>A	KCNH2x1763	ATCGGCTGGCTGCACAACCT	5
PSMB8	c.602G>T	PSMB8x601	ATAAGTGTTCCCACTACCCG	6
KCNE1	c.253G>A	KCNE1x255	TCTACATCGAGTCCGATGCC	7
KCNH2	c.133A>G	KCNH2x134	GCCGTCATCTACTGCAACGA	8
SCN5A	c.4282G>T	SCN5Ax4282	GGACATTATGTATGCAGCTG	9
KCNH2	c.1762A>G	KCNH2x1763	ATCGGCTGGCTGCACAACCT	10
APRT	c.407T>C	APRTx400	GGCAGCGTTCATGGTTCCTG	11
HES7	c.73C>T	HES7x70	GCTTGTGGAGAAGCGGCGCC	12
KCNJ11	c.878C>A	KCNJ11x878	GAAGGCGTGGTGGAAACCAC	13
KCNJ11	c.881C>T	KCNJ11x878	GAAGGCGTGGTGGAAACCAC	14

[0158]

[Table 2]

ssODN templates

Gene	Target Site	Name	Sequence	Seq ID No:
EGFP	c.196T>C	GFPc.196C-50/50-t	CGGCAAGCTGCCCGTGCCCTGGCCCACCCTCGTGACCACCCTGAGCCATGGGGTGCAGTGCTTCAGCCGCTACCCCGACCACATGAAGCAGCACGACTTC	15
	c.195C>G	GFP-50/50-b-t	CGGCAAGCTGCCCGTGCCCTGGCCCACCCTCGTGACCACCCTGACGTACGGCGTGCAGTGCTTCAGCCGCTACCCCGACCACATGAAGCAGCACGACTTC	16
	c.196T	GFP-50/50-t	CGGCAAGCTGCCCGTGCCCTGGCCCACCCTCGTGACCACCCTGACCTACGGCGTGCAGTGCTTCAGCCGCTACCCCGACCACATGAAGCAGCACGACTTC	17
ATP1A1	RD	ATP1A1-RD	CAATGTTACTGTGGATTGGAGCGATTCTTTGTTTCTTGGCTTATAGCATCAGAGCTGCTACAGAAGAGGAACCTCAAAACGATGACGTGAGTTCTGTAATTCAGCATATCGATTTGTAGTACACATCAGATATCTT	18
KCNH2	c.1764C>A	KCNH2-	GGCCGCCCAGGCCGCTGCTGTTGTAGG	19

		N588K-50/50-t	GTTTGCCTATCTGGTCGCCCAGTTTGTGCAGCCAGCCGATGCGTGAGTCCATGTGTGGCTGCTCCATGTTGCC	
	c.1765C>T	KCNH2-L589L-50/50-t	GGCCGCCCAGGCCGCTGCTGTTGTAGGGTTTGCCTATCTGGTCGCCCAAGTTGTGCAGCCAGCCGATGCGTGAGTCCATGTGTGGCTGCTCCATGTTGCC	20
PSMB8	c.602G>T	PSMB8-G201V-50/50-t	CTACGTGGATGAACATGGGACTCGGCTCTCAGGAAATATGTTCTCCACGGTTAGTGGGAACACTTATGCCTACGGGGTCATGGACAGTGGCTATCGGCCT	21
	c.600G>T	PSMB8-T200T-50/50-t	CTACGTGGATGAACATGGGACTCGGCTCTCAGGAAATATGTTCTCCACTGGTAGTGGGAACACTTATGCCTACGGGGTCATGGACAGTGGCTATCGGCCT	22

[Table 3]

ssODN templates (continued)

KCNE1	c.253G>A	KCNE1-D85N-50/50-t	CTCTCCAGGACCCGGGCCTGGACATAGGCCTTGTCCTTCTCTTGCCAGGCATTGGACTCGATGTAGACGTTGAATGGGTCGTTCGAGTGCTCCAGCTTCT	23
	c.255T>C	KCNE1-D85D-50/50-nt	AGAAGCTGGAGCACTCGAACGACCCATTCAACGTCTACATCGAGTCCGACGCCTGGCAAGAGAAGGACAAGGCCTATGTCCAGGCCCGGGTCCTGGAGAG	24
KCNH2	c.133A>G	KCNH2-N45D-50/50-t	GCTGCATCACCTCGGCCCGCGAGTAGCCGCACAGCTCGCAGAAGCCGTCGTCGCAGTAGATGACGGCGCAGTTCTCCACCCGAGCGTTGGCGATGATGAA	25
	c.135C>T	KCNH2-N45N-50/50-nt	TTCATCATCGCCAACGCTCGGGTGGAGAACTGCGCCGTCATCTACTGCAATGACGGCTTCTGCGAGCTGTGCGGCTACTCGCGGGCCGAGGTGATGCAGC	26
SCN5A	c.4282G>T	SCN5AA1428S-50/50-t	GACTTGGTGGAAGAAGCCACTGTGGCAACCTACCCCCCTGGAGTCCACAGATGCATACATAATGTCCATCCAGCCTTTAAATGTTGCCTGGGAGGAAAAG	27
	c.4287G>T	SCN5AV1429V-50/50-nt	CTTTTCCTCCCAGGCAACATTTAAAGGCTGGATGGACATTATGTATGCAGCTGTTGACTCCAGGGGGGTAGGTTGCCACAGTGGCTTCTTCCACCAAGTC	28
KCNH2	c.1762A>G	KCNH2-N588D-50/50-t	GGCCGCCCAGGCCGCTGCTGTTGTAGGGTTTGCCTATCTGGTCGCCCAGGTCGTGCAGCCAGCCGATGCGTGAGTCCATGTGTGGCTGCTCCATGTTGCC	29

	c.1765C>T	KCNH2-L589L-50/50-t	GGCCGCCCAGGCCGCTGCTGTTGTAGG GTTTGCCTATCTGGTCGCCCAAGTTGTG CAGCCAGCCGATGCGTGAGTCCATGTG TGGCTGCTCCATGTTGCC	30

[Table 4]

ssODN templates (continued)

APRT	c.407T>C c.402A>T	APRT-M136T-50/50-t	CTGCTCTCTGCAGCCCAGGCCAACTGG GGACCTCACCCTCCCATCCCCAGGTACC ACGAACGCTGCCTGTGAGCTGCTGGGC CGCCTGCAGGCTGAGGTC	31
HES7	c.73C>T	HES7-R25W-50/50-nt	CTCCTTTTCTCGCTGGTCGCAGATGCTC AAGCCGCTTGTGGAGAAGCGGCGCTGG GACCGCATCAACCGCAGCCTGGAAGAG CTGAGGCTGCTGCTGCTG	32
KCNJ11	c.878C>A	KCNJ11-T293N-50/50-t	GGATCTCATCGGCCAGGTAGGAGGTGC GGGCCTGGGTGGTGATGCCCGTGTTTT CCACCACGCCTTCCAGGATGACGATGA TCTCGAGGTCCTGGTGGTG	33
KCNJ11	c.881C>T	KCNJ11-T294M-50/50-t	GGATCTCATCGGCCAGGTAGGAGGTGC GGGCCTGGGTGGTGATGCCCATGGTTT CCACCACGCCTTCCAGGATGACGATGA TCTCGAGGTCCTGGTGGTG	34

[0159]

In the case of plasmid-based delivery, a target-specific gRNA sequence (GFPx199 gRNA: caccGCTGAAGCACTGCACGCCGT (Seq ID No: 1) sense and aaacACGGCGTGCAGTGCTTCAGC (Seq ID No: 2) anti-sense oligos) was cloned into the pX459v2 vector (a gift from F. Zhang, Addgene #62988)70. Then, 3 μg of targeting vector and 3 μg (98 pmol) of ssODN repair templates were mixed, 1×10^6 cells resuspended in Opti-MEM were added to the mixture and a total volume of 100 μl was electroporated in a Nepa Electroporation Cuvette 2mm gap (Nepa Gene, Cat. No. EC-002) using the NEPA21 Electroporator (Poring pulse: 125 V voltage, 5 ms pulse length, 50 ms pulse gap, 2 pulses, 10% pulse decay, +orientation; Transfer pulse: 20 V voltage, 50 ms pulse length, 50 ms pulse gap, 5 pulses, 40% pulse decay, ±orientation). Electroporated cells were then transferred to an iMatrix511-coated plate in StemFit

AK02N medium supplemented with ROCK inhibitor and treated with 1 μg/mL puromycin (Merck, Cat. No. P7255-25MG) 24 h post-EP for 48 h. Medium exchange was then performed using StemFit AK02N without ROCK inhibitor, and cells were standardly maintained until FACS analysis on day 8.

[0160]

For gene editing experiments performed on the MaxCyte STX (MaxCyte) instrument, cells were first harvested 1 day before EP and plated at a density of 1.5×10^6 cells on iMatrix511-coated 6-well plates in StemFit AK02N medium supplemented with ROCK inhibitor, as recommended by the manufacturer's instructions. On the day of electroporation, RNP complexes were formed in individual 1.5mL tubes by mixing 61 pmol gRNA with 61 pmol Cas9 nuclease (1:1 gRNA:Cas9 ratio), and 328 pmol ssODN repair templates. Cells were harvested, counted and resuspended in MaxCyte buffer (MaxCyte, Cat. No. EPB-1) at a density of 2×10^6 cells/100 μl, then 1×10^6 cells were added to the RNP and ssODN mixture and a total volume of 50 μl was electroporated in an OC-100 (MaxCyte, Cat. No. SOC-1) or OC-100 × 2 (MaxCyte, Cat. No. SOC-1 × 2) processing assembly on the MaxCyte STX (Optimized protocol 8). After electroporation, processing assemblies were incubated for 20 min at 37 °C, then electroporated cells were transferred to an iMatrix511-coated plate in StemFit AK02N medium supplemented with ROCK inhibitor and incubated at 37 °C, or at 32 °C for cold shock treatment. Medium exchange was performed after 48 h with StemFit AK02N without ROCK inhibitor, and cells were standardly maintained until FACS analysis on day 8.

[0161]

(Small molecule treatment)

For screening and optimization purposes, 5 μg Cas9 (30.5 pmol) was set as a standard editing condition, although higher Cas9 amounts resulted in higher editing

efficiency. All small molecules were dissolved in dimethylsulfoxide (DMSO) as recommended by the manufacturer's instructions, except for XL413 that was dissolved in water. Small molecules were supplemented in StemFit AK02N medium at a final concentration of 3 μM for KU-55933 (Selleck Chemicals, Cat. No. S1092), 1 μM for VE-821 (Selleck Chemicals, Cat. No. S8007), 2 μM for NU7441 (Tocris Bioscience, Cat. No. 3712), 3 μM for Mirin (Sigma-Aldrich, Cat. No. M9948-5MG), 10 μM for PFM01 (Sigma-Aldrich, Cat. No. SML1735-5MG), 20 μM for TDRL-505 (Calbiochem, Cat. No. 530535), 10 μM for RS-1 (Sigma-Aldrich, Cat. No. R9782-5MG), 1 μM for SCR7 (Xcess Bioscience, Cat. No. M60082-2S) and 5 μM for L755507 (Sigma-Aldrich, Cat. No. SML1362-5MG), which are the maximum non-toxic concentrations in iPS cells defined by a titration curve and colony count after 48 h treatment. XL413 (Sigma-Aldrich, Cat. No. SML1401-5MG) was supplemented at a final concentration of 33 μM, and Nocodazole (Sigma-Aldrich, Cat. No. M1404-2MG) at 100 ng/mL. When combining several small molecules, the concentrations were equivalent to individual treatments. The DMSO control was supplemented at a volume equal to the largest volume of individual or combined small molecules used in treated conditions. For gene editing, cells were pretreated for 4 h before EP and for 48 h after EP (pre) with each small molecule, or when specified only for 48 h after EP without pretreatment (post). Pretreated cells were harvested and resuspended in medium supplemented with small molecule during cell counting, before being resuspended in Opti-MEM medium for electroporation. After EP, cells were transferred to an iMatrix511-coated plate in StemFit AK02N medium supplemented with ROCK inhibitor and small molecule and incubated at 37 °C, or at 32 °C for 48 h for cold shock treatment and then incubated at 37 °C. Medium exchange was performed 48 h after EP with StemFit AK02N medium, and cells were standardly maintained until FACS analysis on day 8. For cell-cycle synchronization and gene

editing, XL413 treatment was performed for 24 h after EP, replaced by StemFit AK02N medium supplemented with ROCK inhibitor for 24 h and then by StemFit AK02N medium without ROCK inhibitor. Nocodazole treatment was applied 16 h before EP, supplemented during cell harvest and counting, and replaced by StemFit AK02N medium supplemented with ROCK inhibitor after EP.

[0162]

(Cell-cycle analysis)

Using the Click-iT EdU Alexa Fluor 647 Flow Cytometry Assay Kit (Thermo Fischer Scientific, Cat. No. C10424), cells were first incubated for 2 h 15 min with 10 μM 5-ethynyl-2'-deoxyuridine (EdU) in addition to the small molecule or culture condition being tested. Cells were then harvested, counted, and an equal number of cells was transferred to a new 1.5mL tube. According to the manufacturer's instructions, cells were washed with 1% BSA in 1X DPBS, fixed with Click-iT fixative (4% paraformaldehyde in DPBS), incubated for 15min at room temperature (RT) and protected from light, and washed with 1% BSA in DPBS. Cells were then permeabilized in 1X Click-iT saponin-based permeabilization and wash reagent. The Click-iT labelling reaction was performed by adding a mixture of Alexa Fluor 647 azide fluorescent dye, 2mM CuSO4 and 1X Click-iT EdU buffer additive to the samples, incubating the reaction mixture for 30min at RT and protected from light, and then washing and resuspending the samples in 1X Click-iT saponin-based permeabilization and wash reagent. Finally, a propidium iodide (PI) (Wako, Cat. No. 169-26281) staining solution composed of Triton-X 100 (Nacalai Tesque, Cat. No. 282-29) at a final concentration of 0.1%, RNase A at 0.2mg/mL (Invitrogen, Cat. No. 12091-021) and PI at 20 μg/mL in DPBS was mixed to the samples and incubated for 30 min at RT, protected from light.

[0163]

(Flow cytometry and cell sorting)

Measurement of fluorescence intensities was performed using 5×10^5 cells resuspended in FACS buffer (2% FBS in DPBS) on a BD LSRFortessa Cell Analyzer (BD Biosciences) with BD FACSDiva software (BD Bioscience), and raw data were analyzed with FlowJo (FlowJo LLC). For editing experiments in GFP iPS cells, cells were acquired using the Pacific Blue (450/50 nm) and FITC (530/30 nm) filters. Cells stained with EdU and PI were acquired using Alexa Fluor 647 (660/20 nm) and PE-Tx-Red-GR filters. For characterization of DNA repair outcomes, BFP+, BFP-/GFP-, and GFP+ populations were sorted from edited heterozygous GFP iPS cells, and for the clonal isolation of compound heterozygous cells, the BFP+/GFP+ population was sorted from edited homozygous GFP iPS cells targeted with mixed ssODN repair templa/cates. Cells were harvested in FACS buffer at a density of 1×10^6 cells/mL and filtered through a cell-strainer for dissociation. Sorting gates were set for singlets, and the desired populations were collected on a BD FACSAria II cell sorter (BD Bioscience) into StemFit AK02N medium containing 10-20 μM ROCK inhibitor.

[0164]

(HDR quantification assay)

Ouabain octahydrate (Sigma-Aldrich, Cat. No. O3125-250MG) was dissolved in water. Cells targeted at the ATP1A1 locus and being tested for small molecule or culture conditions were treated 48 h after EP with 1 mM Ouabain in StemFit AK02N medium supplemented with ROCK inhibitor until day 6, in order to selectively obtain HDR-edited colonies. Cells were then maintained normally with StemFit AK02N medium until day 13, and forming colonies were stained with crystal violet. Tissue culture plates were placed on ice, washed twice with ice-cold 1X DPBS, fixed with ice-cold methanol for 10 min, then cells were removed from the ice and incubated with 0.05-0.1% Crystal Violet

(Nacalai, Cat. No. 09804-52) in 25-100% methanol for 10 min at RT. Excess Crystal Violet was removed by washing with water, and the plates photographed for manual colony counting.

[0165]

(Clonal analysis)

For characterization of DNA repair outcomes of single clones, cells were harvested on day 7 after EP and 5×10^5 cells were used for genomic DNA extraction (described below), two cryogenic tubes with 5×10^5 cells each resuspended in STEM-CELLBANKER GMP grade (TAKARA BIO, Cat. No. CB047) were frozen down for total population stocks, and 300-600 cells were plated in iMatrix511-coated 6 cm dishes. Ten days after plating, colonies ~1mm in diameter were picked in 5 μl of media under the microscope and transferred to a 96-well PCR plate. Afterwards, 10 μl of QuickExtract DNA Extraction Solution (Epicenter, Cat. No. QE09050) was added, and plates were incubated for 6 min at 65 °C then 2 min at 98 °C before being stored at -30 °C.

[0166]

(Genotyping)

For genomic DNA extraction, $0.5\text{-}1 \times 10^6$ cells were washed with 1X DPBS, DNA was purified using the DNeasy Blood & Tissue Kit (Qiagen, Cat. No. 69506) as recommended by manufacturer's instructions, and purified DNA was resuspended in 100 μl of water. Target sequences were amplified using KAPA HiFi HS ReadyMix (Kapa Biosystems, Cat. No. KK2602) polymerase chain reaction (PCR), enzymatic PCR product cleanup was performed with ExoSAP-IT Express reagent (Thermo Fischer Scientific, Cat. No. 75001), and Sanger sequencing was performed using the BigDye Terminator v3.1 CS Kit (Thermo Fischer Scientific, Cat. No. 4337456) according to the manufacturer's instructions. Genotyping primers are listed in Tables 5 and 6. Reactions

were then purified by ethanol precipitation and acquired on a 3130xl Genetic Analyzer (Applied Biosystems). Sequence alignments were analyzed with Snapgene (GSL Biotech LLC), and sequence trace files with low base calling confidence were excluded from analyses.

[0167]

[Table 5]

Genotyping primers

Gene	Target Site	Name	Sequence	Seq ID No:
EGFP	c.196T>C	dna549	AGCAAGGGCGAGGAGCTGTT	35
		dna649	GCCGTTCTTCTGCTTGTCGG	36
ATP1A1	RD	dna2778-ATP1A1_Fwd	TATTGCAACCGTCCAGCTAC	37
		dna2779-ATP1A1_Rev	GAATGGCCACCAAGCATTTC	38
KCNH2	c.1764C>A	dna2093-HERG-Exon8, 9-F	CTCTGTCCCAAAGCTAGCAC	39
		dna2094-HERG-Exon8, 9-R	GGGTCCTTACTACTGACTGTGA	40
PSMB8	c.602G>T	dna3253-PSMB8 p.G201V-R	GGATAAGAAGGTGGGTGCTCT	41
		dna3252-PSMB8 p.G201V-F	AAACCATATGACTGGGCCTTTA	42
KCNE1	c.253G>A	dna463-kcne1.3F3	AAACCAAAATGCACACATGCAACC	43
		dna508-hKCNE1.3R_4696-4669	TGGAAATGTCATGCCTTTAGGTTCAGTC	44
		dna005-kcne1F3	GTTCAGCAGGGTGGCAACAT	45
KCNH2	c.133A>G	dna2081-HERG-Exon2-F	CTGTGTGAGTGGAGAATGTGG	46
		dna2082-HERG-Exon2-R	GTCACACCCCCACAGAAC	47
SCN5A	c.4282G>T	dna3177-SCN5A-RP	CCTTCTTGGGGCATCTTCTC	48
		dna3176-SCN5A-FP	CCAGAGGTGGGTAGGGATAG	49
KCNH2	c.1762A>G	dna2093-HERG-	CTCTGTCCCAAAGCTAGCAC	50

		Exon8, 9-F		
		dna2094-HERG-Exon8, 9-R	GGGTCCTTACTACTGACTGTGA	51

[0168]

[Table 6]

Genotyping primers (continued)

APRT	c.407T>C	dna1711-hAPRT-T7F5	GTCGTGGATGATCTGCTGG	52
		dna1712-hAPRT-T7R5	TGCCCAAGGCTGATATTTCCC	53
HES7	c.73C>T	dna2227-HES7-Exon2+3-F	GCGAGCTACAGAAACTGATCT	54
		dna2228-HES7-Exon2+3-R	GGGAGAAAATGAGGGAGACAC	55
KCNJ11	c.878C>A	dna3116-KCNJ11-FP	GTGGTACGCAAGACCACCAG	56
		dna3117-KCNJ11-RP	GGGCTACATACCACATGGTCC	57
KCNJ11	c.881C>T	dna3116-KCNJ11-FP	GTGGTACGCAAGACCACCAG	58
		dna3117-KCNJ11-RP	GGGCTACATACCACATGGTCC	59

[0169]

(RFLP analyses)

ssODN-mediated modification of the GFP target sequence was verified by Restriction Fragment Length Polymorphism (RFLP) of a newly created silent restriction site. The target sequences were PCR amplified from purified gDNA using KAPA HiFi HS ReadyMix, then amplicons were cleaved with FastDigest NcoI (Thermo Fischer Scientific, Cat. No. FD0573) restriction enzyme in FastDigest Buffer (Thermo Fischer Scientific, Cat. No. B64) and incubation for 30 min at 37 °C. Cleaved amplicons were then resolved by gel electrophoresis, acquired on an AE-9000N E-Graph (Atto) gel documentation system and quantified with the ImageJ software.

[0170]

(TIDE analysis)

TIDE analysis was performed on mixed sequences using the online tool at https://tide.nki.nl/71. Sequence data from 409B2-derived heterozygous GFP iPS cells were used as a reference. The deletion size window was extended to 50 bp to visualize larger deletions, while other parameters were kept as default.

[0171]

(Fluorescent microscopy)

Cells plated on iMatrix511-coated 6-well plates with StemFit AK02N medium were directly imaged using an LSM 710 (ZEISS) confocal microscope and LSM Software ZEN 2009 (ZEISS). Images were obtained with a ×10 objective, and GFP and DAPI filters with appropriate gain and exposure times.

[0172]

[Results]

(Fluorescent DNA repair assay in human iPS cells)

Fluorescent reporters provide a means to visualize and quantify gene editing outcomes. GFP and BFP share high sequence homology, and a single tyrosine to histidine (Y66H) amino-acid change in the fluorophore region is sufficient to convert GFP to BFP fluorescence emission42. We generated an iPS cell line heterozygously targeted at the AAVS1 locus in the 1383D6 parental background (Fig. 8A to Fig. 8C) with a stably expressing GFP fluorescent reporter following our previously published method. A Cas9-mediated DSB in GFP was repaired using a 100 bp ssODN template designed to make four nucleotide changes resulting in conversion of GFP to BFP (Y66H), insertion of a PAM blocking mutation to prevent Cas9 recleavage and stabilize the BFP protein (T65S), and creation of a NcoI restriction site for genotyping by restriction fragment length polymorphism (RFLP) (Fig. 1A).

[0173]

Three possible fluorescent outcomes reflect DNA repair choices: BFP, loss of fluorescence (Δ), and GFP, corresponding to HDR, MutEJ, and unmodified alleles, respectively (Fig. 1B). Due to uniform expression of the reporter from the AAVS1 locus, these three outcomes could be clearly discriminated and quantified following nuclease treatment (Fig. 1C to Fig. 1E; Fig. 9A to Fig. 9C).

[0174]

(Cell-cycle control favors HDR outcomes)

Considering the link between cell-cycle phase and DNA repair pathway choice, we aimed to synchronize cells using various culture conditions and chemical inhibitors. Mild hypothermia has been shown to cause cell-cycle arrest and slow cell metabolism in vitro44. We observed that applying a 32 °C cold shock for 48 h directly following electroporation (EP) improved HDR frequency 1.4-fold (30.1% vs 21.3%) and the HDR/MutEJ ratio 1.6-fold compared to normal culture conditions at 37 °C (Fig. 2A, Fig.2B; Fig. 10A, Fig. 10B), confirming previously published results.

[0175]

In order to elucidate the effect of cold shock on iPS cells, we performed cell-cycle analysis using a 5-ethynyl-2'-deoxyuridine (EdU) proliferation assay combined with propidium iodide (PI) staining for total DNA content, and quantified the cell-cycle phase after EP and cold shock treatment (Fig. 2C). Cells undergoing cold shock for 48 h after EP showed 25.5% of cellcycle phase accumulation in the G2/M phase compared to 6.0% under normal culture conditions. In addition, the mean intensity of EdU incorporation was reduced 2.4-fold in S-phase cells in the cold shock condition, indicating a reduced DNA synthesis rate. We tested the effect of cell-cycle synchronization in late G2/M phase by pretreating cells with Nocodazole for 16 h before

EP but, in disagreement to previous reports, we observed no increase in HDR efficiency (Fig. 10C to Fig. 10E). This might suggest that slowed cell-cycle progression in the presence of nuclease is more important than G2/M synchronization prenuclease. Nocodazole inhibits microtubule polymerization, activating the spindle assembly checkpoint and arresting cells in prometaphase, likely causing cells to immediately complete mitosis upon nocodazole release.

[0176]

Since HDR is most active in S/G2 phase, we investigated the effect of synchronizing cells using the CDC7 inhibitor XL413, which halts S-phase progression and arrests karyotypically normal cells in G1/S45,46. As expected, EdU/PI staining revealed accumulation of >90% of cells in G1 and early S phase after 24 h treatment with XL413 after EP (Fig. 2D to Fig. 2F). XL413 increased the HDR frequency 1.7-fold (33.7% vs 19.4%), and the HDR/MutEJ ratio 2.2-fold compared to the untreated control. When combining XL413 treatment for 24 h with cold shock for 48 h, the HDR frequency was increased further by 2-fold (39.4% vs 19.4%) and the HDR/MutEJ ratio by 2.7-fold (0.86 vs 0.32), such that HDR events became nearly as frequent as MutEJ. Interestingly, pretreatment of cells with XL413 before EP did not improve HDR (Fig. 10F to Fig. 10H). These results indicate that chemical and environmental factors modulating cell-cycle synchronization and progression can individually and synergistically affect DNA repair pathway choice in favor of higher HDR outcomes.

[0177]

(Modulating DNA repair pathways to bias HDR outcomes)

To further improve precise gene editing, we treated cells with various small molecules (Fig. 3A) reported to inhibit particular DNA repair pathway components: KU-5593347, VE-82148, NU744149, Mirin50, PFM0151, TDRL-50552, and SCR753; or

enhance HDR rates: RS-154 and L75550755. Human iPS cells were treated with small molecules for 4 h before and 48 h following EP, in addition to 48 h cold shock. Among screened compounds, NU7441 (a DNA-PKcs inhibitor) and SCR7 (a ligase IV inhibitor) increased the HDR frequency 1.6-fold and 1.4-fold (35.5% and 32.3% vs 22.6%; Fig. 3B) and were the only two compounds with an HDR/MutEJ ratio > 0.5. Interestingly, compared to NU7441, SCR7-treated samples also showed a larger fraction of MutEJ,resulting in a reduced HDR/MutEJ ratio increase (1.4-fold vs 2.2-fold for NU7441) despite similar proportions of HDR (Fig. 3C).

[0178]

When combined, NU7441+ SCR7 (N + S) had a cumulative effect further improving HDR frequency by 1.8-fold (49.6% vs 27.3%) and the HDR/MutEJ ratio by 2.7-fold compared to untreated control (1.11 vs 0.41), resulting in a majority of HDR events (Fig. 3D, Fig. 3E). On the other hand, previously reported HDR enhancers such as RS-1 and L755507 showed only a modest change in HDR frequency. These data suggest that inhibiting several molecular targets within the NHEJ repair pathway can have an additive effect, further promoting the use of HDR for DSB repair.

[0179]

We next combined chemical cell-cycle synchronization with XL413 and NHEJ repression with N + S treatment, in order to verify possible additive effects improving HDR rates (Fig. 3F to Fig. 3J). Under normal culture conditions, treatment with XL413 (XL) or N + S alone increased HDR frequency by 1.8-fold and 2.3-fold (30.5 and 39% vs 17%), respectively, while combining XL413 with N + S further increased the HDR frequency by 2.7-fold (45.7% vs 17%) compared to an untreated control. Under cold-shock conditions, comparable changes in HDR frequency were observed for individual treatments, but the combination of XL413 with N + S did not show improvement in HDR

frequency compared to N + S treatment alone. In brief, we show evidence for the existence of synergistic gene editing enhancing HDR outcome frequencies when combining modulation of DNA repair with cold shock, or with cell-cycle synchronization in G1/S phase.

[0180]

(Highly efficient biallelic gene editing)

In diploid iPS cells, both paternal and maternal alleles are candidates for editing. In order to recapitulate this scenario, we generated a homozygous GFP reporter iPS cell line in the 1383D6 parental background (Fig. 8A to Fig. 8C) and evaluated biallelic gene targeting outcomes (Fig. 4A). We first compared monoallelic and biallelic targeting efficiencies and DNA repair outcome frequencies between heterozygous and homozygous GFP reporter lines (Fig. 4B) and found comparable HDR frequencies in both lines (24.3% and 29.2%). In the homozygous context, we gated cells having at least one BFP allele as HDR outcomes, and cells having at least one GFP allele as unmodified, which results in a reduced fraction of MutEJ cells and a 1.4-fold higher HDR/MutEJ ratio compared to the heterozygous cell line (Fig. 4C). Surprisingly, there was no detectable double-positive population that represents heterozygote mutants bearing one HDR allele (BFP) and one unmodified allele (GFP), referred to as HDR* (Fig. 4A). To further explore the cause, we deconvolved all possible biallelic repair outcomes to estimate individual allele repair efficiencies (Fig. 4D). Here, we obtained 16.1% BFP/BFP precise biallelic editing, and a predominant fraction of MutEJ alleles distributed across BFP/Δ (13.1%), Δ/Δ (44%), and GFP/Δ (2.1%) repair outcomes. In summary, this data revealed that both alleles are mostly coedited or unmodified, as shown by the low frequency of monoallelic editing in GFP/Δ (2.1%) and BFP/GFP (0.3%) repair outcomes.

[0181]

We further applied NU7441, SCR7, and N + S under cold shock treatment to the homozygous GFP line and observed a 4-fold increase in HDR frequency (48.9% vs 12.2%) and a 3.7-fold increase in HDR/MutEJ ratio (1.73 vs 0.49) compared to untreated control (Fig. 4E, Fig. 4F). Deconvolution of biallelic repair outcomes showed 30.5% BFP/BFP biallelic repair outcomes when using N + S treatment, 5.7-fold higher than the untreated condition (5.3%) (Fig. 4G). These results demonstrated high biallelic targeting efficiency when combining cold shock treatment and DNA repair pathway inhibitors, leading to the effective generation of homozygous mutants containing single-nucleotide modifications. Interestingly, under the conditions we tested, the proportion of heterozygous BFP/GFP outcomes was consistently low (0.7% and 0.5% with and without N + S treatment) indicating that although homozygous outcomes are frequent, an alternative targeting strategy would be required to efficiently generate heterozygous mutations.

[0182]

(Generation of heterozygous mutations)

In order to resolve low monoallelic editing rates while retaining high overall HDR frequencies, we adopted a mixed ssODN repair template strategy. Herein, we leveraged high biallelic modification rates to generate HDR-mediated compound heterozygous mutations composed of one edited allele and one protected allele bearing a silent blocking mutation, thereby preventing subsequent Cas9 recleavage and indel formation at the target site (Fig. 5A). Along with the Y66Hmutant ssODN (ssODN 'M'), we designed an ssODN carrying a silent T65T blocking mutation (ssODN 'B'), and a wild-type (WT) ssODN identical to the GFP target sequence (ssODN 'W') as a control. HDR-mediated editing of T65T with ssODN B destroys the PAM sequence at the target site, resulting in a Cas9-protected GFP allele (pGFP) (Fig. 11A, Fig. 11B). Alleles

incorporating ssODN W were expected to be susceptible to recleavage. Biallelic HDR repair outcomes were expected to result in the generation of homozygous BFP/BFP and pGFP/pGFP cells, as well as a fraction of desired compound heterozygous BFP/pGFP cells referred to as HDR*.

[0183]

Single ssODN templates and ssODN combinations were tested (Fig. 5B, Fig. 5C). ssODN B showed a 1.5-fold increase in GFP-positive cells (57.2%) suggesting the generation of pGFP alleles by HDR, while ssODN W showed a 1.8-fold decrease (22.2%) compared to ssODN M (39.1%), suggesting that WT GFP alleles generated through HDR are subject to recleavage as predicted. Combinations of ssODN M+ B and ssODN M+W yielded similar total repair frequencies. Nonetheless, among all ssODN conditions only the combination of ssODN M and B resulted in a population of heterozygous BFP/GFP double-positive cells, with an efficiency of 3.6% (Fig. 5D, Fig. 5 E), 12-fold higher than using ssODN M alone (0.3%) and 20-fold higher than using a combination of ssODN M and W (0.18%). When applying N + S treatment in addition to cold shock, the efficiency of compound heterozygous BFP/pGFP generation retained a similar fold-enrichment over ssODN M (12.4-fold) or ssODN M+W (16.2-fold) alone but increased to 11.2% of the total population (Fig. 11C to Fig. 11F). These results suggest that under conditions of high HDR efficiency, protection of one allele against Cas9-mediated recleavage is required in order to obtain heterozygous mutant alleles without a mutagenic indel in the second allele.

[0184]

Consequently, we verified the applicability of this approach to endogenous loci. First, we targeted ATP1A1 (Fig. 12A) that is known to cause 2000-fold increase in dominant cellular resistance to the cytotoxic inhibitor ouabain when introducing Q118R

and N129D missense mutations compared to making in-frame indel mutations56. Selecting for HDR clones under high ouabain concentration, we observed a 1.8-fold increase in colony number with combined cold shock and N + S treatment, indicating synergistic increase in frequency at an endogenous locus (Fig. 12B). Next, we aimed to edit nonselectable endogenous loci. We independently generated the N588K (c.1764C > A) mutation in KCNH2 and G201V (c.602 G > T) mutation in PSMB8, either using an ssODN carrying the mutation (ssODN M) or a combination of ssODN M and an ssODN carrying a silent blocking mutation (ssODN M+ B) and performed clonal analysis (Fig. 12C, Fig. 12D). Under optimal cold shock and drug treatment conditions, we obtained 14 out of 96 homozygous clones edited at KCNH2 and 18 out of 91 at PSMB8 when using KCNH2 or PSMB8 ssODN M only, corresponding to biallelic HDR events (Fig. 12E, Fig. 12F). Moreover, we could only obtain compound heterozygous clones at KCNH2 (4/92) or PSMB8 (4/95) when using the ssODN M+ B combination, corresponding to biallelic HDR events incorporating mutant ssODN M and silent blocking ssODN B at cognate alleles. These results confirm that our approach is highly effective to generate both homozygous and heterozygous clones at endogenous loci in human iPS cells.

[0185]

(Synergistic gene editing enhances HDR at endogenous loci)

Finally, in considering the application of gene-edited iPS cells for cell therapy, we tested our defined conditions using a transfection instrument approved for GMP cell applications. We compared DNA repair outcome frequencies in normal culture, cold shock, and combined cold shock and N + S conditions in heterozygous and homozygous GFP iPS cell lines generated in two different donor genetic backgrounds (Fig. 13A to Fig. 13H). In the 1383D6 genetic background, HDR efficiency increased 1.2-fold with cold

shock and 1.6-fold with combined cold shock and N + S treatment both in heterozygous (59.1% and 75.6% vs 47.9%) and homozygous (64.6% and 84.1% vs 52.9%) cell lines compared to an untreated control. When editing homozygous GFP iPS cells with ssODN M and B, the efficiency of compound heterozygous BFP/pGFP editing increased by 1.5-fold with cold shock and 2.5-fold with combined cold shock and N + S treatment (14.4% to 24.1% vs 9.8%). Similar results were obtained in the 409B2 genetic background.

[0186]

Furthermore, cell-cycle synchronization with XL413 and DNA repair modulation with N + S treatment again showed evidence of synergistic gene editing enhancing HDR frequencies (Fig. 6A to Fig. 6H). Remarkably, HDR outcomes reached 83.3% during monoallelic editing of heterozygous GFP iPS cells (Fig. 6A, Fig. 6B), and 96.6% during biallelic editing of homozygous GFP iPS cells when combining XL413 and N + S treatment under cold shock conditions (Fig. 6C, Fig. 6D; Fig. 14A, Fig. 14B), including 84.8% biallelic HDR editing outcomes. Moreover, 32.2% of cells became compound heterozygotes when editing homozygous GFP iPS cells with mixed ssODN M and B repair templates (Fig. 6E, Fig. 6F; Fig. 14C, Fig. 14D). We ultimately verified HDR frequencies of synergistic gene editing at endogenous loci (Fig. 15A to Fig. 15J), using combined XL413 and N + S (XL + N + S) or combined cold shock and N + S (32 °C + N + S) compared to untreated (-) baseline HDR levels (Fig. 6G, Fig. 6H). HDR outcomes included clones with template-mediated repair events on one or both alleles, while MutEJ outcomes included clones with an indel on at least one allele. Overall, synergistic gene editing resulted in several-fold increase in HDR frequencies at all targeted loci, confirming broad applicability of this strategy to targeting the human genome (Fig. 6G). At 5 loci (KCNH2 N588D/N588K, APRT M136T, HES7 R25W, and PSMB8 G201V), we obtained from 18 to 23 out of 32 clones with HDR alleles under XL

+ N + S treatment, representing 56 to 72% total HDR efficiency. Interestingly, cell-cycle arrest with XL413 had a stronger effect on HDR rates than cold shock, when combined with N + S treatment. At the other 5 loci (KCNE1 D85N, KCNH2 N45D, SCN5A A1428S, and KCNJ11 T293N/T294M), total editing efficiency was low as shown by the greater proportion of unmodified wild-type clones, suggesting poor gRNA activity. In this case, between 0 and 8 out of 32 HDR clones or 0 to 25% HDR efficiency was achieved. Similarly, HDR/MutEJ ratios were improved with synergistic gene editing, with a stronger effect observed in most cases for XL413 compared to cold shock (Fig. 6H). In summary, these results confirm that synergistic gene editing via cell-cycle synchronization and DNA repair pathway modulation is transferrable between electroporation instruments and to other iPS cell lines, resulting in the efficient clonal generation of homozygous and compound heterozygous mutations at multiple endogenous loci.

[0187]

(Discussion)

In this study, we sought to bias DNA repair outcomes towards HDR during ssODN-mediated gene editing in human iPS cells, using chemical and cell-culture condition interventions (Fig. 7). Cold shock was shown to have various effects on cellular function under severe (4-16 °C), moderate (16-25 °C), and mild (25-35 °C) hypothermia, such as slowed metabolism, activation of apoptotic pathways, changes in gene expression and cell-cycle arrest. Mild cold shock of 32 °C is characterized by peak levels of cold-inducible RNA-binding protein (CIRP) and RNA-binding motif protein 3 (RBM3) that have important functions in cellular protection against various endogenous and environmental stresses. In the context of gene editing, cold shock was shown to improve HDR efficiency, yet the mechanism remains unclear. Here we showed that cold

shock slowed cell-cycle progression, accumulated cells in G2/M phase, and reduced DNA synthesis rates. Alternatively, cold shock could manifest through other noncell-cycle-dependent effects such as nuclease stability, gRNA association or DNA cleavage kinetics and stabilization of repair intermediates, post-translational regulation, and cell viability. These additional effects of cold shock may explain the synergy observed in combination with the XL413-induced cell-cycle arrest in G1/S phase.

[0188]

Regulation of the cell cycle is an ongoing area of interest in the fields of DNA repair and gene editing. It has been proposed that increased CDK activity in S phase stimulates phosphorylation of key HDR proteins such as CtIP, promoting DSB end resection and HDR. Cell-cycle synchronization at the G1/S boundary with Aphidicolin and in late G2/M phase with Nocodazole was shown to enhance HDR frequency. Furthermore, simultaneous promotion of G1/S transition by Cyclin D1 (CCND1) overexpression and cell-cycle synchronization in G2/M phase with nocodazole was reported to further improve HDR efficiency. Here, we report enhanced gene editing by the CDC7 inhibitor XL413 in iPS cells. XL413 was reported to accumulate cells in S/G2/M phases in cancer cell lines46, while arrest in G1/early S phase was reported in karyotypically normal cells45, in agreement with our observations in iPS cells. It is also known that human iPS cells, similar to embryonic stem (ES) cells, have an abbreviated G1 phase of ~2.5 h and enter S phase ~4 h after nocodazole-induced synchronization in G2/M phase. During CRISPR-Cas9 targeting, RNP activity is initiated within 4 h of delivery and is mostly completed after ~24 h due to RNP degradation64, leaving a limited time window for DSB formation and recruitment of the HDR pathway in S/G2 phase. Therefore, cell-cycle retardation in G2/M or synchronization in G1/early S phase at a time when nuclease activities are high might ensure rapid cell-cycle entry in S phase,

which is in any case the predominant cell-cycle state in iPS cells and favors HDR repair. While it is interesting that nocodazole failed to enhance iPS cell gene editing in our experiments, XL413 had a clear positive effect, warranting further exploration.

[0189]

We found that the NHEJ inhibitors NU7441 and SCR7 individually improve HDR efficiency in iPS cells, and further improve HDR efficiency when combined. DNA-PKcs is specifically activated upon DSB formation and recruits protein components of the NHEJ pathway including DNA ligase IV, which acts to join DNA ends. We suspect that inhibition of DNA-PKcs with NU7441 might circumvent NHEJ complex assembly and allow for alternative DNA repair pathway choices, whereas for downstream inhibition of DNA ligase IV with SCR7, cells may already be committed to NHEJ or some alternative MutEJ repair. This may explain the higher HDR efficiency with NU7441 compared to SCR7 treatment. Interestingly, we did not observe enhancement of HDR by RS-1 or L755507. With regard to the specific type of HDR we are aiming to induce, recent reports speculate that ssODN-mediated DSB repair undergoes synthesis dependent strand annealing (SDSA), which is a RAD51-independent process and thus might explain the limited effect of HDR enhancers RS-1 and possibly L755507 in our system.

[0190]

Previous studies attempted to combine cell-cycle synchronization with NHEJ inhibition but did not observe improved HDR efficiency compared to individual conditions. This may be due to the use of karyotypically abnormal cell lines as HEK293T cells or because of the low efficiency of the SCR7 inhibitor alone in pluripotent stem cells. In addition, HDR activity peaks in mid S phase and decreases in G2 phase in karyotypically normal cells, which might indicate the limited efficiency we observed in

iPS cells with late G2/M phase synchronization by Nocodazole. Taken together, these results demonstrate that different conditions simultaneously modulating cell-cycle phase and DNA repair pathway choice synergistically improve HDR frequency. To our knowledge, we are the first to report synergistic effects of cellcycle synchronization and DNA repair pathway modulation on precise gene editing.

[0191]

Using this approach, we obtained up to 96.6% of cells with HDR alleles during biallelic editing, including 84.8% biallelic HDR editing when generating homozygous mutations. Surprisingly, high editing efficiencies were associated with nearly nonexistent heterozygous mutant cells. Single HDR alleles formed by precise monoallelic editing were predominantly paired with an indel in the second allele, in agreement with previous reports.

[0192]

Therefore, we adopted a mixed ssODN strategy to create compound heterozygous mutant alleles protected from Cas9-recleavage, and generated up to 32.2% compound heterozygous mutants at the GFP reporter. Considering endogenous targets for disease modeling, we generated homozygous and compound heterozygous mutations at multiple loci and demonstrated that synergistic gene editing consistently improves HDR outcome frequencies several-fold compared to baseline HDR levels. Eventually, obtaining heterozygous mutants without silent mutations protecting the second allele may require a second round of editing, or use of a two-step donor vector targeting and excision process such as the MhAX method. Other strategies could leverage haplotype specificity, conversion tract, or nuclease titration to bias towards monoallelic editing, but these approaches will be locus-dependent and come at the cost of lower editing efficiency. We expect that synergistic gene editing will improve ssODN-based strategies

for introducing and removing blocking mutations using two-step targeting. In conclusion, we established a biallelic reporter system capable of resolving allele-specific DNA repair outcomes and defined synergistic gene editing conditions improving HDR and HDR/MutEJ rates using cold shock, cell-cycle synchronization and DNA repair modulation. Leveraging high efficiency biallelic modification, we demonstrated a strategy to generate compound heterozygous iPS cell lines. We expect that improving the reliability of biallelic editing outcomes will greatly facilitate the generation of dominant and recessive genetic disease models and possibly even therapies using human iPS cells.

Industrial Applicability

[0193]

According to the present invention, a technique for efficiently produce genome-edited cells, in which targeted DNA double strand breaks (DSBs) in the genome are repaired by homology-directed repair (HDR) or comparable pathway is provided.

CLAIMS

1. A production method of genome-edited cells, comprising:

synchronizing the cell cycle of the cells,

treating the cells with an agent that modifies a DNA repair pathway,

introducing a donor DNA into the cells, and

inducing a sequence-specific double-strand break in the genomic DNA of the cells in the presence of the donor DNA, so that the double-strand break is repaired according to all or part of the donor DNA sequence by homology directed repair or comparable pathway so that genome-edited cells are obtained.

2. The production method according to claim 1, wherein synchronizing the cell cycle of the cells includes incubating the cells at 25 to 35°C for 24 to 72 hours.

3. The production method according to claim 1 or 2, wherein synchronizing the cell cycle of the cells includes treating the cells with Cell Division Cycle 7 (CDC7) inhibitor.

4. The production method according to any one of claims 1 to 3, wherein the agent that modifies a DNA repair pathway includes a DNA-PK inhibitor or a DNA ligase IV inhibitor.

5. The production method according to any one of claims 1 to 4, wherein the agent that modifies a DNA repair pathway includes a combination of a DNA-PK inhibitor and a DNA ligase IV inhibitor.

6. The production method according to any one of claims 1 to 5, wherein the sequence-specific double-strand break is induced by a ribonucleoprotein (RNP) complex comprising a Cas9 and a gRNA.

7. The production method according to any one of claims 1 to 6, wherein the donor DNA is a single-stranded donor oligonucleotide.

8. The production method according to claim 7, wherein the donor DNA has a nucleotide sequence that modifies a protospacer sequence or Protospacer Adjacent Motif (PAM) sequence.

9. The production method according to any one of claims 1 to 8, wherein the donor DNA has a mutation, and cells in which the mutation is introduced into one or both alleles are obtained.

10. The production method according to any one of claims 1 to 9, wherein the donor DNA comprises a combination of a plurality of kinds of donor DNAs corresponding to the same region on the genome.

11. The production method according to claim 10,

wherein the donor DNA comprises a combination of a first donor DNA and a second donor DNA,

wherein the first donor DNA has a mutation of interest, and the second donor DNA has a mutation that modifies a protospacer sequence or PAM sequence, and

cells in which the mutation of interest is introduced into only one allele and

protospacer sequence or PAM sequence of the other allele is modified are obtained.

12. The production method according to any one of claims 1 to 11, wherein the cells are induced pluripotent stem (iPS) cells.

13. A method of editing genome of cells, comprising:

synchronizing the cell cycle of the cells,

treating the cells with an agent that modifies a DNA repair pathway,

introducing a donor DNA into the cells, and

inducing a sequence-specific double-strand break in the genomic DNA of the cells in the presence of the donor DNA, so that the double-strand break is repaired according to all or part of the donor DNA sequence by homology directed repair or compatible pathway so that genome of the cells are edited.

14. A method of detecting genome editing on one or both allele, comprising:

introducing a donor DNA into a cell, wherein the cell has genes encoding a fluorescent protein that emits a first fluorescence in both allele, and wherein the donor DNA has a mutation that modifies the first fluorescence of the fluorescent protein into a second fluorescence;

inducing a sequence-specific double-strand break in the genomic DNA of the cell in the presence of the donor DNA, so that the double-strand break is repaired according to all or part of the donor DNA sequence by homology directed repair or comparable pathway so that genome-edited cells are obtained; and

analyzing the fluorescence of the genome-edited cells, and as a result,

(i) if the first fluorescence is detected and the second fluorescence is not

detected, it is indicated that

(i-1) both alleles of the locus of the fluorescent protein did not change, or

(i-2) one allele of the locus of the fluorescent protein did not change and an insertion or deletion mutation occurred in the other allele,

(ii) if the first fluorescence is not detected and the second fluorescence is detected, it is indicated that

(ii-1) both alleles of the fluorescent protein locus were repaired according to all or part of the donor DNA sequence by homology directed repair or comparable pathway, or

(ii-2) one allele of the locus of the fluorescent protein was repaired according to all or part of the donor DNA sequence by homology directed repair or comparable pathway and an insertion or deletion mutation occurred in the other allele,

(iii) if neither the first fluorescence nor the second fluorescence is detected, it is indicated that an insertion or deletion mutation occurred in both alleles of the locus of the fluorescent protein,

(iv) if both the first fluorescence and the second fluorescence are detected, it is indicated that one allele of the locus of the fluorescent protein was repaired according to all or part of the donor DNA sequence by homology directed repair or comparable pathway and the other allele did not change.

15. The method according to claim 14, wherein the fluorescent protein that emits the first fluorescence is a Green Fluorescent Protein (GFP), the fluorescent protein that emits the second fluorescence is a Blue Fluorescent Protein (BFP), and the donor DNA has a mutation in which the 66th tyrosine residue of GFP is replaced with a histidine residue to

be modified into BFP.

16. A kit for genome editing comprising a CDC7 inhibitor, a DNA-PK inhibitor, and a DNA ligase IV inhibitor.

17. The kit for genome editing according to claim 16, further comprising a sequence-specific DNA-cleaving enzyme and a donor DNA.

18. The kit for genome editing according to claim 17, wherein the donor DNA has a mutation in which the 66th tyrosine residue of GFP is replaced with a histidine residue to be modified into BFP.

FIG. 1A

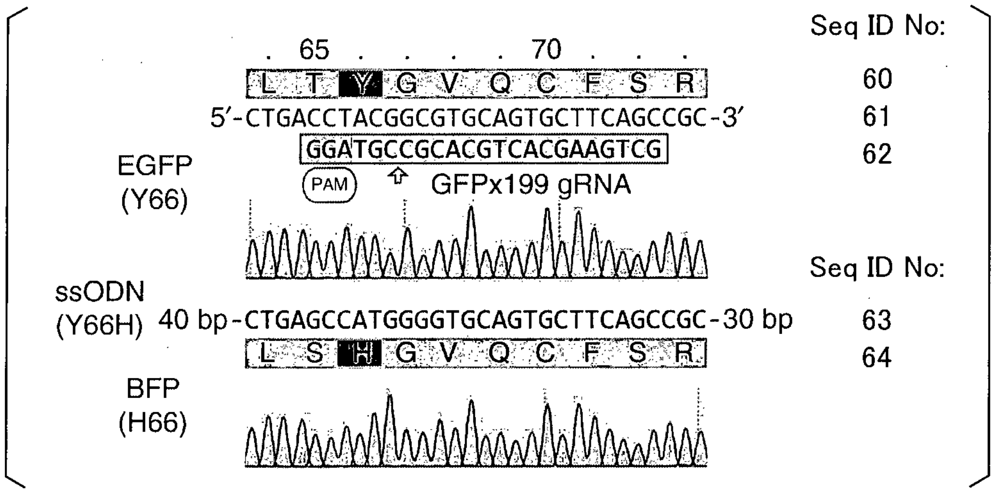
Seq ID No:
. 65 . . . . . 70 . . .
L T Y G V Q C F S R
60
5′-CTGACCTACGGCGTGCAGTGCTTCAGCCGC-3′
61
GGATGCCGCACGTCACGAAGTCG
62
EGFP
(Y66)
PAM
GFPx199 gRNA
Seq ID No:
ssODN
(Y66H)
40 bp-CTGAGCCATGGGGTGCAGTGCTTCAGCCGC-30 bp
63
L S H G V Q C F S R
64
BFP
(H66)

FIG. 1B

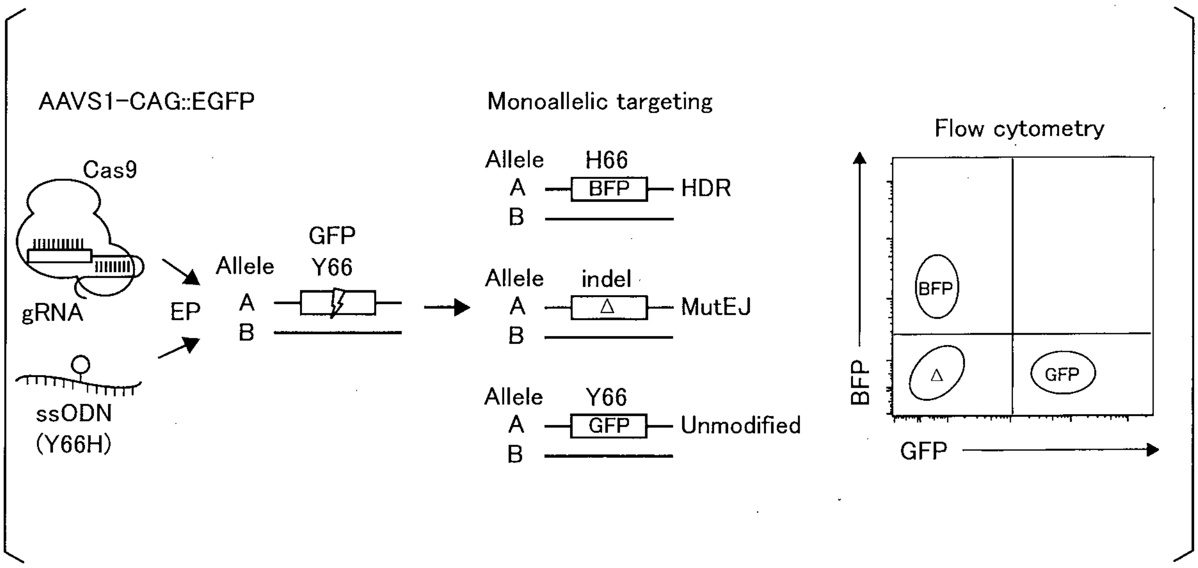
AAVS1-CAG::EGFP
Cas9
gRNA
ssODN
(Y66H)
EP
Allele
A
B
GFP
Y66
Monoallelic targeting
Allele
H66
A
BFP
HDR
B
Allele
indel
A
Δ
MutEJ
B
Allele
Y66
A
GFP
Unmodified
B
Flow cytometry
BFP
Δ
GFP
BFP
GFP

FIG. 1C

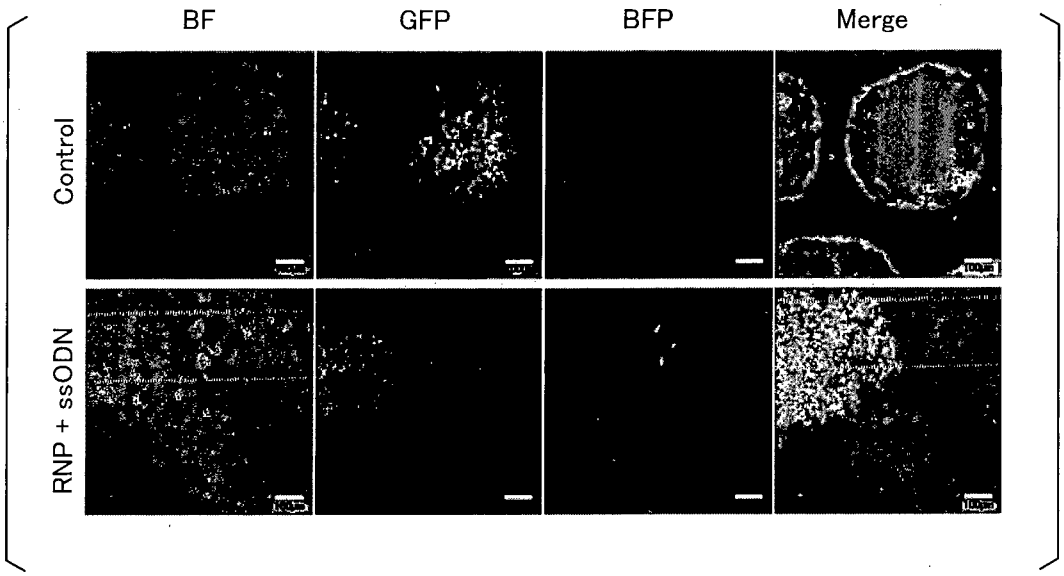
BF
GFP
BFP
Merge
Control
RNP + ssODN

FIG. 1D

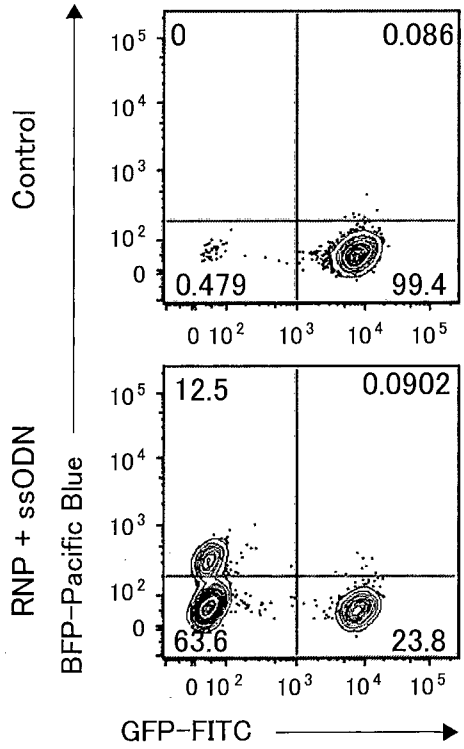
Control
RNP + ssODN
BFP-Pacific Blue
GFP-FITC
0
0.086
0.479
99.4
12.5
0.0902
63.6
23.8
10^5
10^4
10^3
10^2
0

FIG. 1E

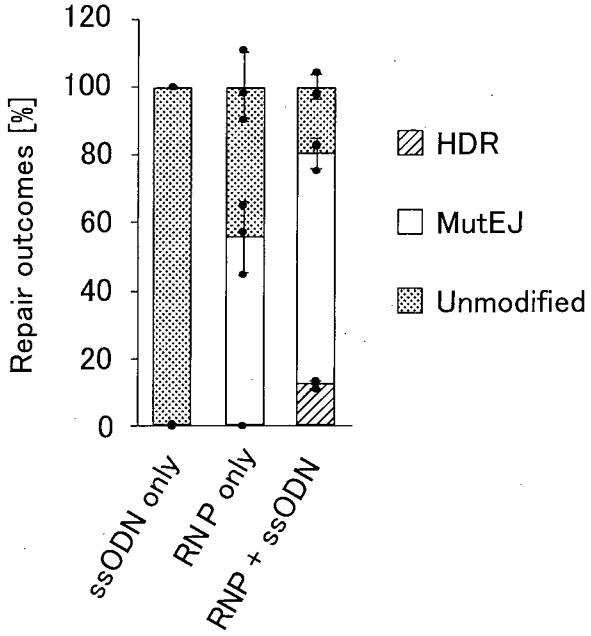
120
100
80
60
40
20
0
Repair outcomes [%]
HDR
MutEJ
Unmodified
ssODN only
RNP only
RNP + ssODN

FIG. 2A

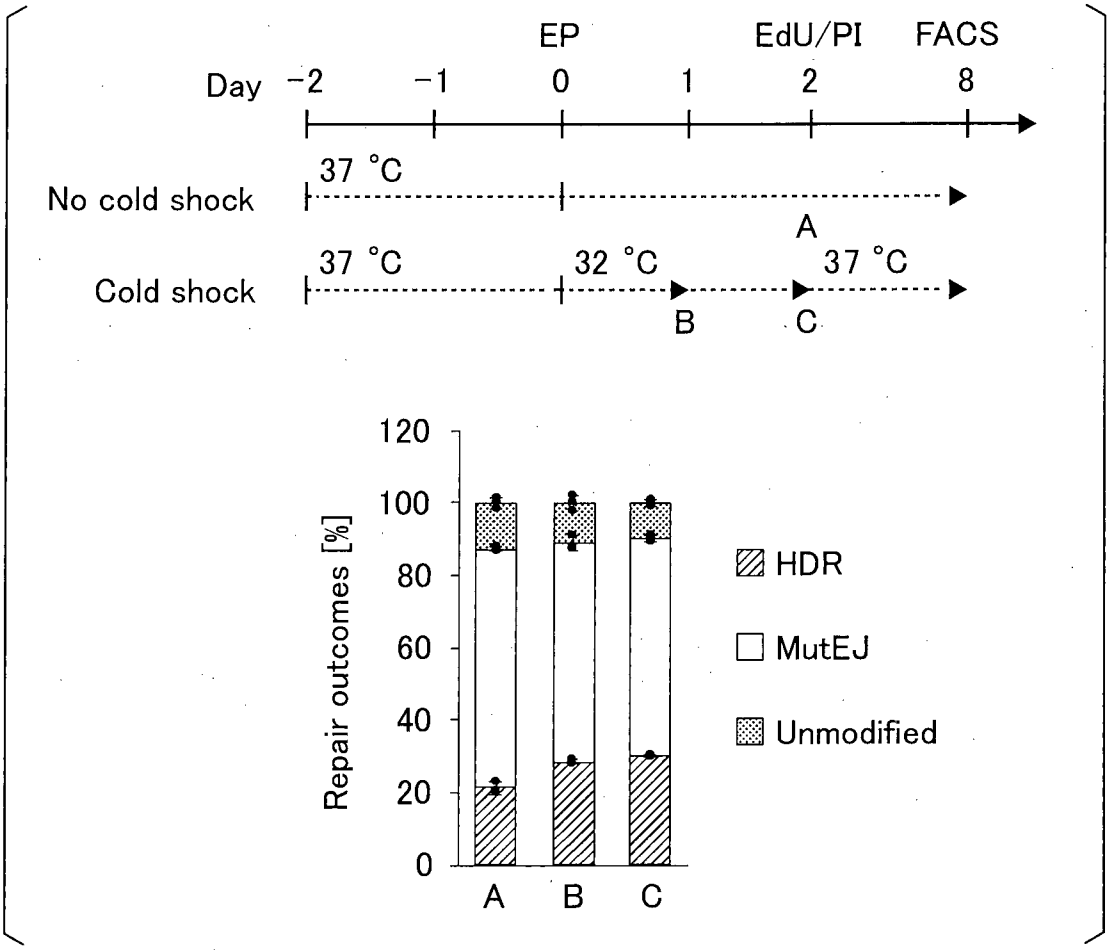
EP
EdU/PI
FACS
Day
-2
-1
0
1
2
8
37 °C
No cold shock
A
37 °C
32 °C
37 °C
Cold shock
B
C
120
100
80
60
40
20
0
Repair outcomes [%]
HDR
MutEJ
Unmodified
A
B
C

FIG. 2B

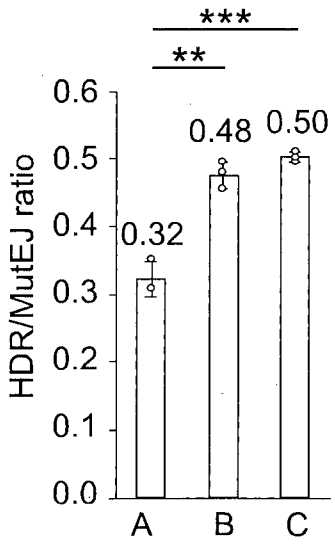
***
**
0.6
0.5
0.4
0.3
0.2
0.1
0.0
HDR/MutEJ ratio
0.32
0.48
0.50
A
B
C

FIG. 2C

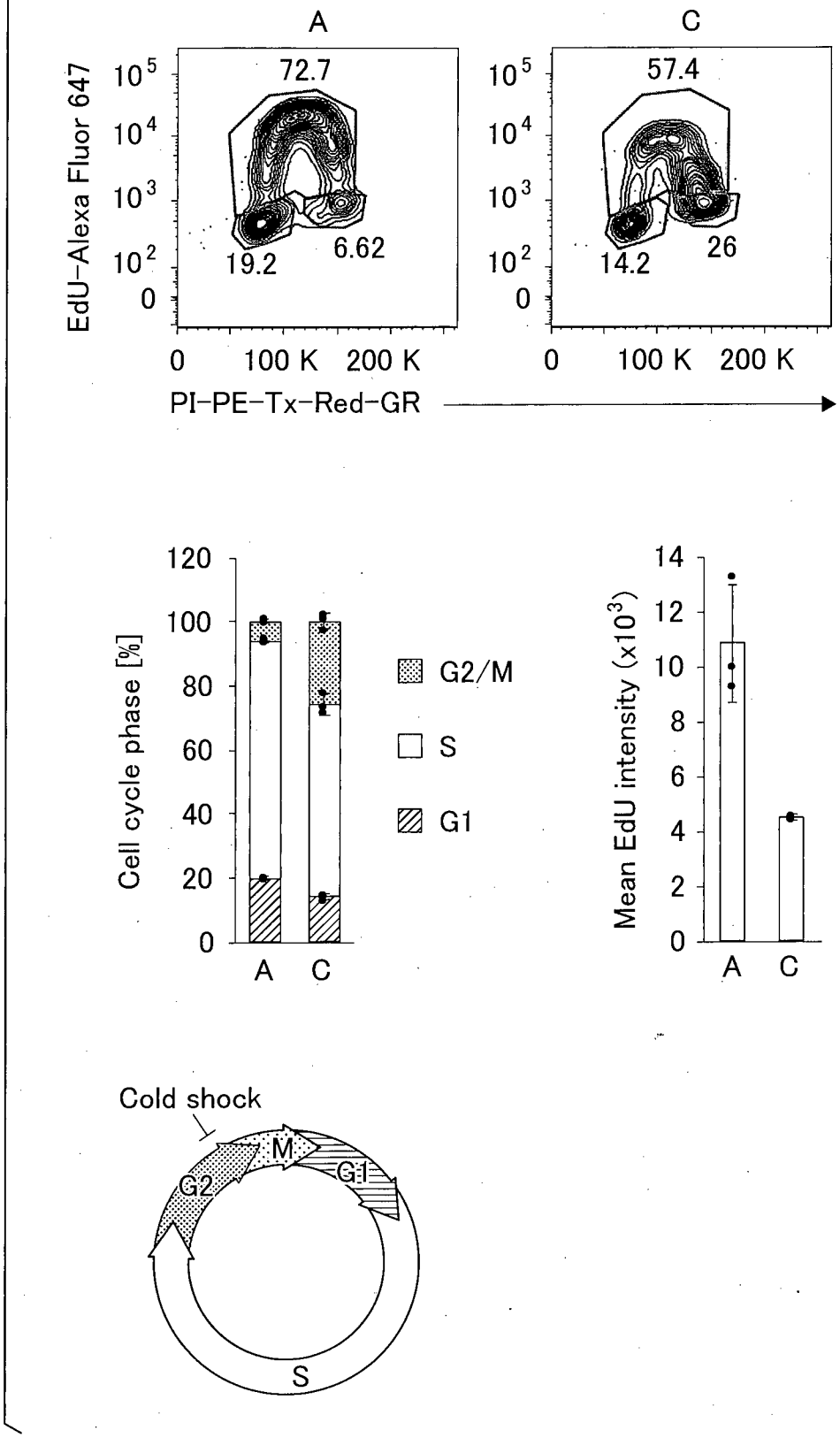
A
C
72.7
6.62
19.2
57.4
26
14.2
EdU-Alexa Fluor 647
PI-PE-Tx-Red-GR
0
100 K
200 K
Cell cycle phase [%]
G2/M
S
G1
Mean EdU intensity (x10³)
Cold shock
M
G1
G2
S

FIG. 2D

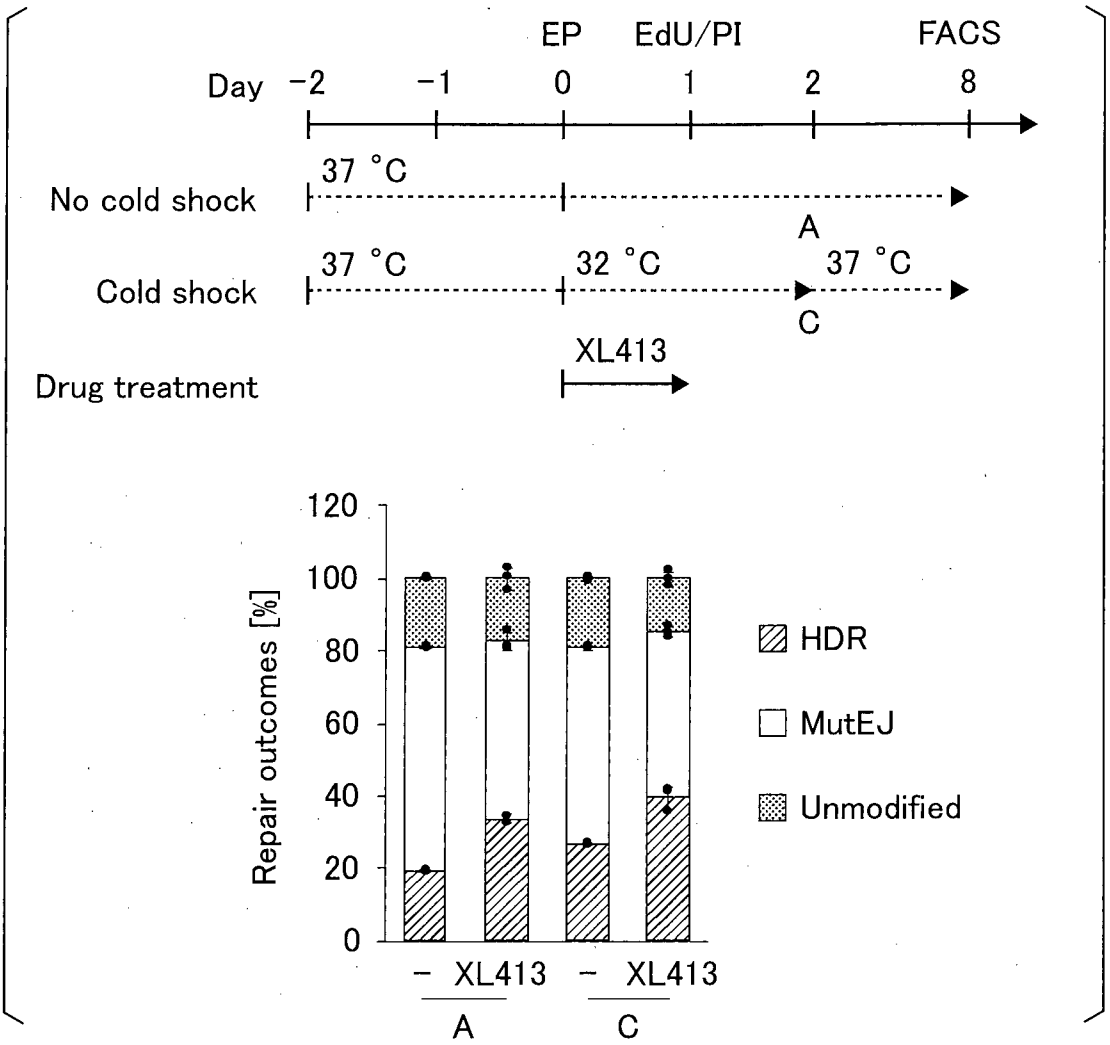
EP
EdU/PI
FACS
Day
-2
-1
0
1
2
8
No cold shock
37 °C
A
Cold shock
37 °C
32 °C
37 °C
C
Drug treatment
XL413
Repair outcomes [%]
120
100
80
60
40
20
0
HDR
MutEJ
Unmodified
- XL413
- XL413
A
C

FIG. 2E

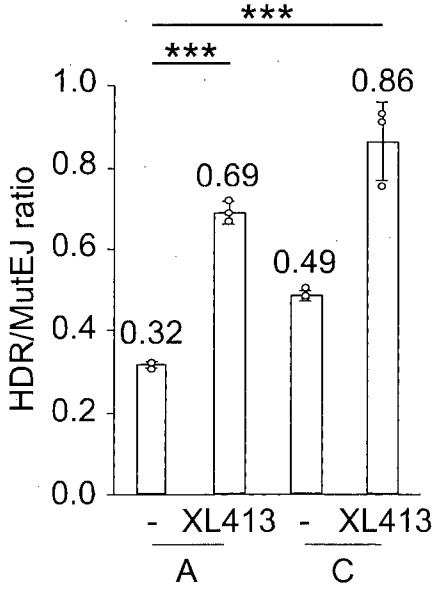
***
***
HDR/MutEJ ratio
1.0
0.8
0.6
0.4
0.2
0.0
0.32
0.69
0.49
0.86
- XL413
- XL413
A
C

FIG. 2F

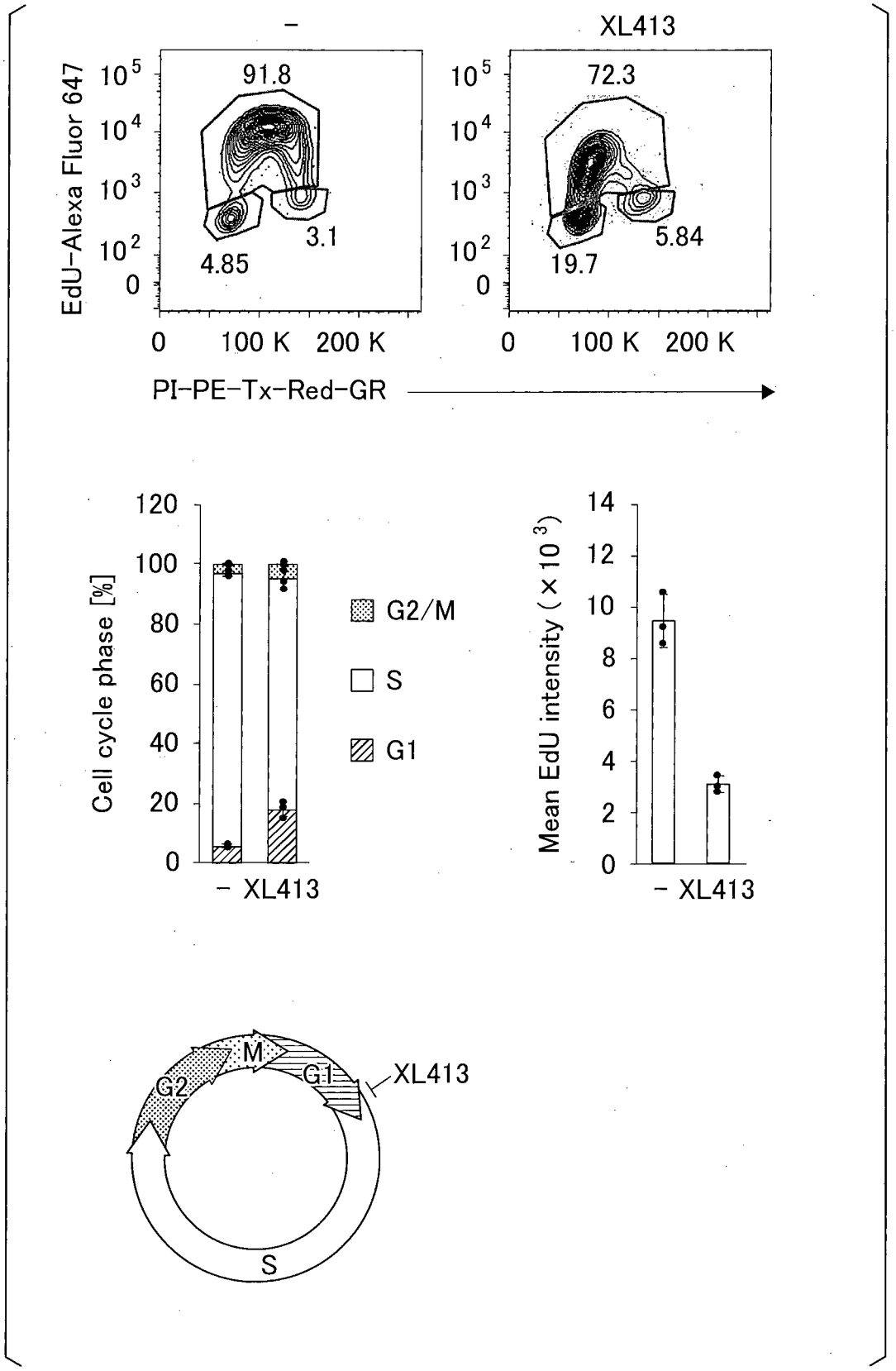
-
XL413
EdU-Alexa Fluor 647
91.8
3.1
4.85
72.3
5.84
19.7
0
100 K
200 K
PI-PE-Tx-Red-GR
Cell cycle phase [%]
G2/M
S
G1
- XL413
Mean EdU intensity (×10 3)
M
G2
G1
S
XL413

FIG. 3A

Compound	Function
KU-55933	ATM inhibitor
VE-821	ATR inhibitor
NU7441	DNA-PK inhibitor
Mirin	MRN-ATM inhibitor
PFM01	MRE11 endonuclease inhibitor
TDRL-505	RPA inhibitor
RS-1	RAD51 stimulator
SCR7	DNA ligase IV inhibitor
L755507	β3 adrenergic receptor agonist

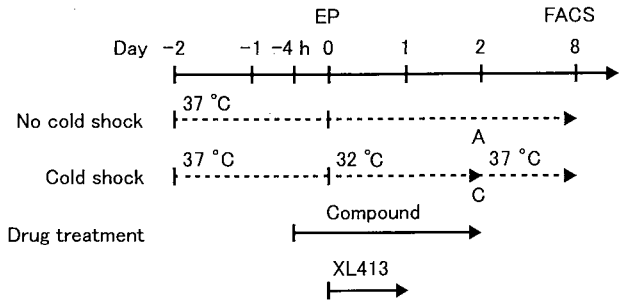

FIG. 3B

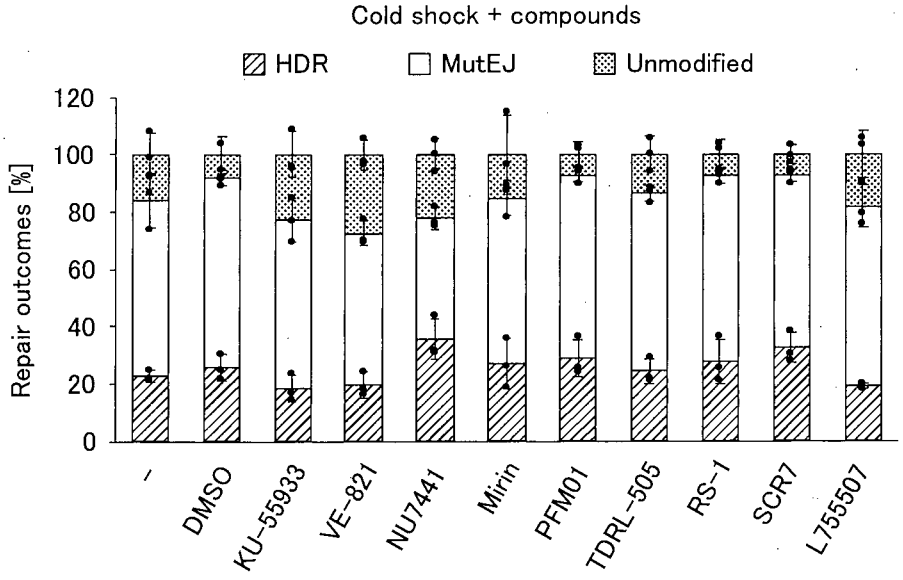

FIG. 3C

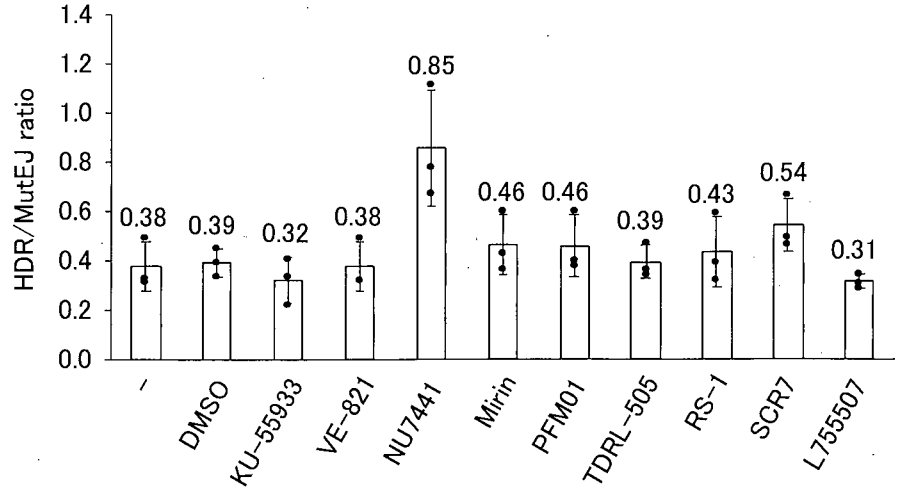

FIG. 3D

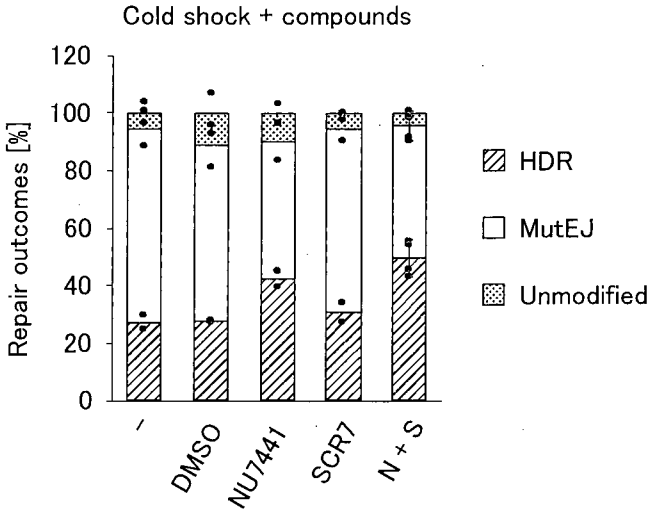

FIG. 3E

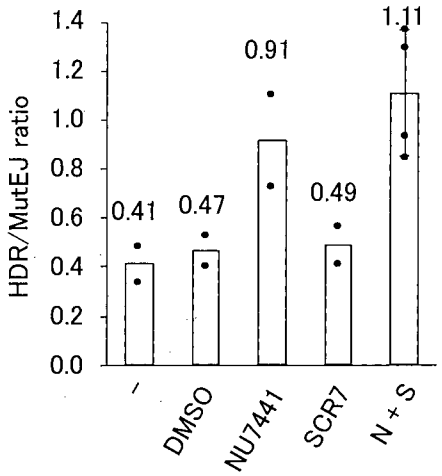

FIG. 3F

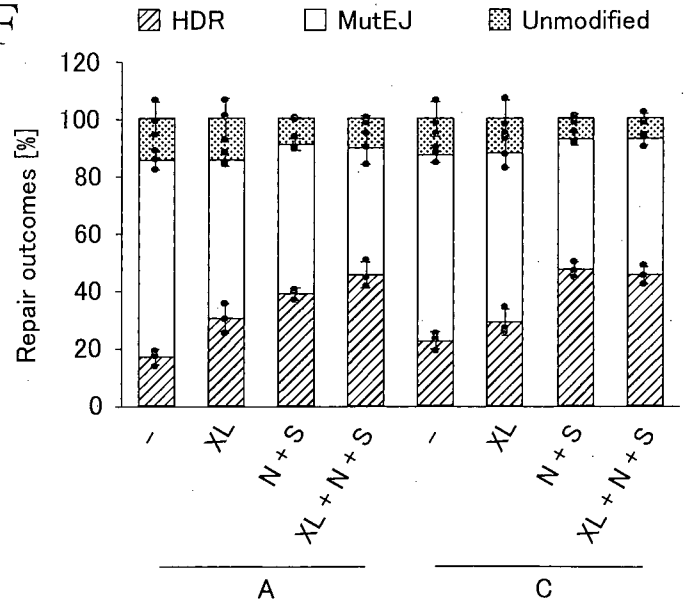

FIG. 3G

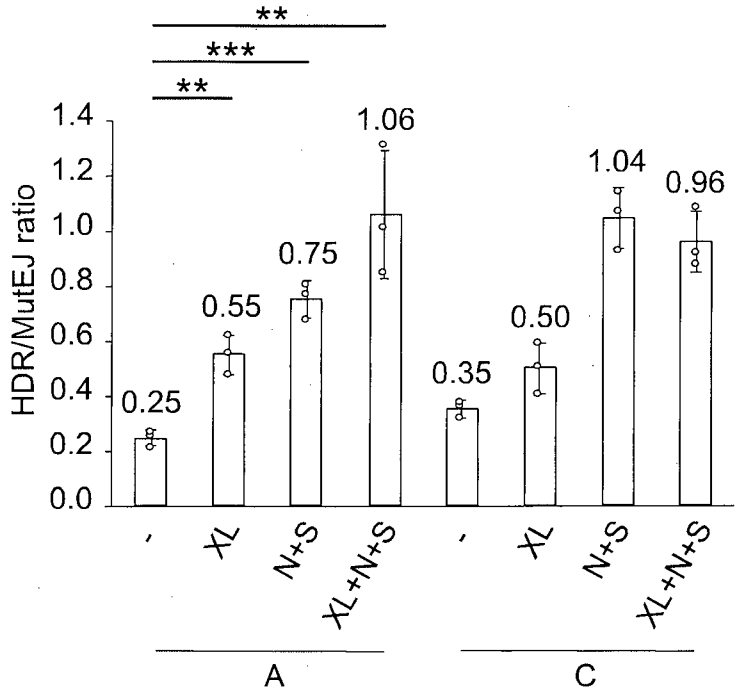
**
***
**
HDR/MutEJ ratio
1.4
1.2
1.0
0.8
0.6
0.4
0.2
0.0
0.25
0.55
0.75
1.06
0.35
0.50
1.04
0.96
-
XL
N+S
XL+N+S
-
XL
N+S
XL+N+S
A
C

FIG. 3H

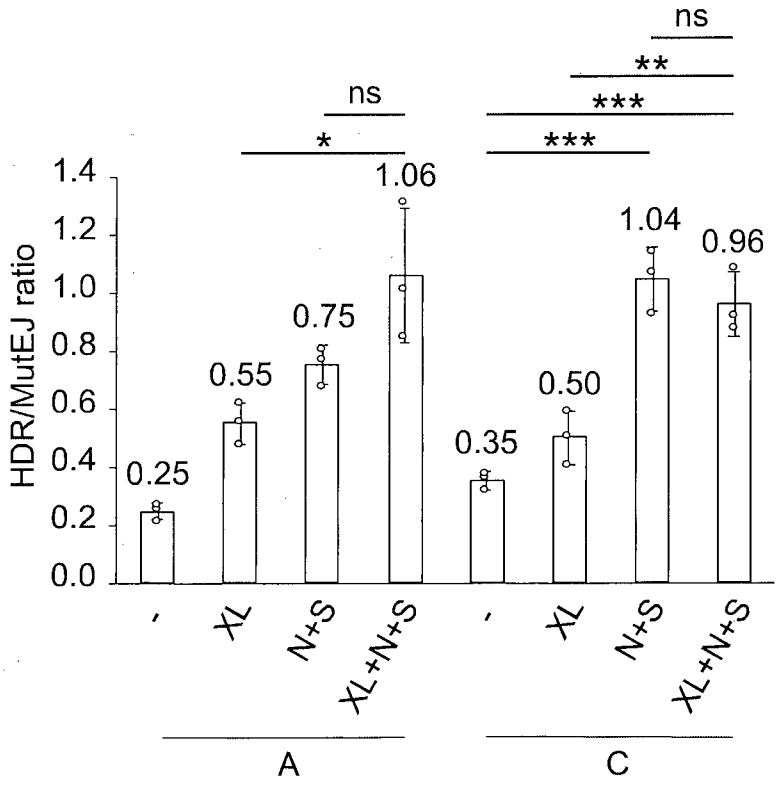
ns
**
***
***
ns
*
HDR/MutEJ ratio
1.4
1.2
1.0
0.8
0.6
0.4
0.2
0.0
0.25
0.55
0.75
1.06
0.35
0.50
1.04
0.96
-
XL
N+S
XL+N+S
-
XL
N+S
XL+N+S
A
C

FIG. 3I

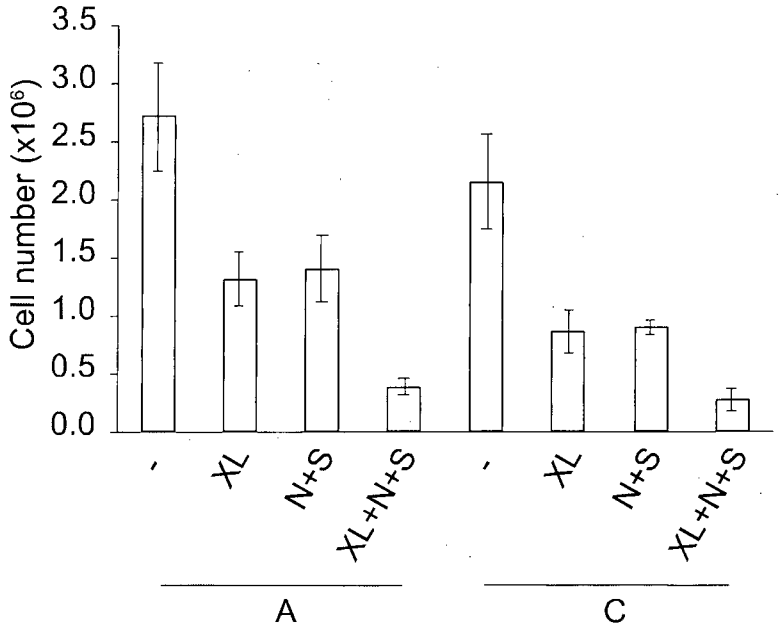
Cell number (x10^6)
3.5
3.0
2.5
2.0
1.5
1.0
0.5
0.0
-
XL
N+S
XL+N+S
-
XL
N+S
XL+N+S
A
C

FIG. 3J

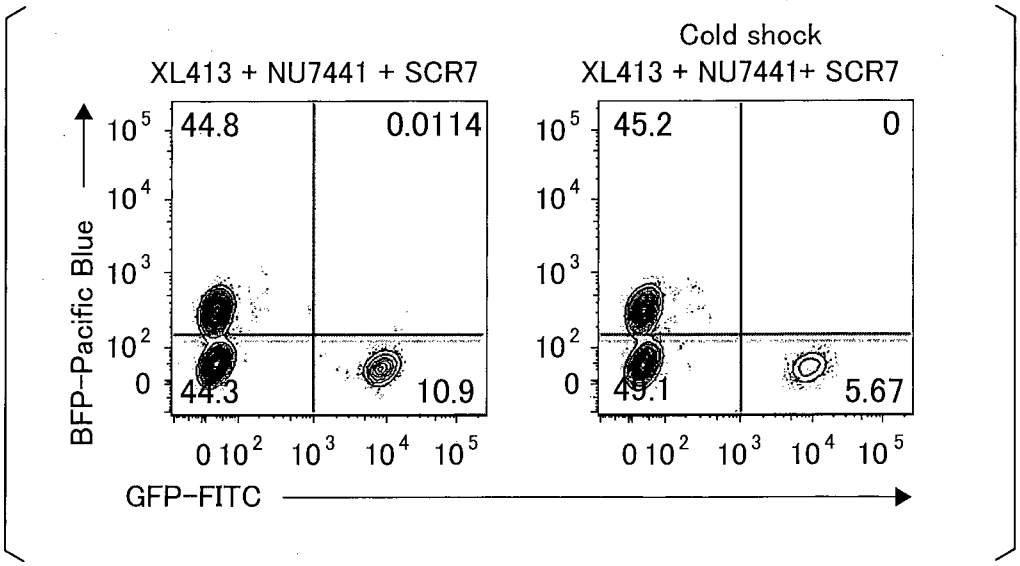
XL413 + NU7441 + SCR7
Cold shock
XL413 + NU7441+ SCR7
BFP-Pacific Blue
GFP-FITC
44.8
0.0114
44.3
10.9
45.2
0
49.1
5.67

FIG. 4A

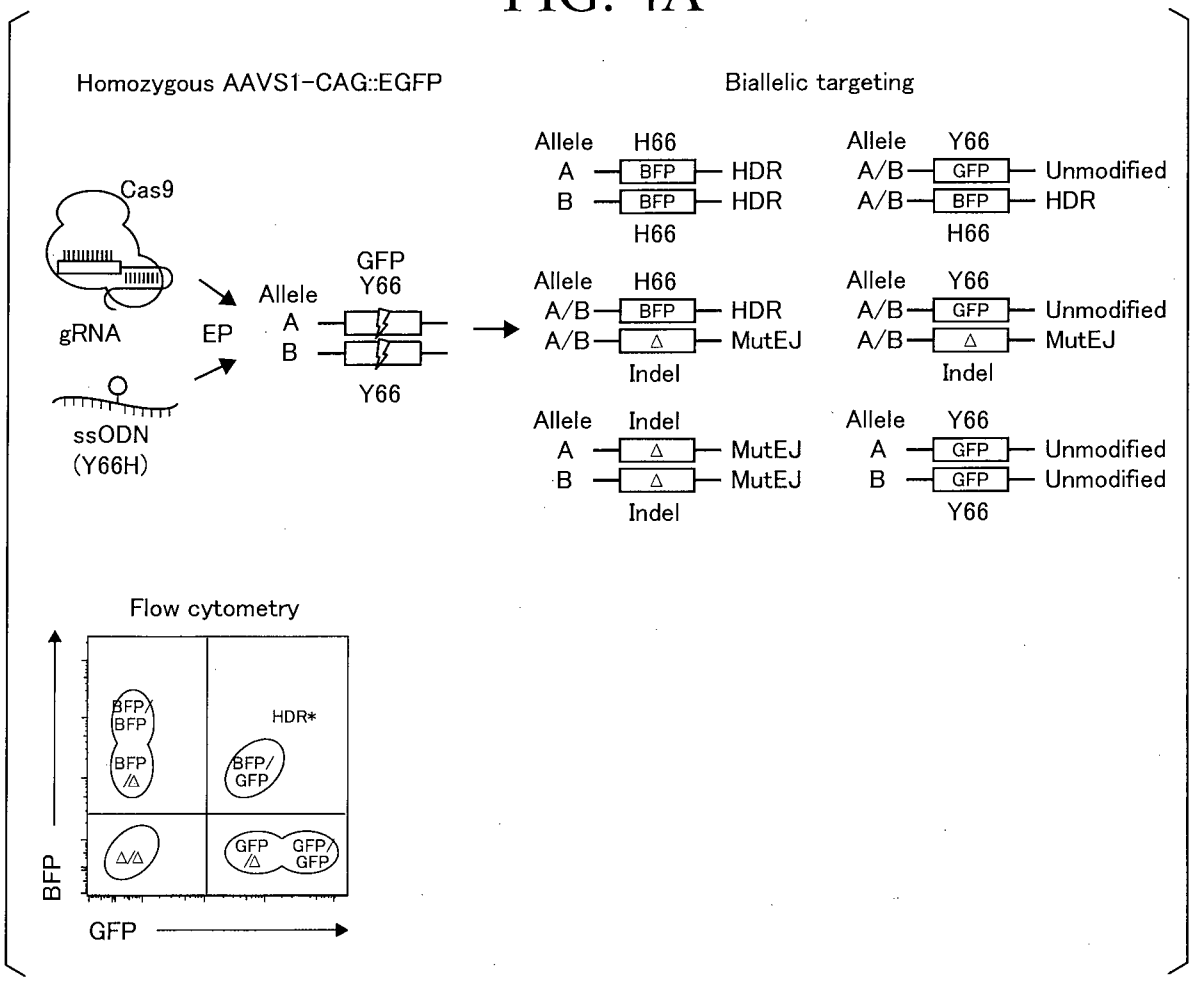
Homozygous AAVS1-CAG::EGFP
Biallelic targeting
Cas9
gRNA
EP
ssODN
(Y66H)
Allele
A
B
GFP
Y66
Y66
Allele H66
A BFP HDR
B BFP HDR
H66
Allele Y66
A/B GFP Unmodified
A/B BFP HDR
H66
Allele H66
A/B BFP HDR
A/B Δ MutEJ
Indel
Allele Y66
A/B GFP Unmodified
A/B Δ MutEJ
Indel
Allele Indel
A Δ MutEJ
B Δ MutEJ
Indel
Allele Y66
A GFP Unmodified
B GFP Unmodified
Y66
Flow cytometry
BFP
GFP
BFP/BFP
BFP/Δ
HDR*
BFP/GFP
Δ/Δ
GFP/Δ
GFP/GFP

FIG. 4B

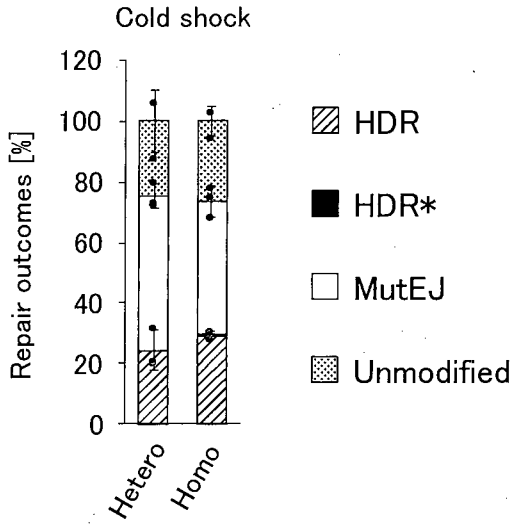

FIG. 4C

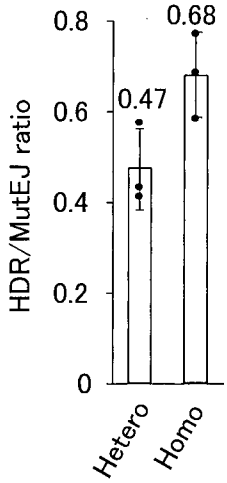

FIG. 4D

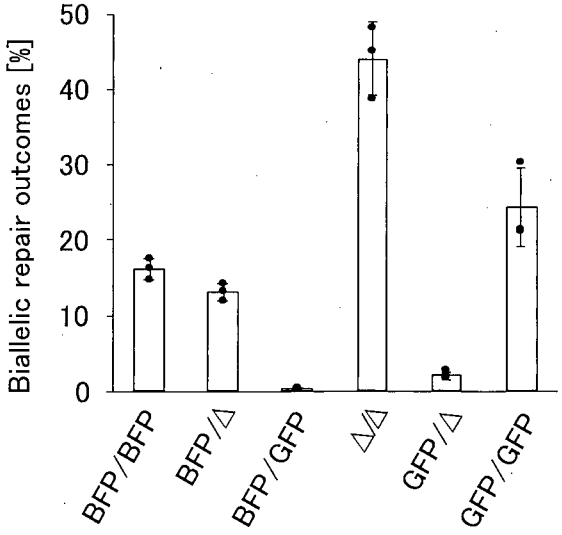

FIG. 4E

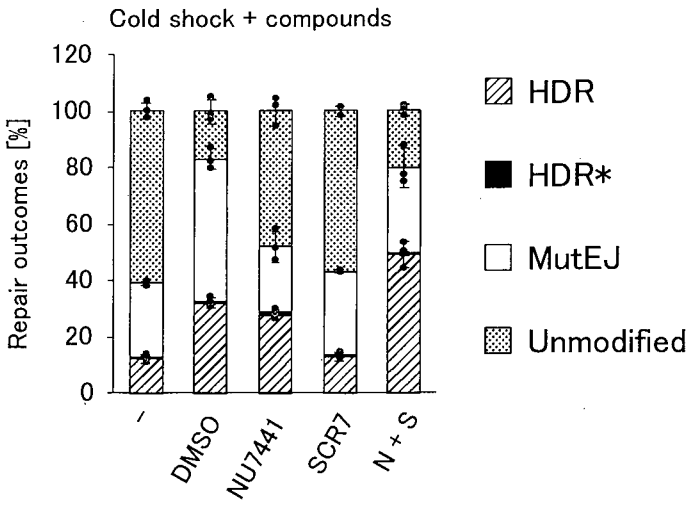

FIG. 4F

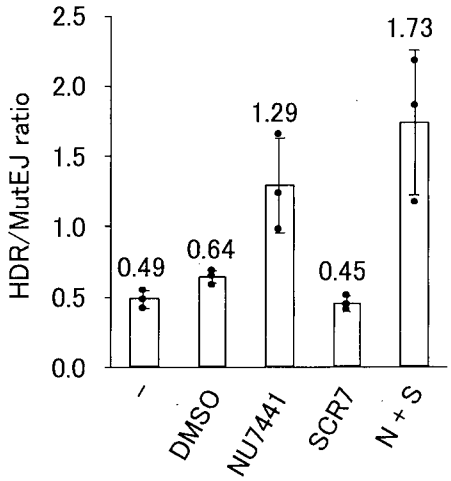

FIG. 4G

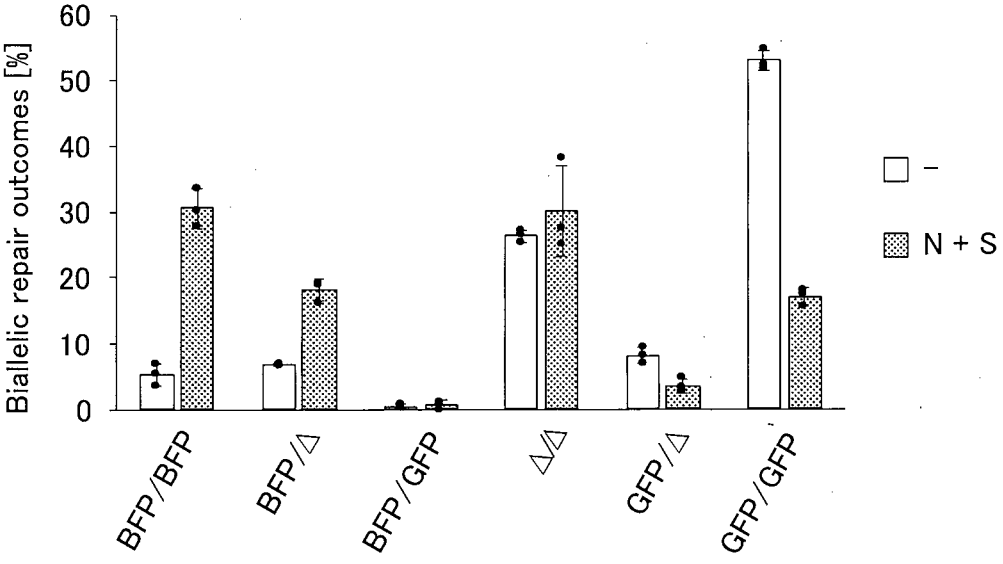

FIG. 5A

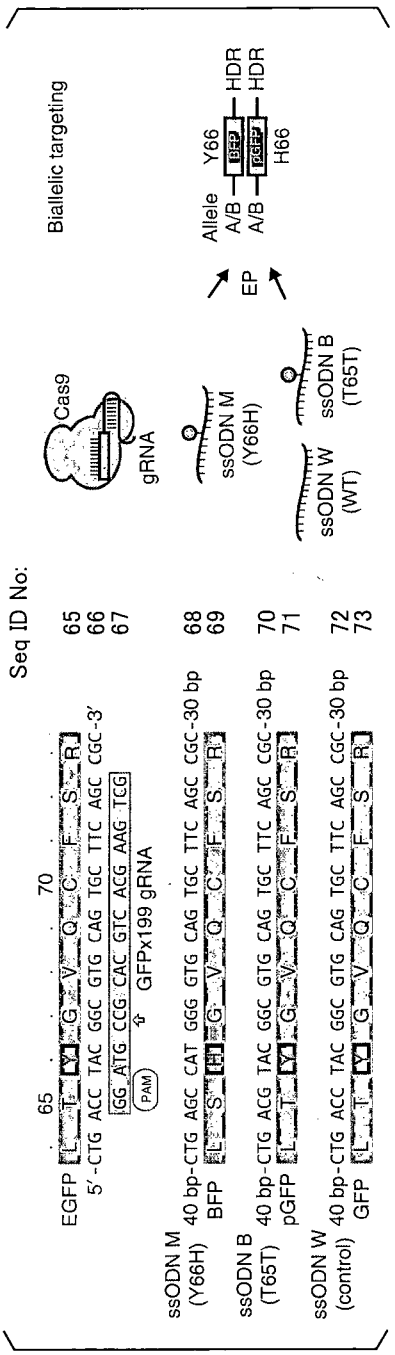
Seq ID No:
65
70
EGFP L T Y G V Q C F S R
5'-CTG ACC TAC GGC GTG CAG TGC TTC AGC CGC-3'
GG ATG CCG CAC GTC ACG AAG TCG
PAM
GFPx199 gRNA
ssODN M (Y66H) 40 bp-CTG AGC CAT GGG GTG CAG TGC TTC AGC CGC-30 bp 68
BFP L S H G V Q C F S R 69
ssODN B (T65T) 40 bp-CTG ACG TAC GGC GTG CAG TGC TTC AGC CGC-30 bp 70
pGFP L T Y G V Q C F S R 71
ssODN W (control) 40 bp-CTG ACC TAC GGC GTG CAG TGC TTC AGC CGC-30 bp 72
GFP L T Y G V Q C F S R 73
Cas9
gRNA
ssODN M (Y66H)
ssODN B (T65T)
ssODN W (WT)
EP
Biallelic targeting
Allele
A/B
A/B
Y66
H66
BFP
pGFP
HDR
HDR

FIG. 5B

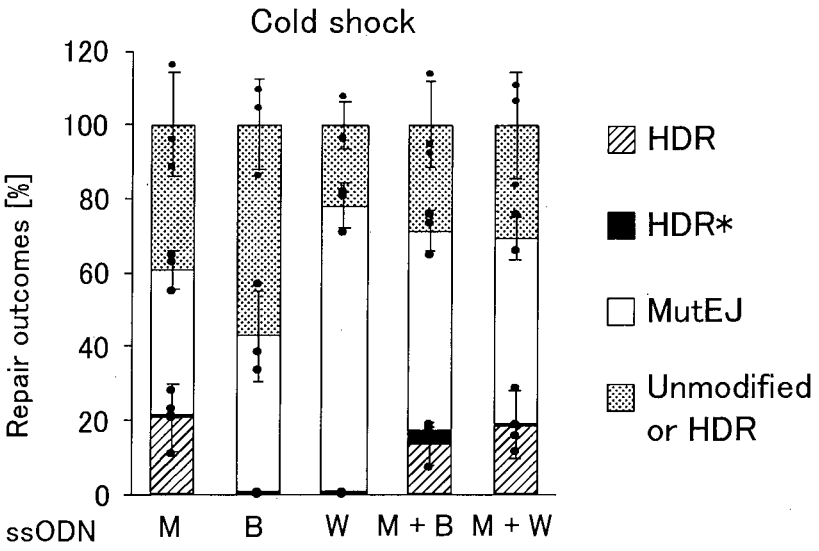
Cold shock
120
100
80
60
40
20
0
Repair outcomes [%]
ssODN
M
B
W
M + B
M + W
HDR
HDR*
MutEJ
Unmodified or HDR

FIG. 5C

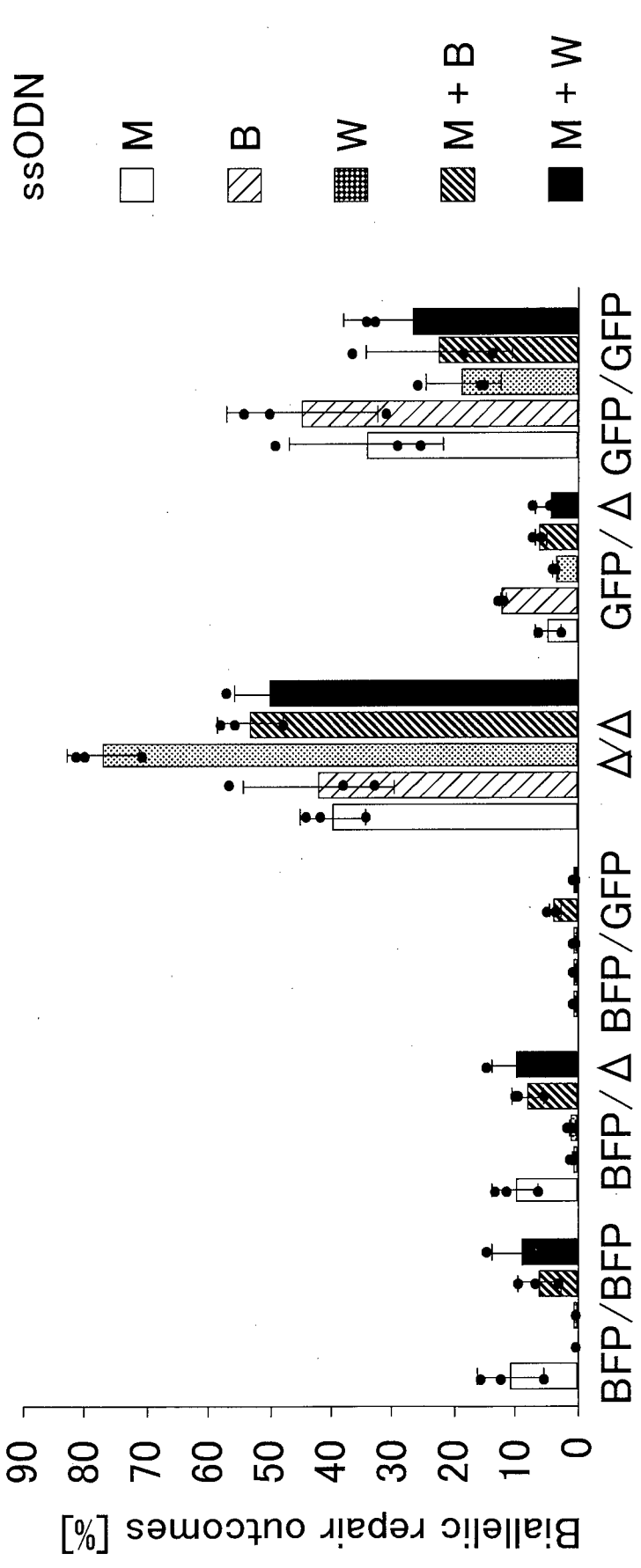
ssODN
M
B
W
M + B
M + W
Biallelic repair outcomes [%]
0
10
20
30
40
50
60
70
80
90
BFP/BFP
BFP/Δ BFP/GFP
Δ/Δ
GFP/Δ GFP/GFP

FIG. 5D

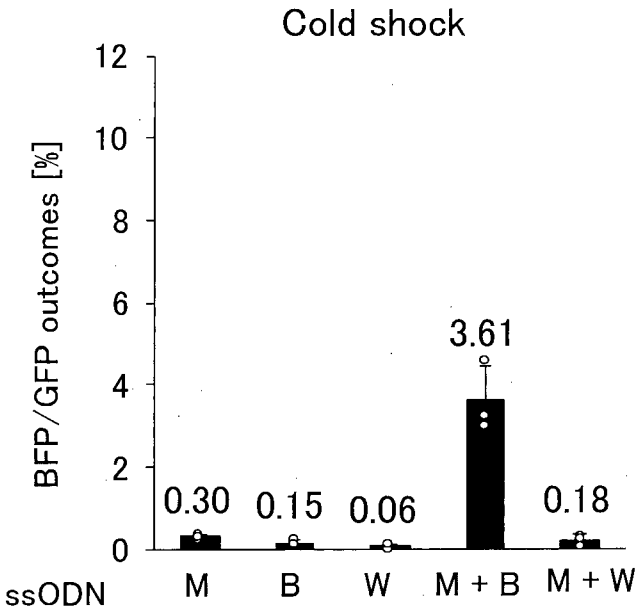
Cold shock
BFP/GFP outcomes [%]
12
10
8
6
4
2
0
0.30
0.15
0.06
3.61
0.18
ssODN
M
B
W
M + B
M + W

FIG. 5E

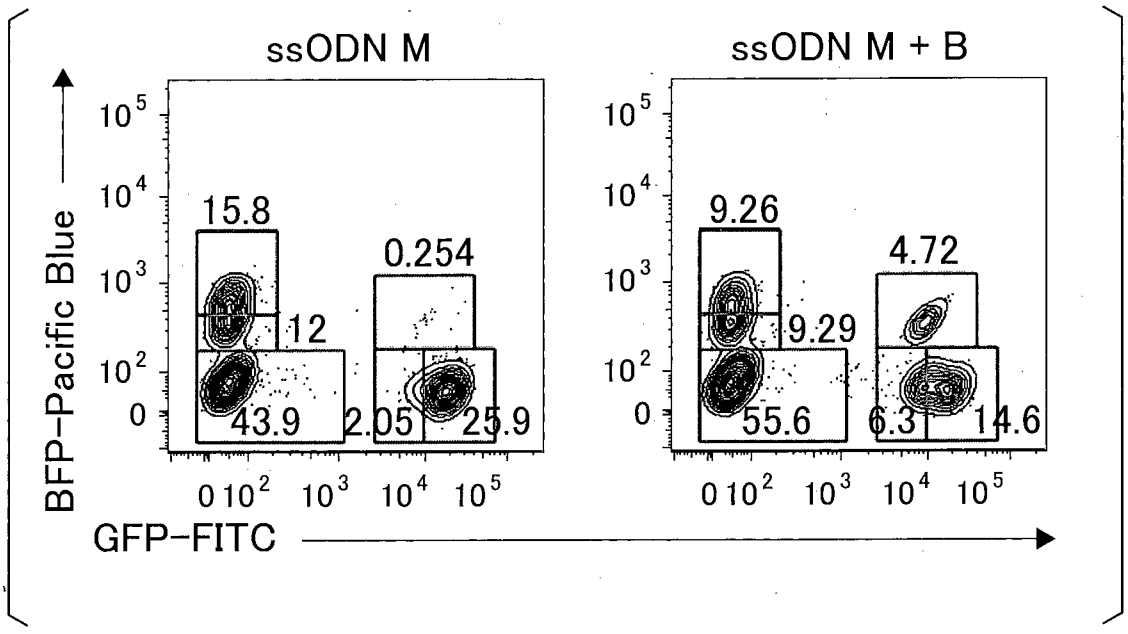
ssODN M
ssODN M + B
BFP-Pacific Blue
GFP-FITC
15.8
12
43.9
0.254
2.05
25.9
9.26
9.29
55.6
4.72
6.3
14.6

FIG. 6A

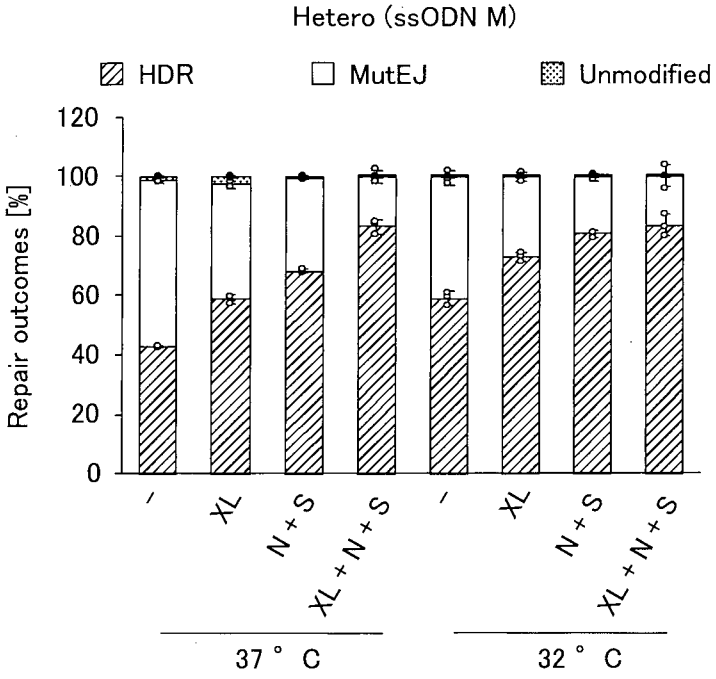
Hetero (ssODN M)
HDR
MutEJ
Unmodified
Repair outcomes [%]
120
100
80
60
40
20
0
-
XL
N+S
XL+N+S
-
XL
N+S
XL+N+S
37° C
32° C

FIG. 6B

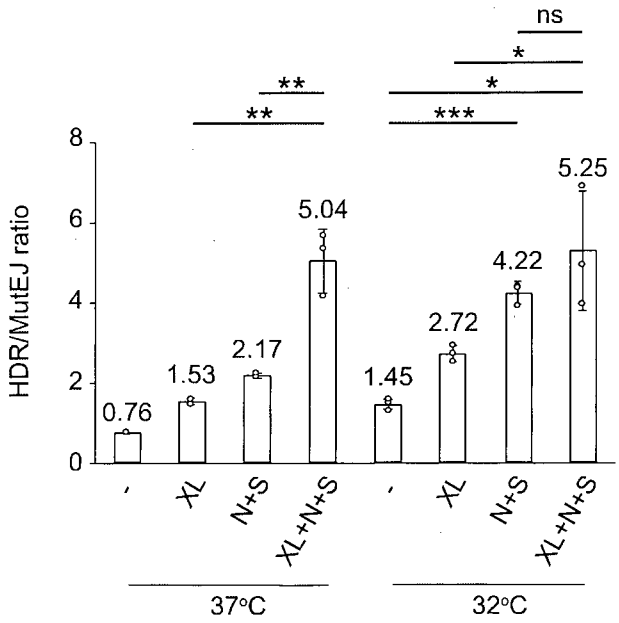
ns
*
*
***
**
**
HDR/MutEJ ratio
8
6
4
2
0
0.76
1.53
2.17
5.04
1.45
2.72
4.22
5.25
-
XL
N+S
XL+N+S
-
XL
N+S
XL+N+S
37°C
32°C

FIG. 6C

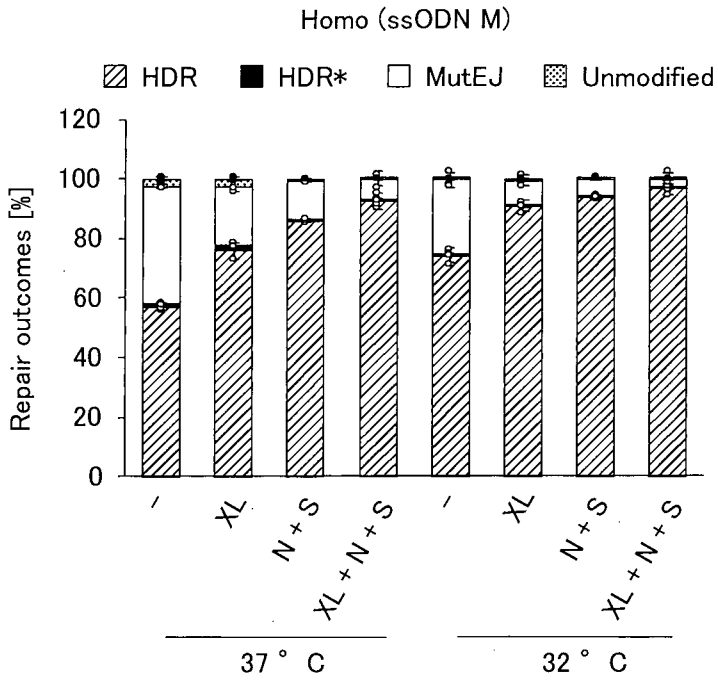
Homo (ssODN M)
HDR
HDR*
MutEJ
Unmodified
Repair outcomes [%]
120
100
80
60
40
20
0
-
XL
N+S
XL+N+S
-
XL
N+S
XL+N+S
37 ° C
32 ° C

FIG. 6D

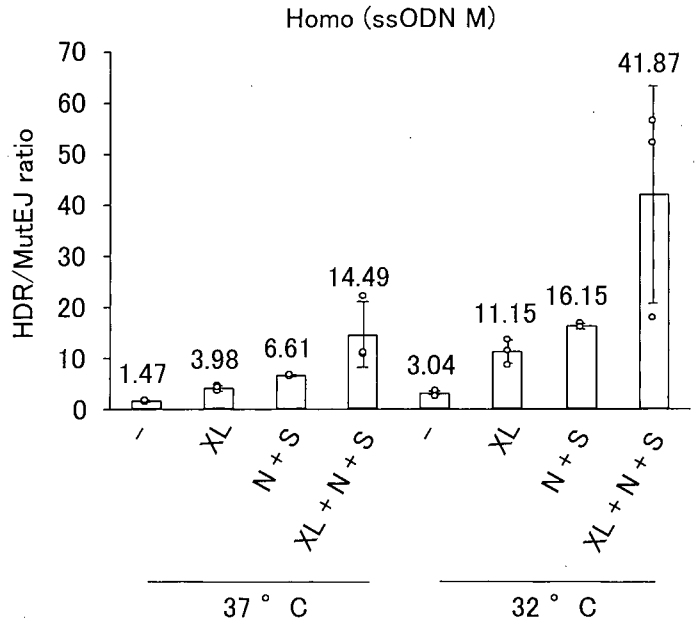
Homo (ssODN M)
HDR/MutEJ ratio
70
60
50
40
30
20
10
0
1.47
3.98
6.61
14.49
3.04
11.15
16.15
41.87
-
XL
N+S
XL+N+S
-
XL
N+S
XL+N+S
37 ° C
32 ° C

FIG. 6E

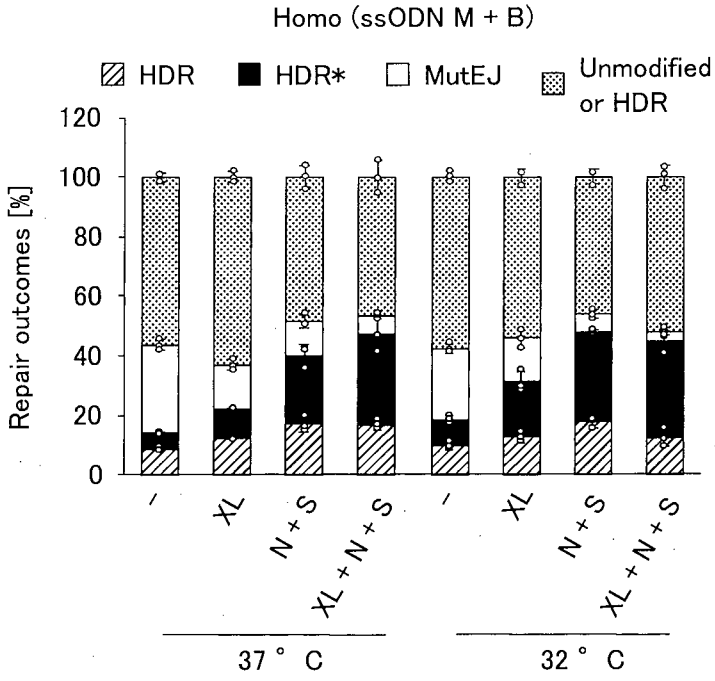
Homo (ssODN M + B)
HDR
HDR*
MutEJ
Unmodified or HDR
Repair outcomes [%]
120
100
80
60
40
20
0
-
XL
N+S
XL+N+S
-
XL
N+S
XL+N+S
37° C
32° C

FIG. 6F

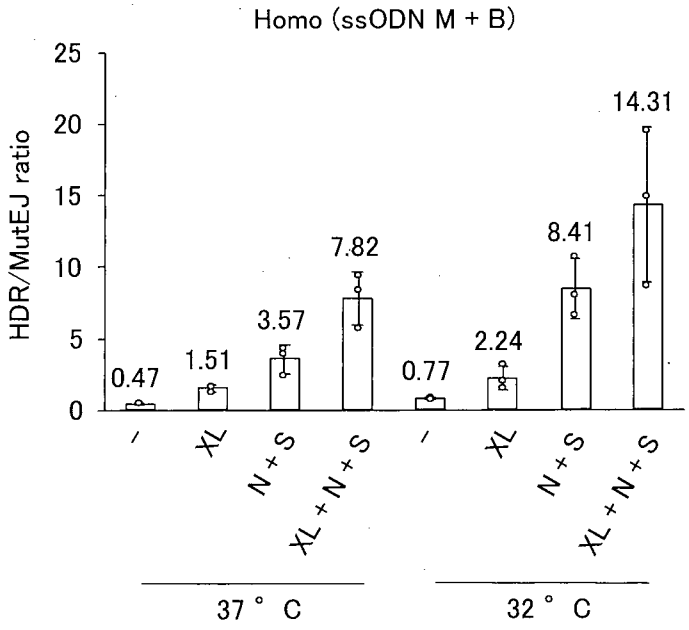
Homo (ssODN M + B)
HDR/MutEJ ratio
25
20
15
10
5
0
0.47
1.51
3.57
7.82
0.77
2.24
8.41
14.31
-
XL
N+S
XL+N+S
-
XL
N+S
XL+N+S
37° C
32° C

FIG. 6G

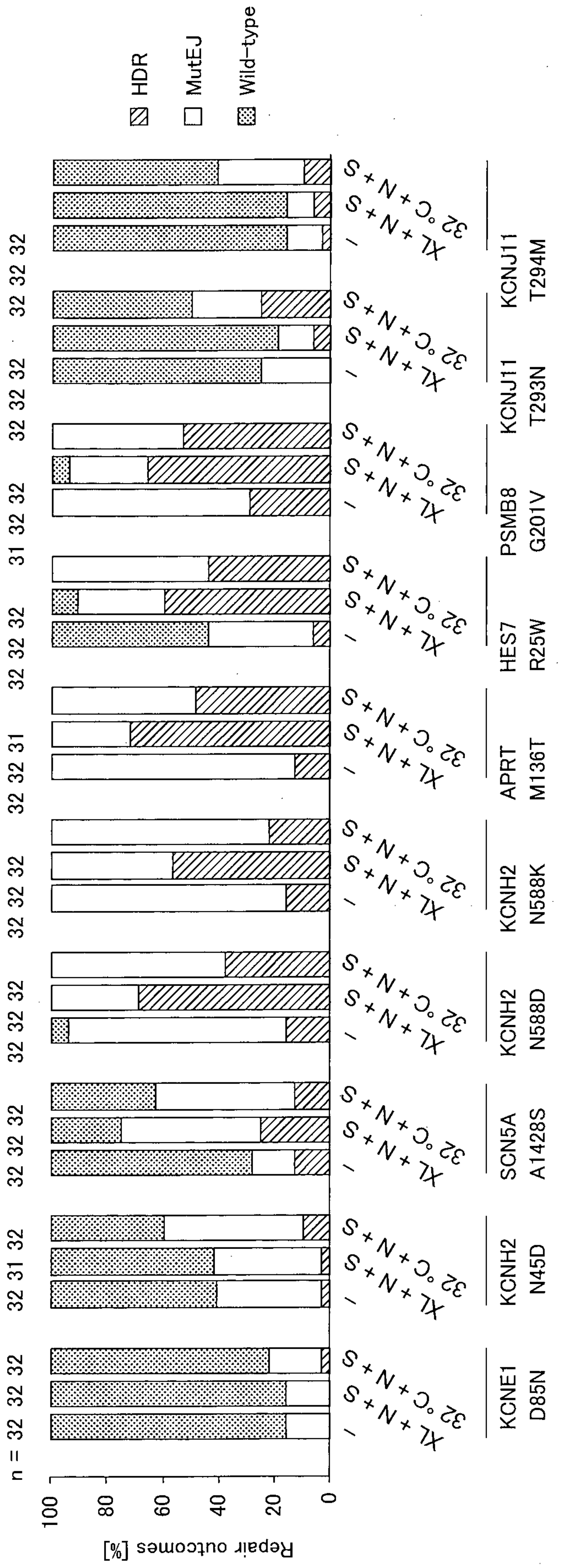
HDR
MutEJ
Wild-type
Repair outcomes [%]
100
80
60
40
20
0
n = 32 32 32
32 31 32
32 32 32
32 32 32
32 32 32
32 32 31
32 32 32
31 32 32
32 32 32
32 32 32
/
XL + N + S
32 °C + N + S
KCNE1 D85N
KCNH2 N45D
SCN5A A1428S
KCNH2 N588D
KCNH2 N588K
APRT M136T
HES7 R25W
PSMB8 G201V
KCNJ11 T293N
KCNJ11 T294M

FIG. 6H

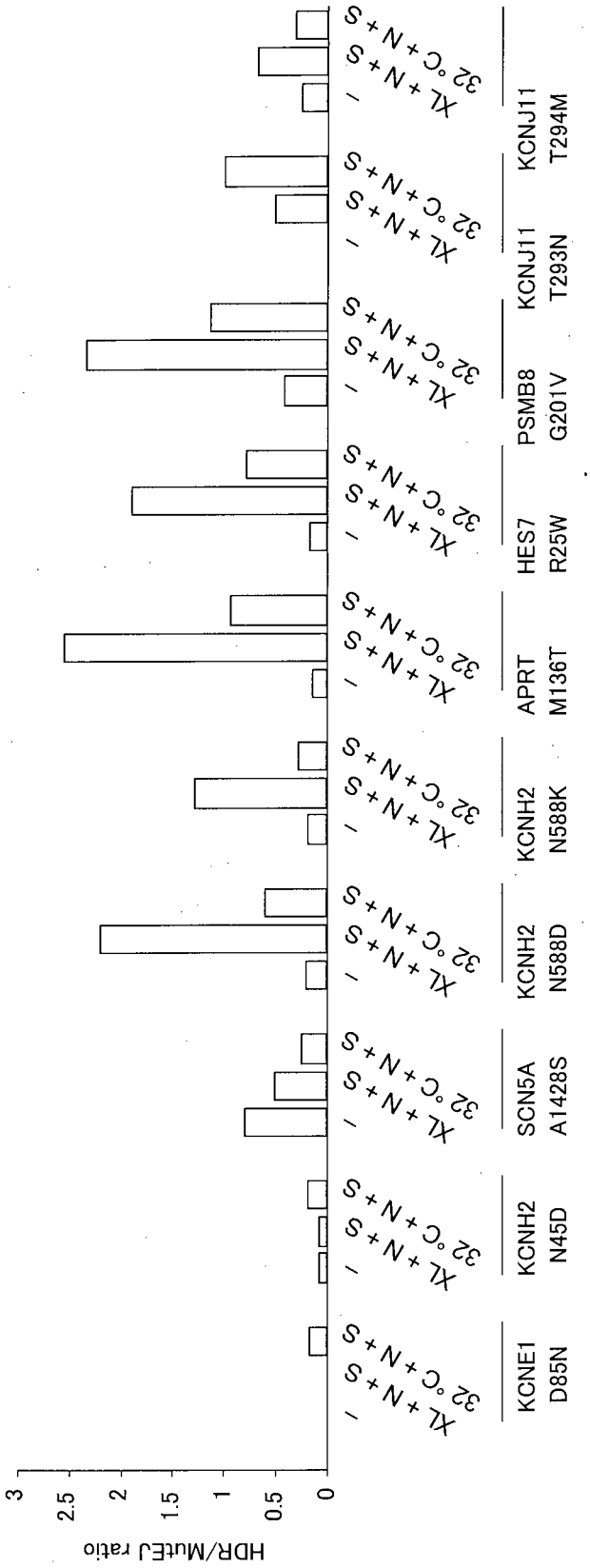
HDR/MutEJ ratio
3
2.5
2
1.5
1
0.5
0
-/-
XL+N+S
32°C+N+S
KCNE1 D85N
KCNH2 N45D
SCN5A A1428S
KCNH2 N588D
KCNH2 N588K
APRT M136T
HES7 R25W
PSMB8 G201V
KCNJ11 T293N
KCNJ11 T294M

FIG. 7

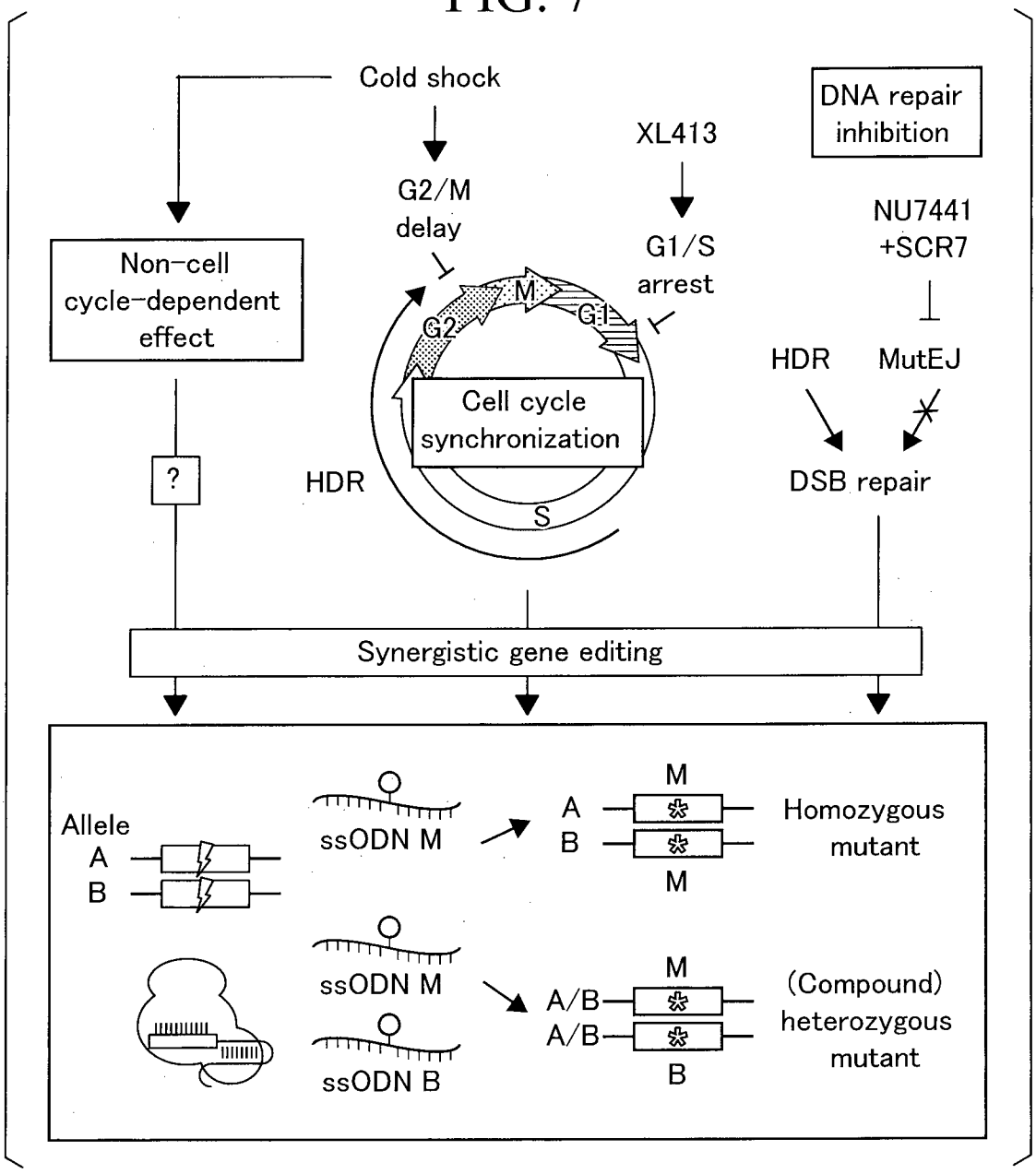
Cold shock
DNA repair inhibition
XL413
G2/M delay
G1/S arrest
NU7441 +SCR7
Non-cell cycle-dependent effect
M
G1
G2
Cell cycle synchronization
HDR
MutEJ
?
HDR
S
DSB repair
Synergistic gene editing
Allele
A
B
ssODN M
M
A
B
M
Homozygous mutant
ssODN M
ssODN B
M
A/B
A/B
B
(Compound) heterozygous mutant

FIG. 8A

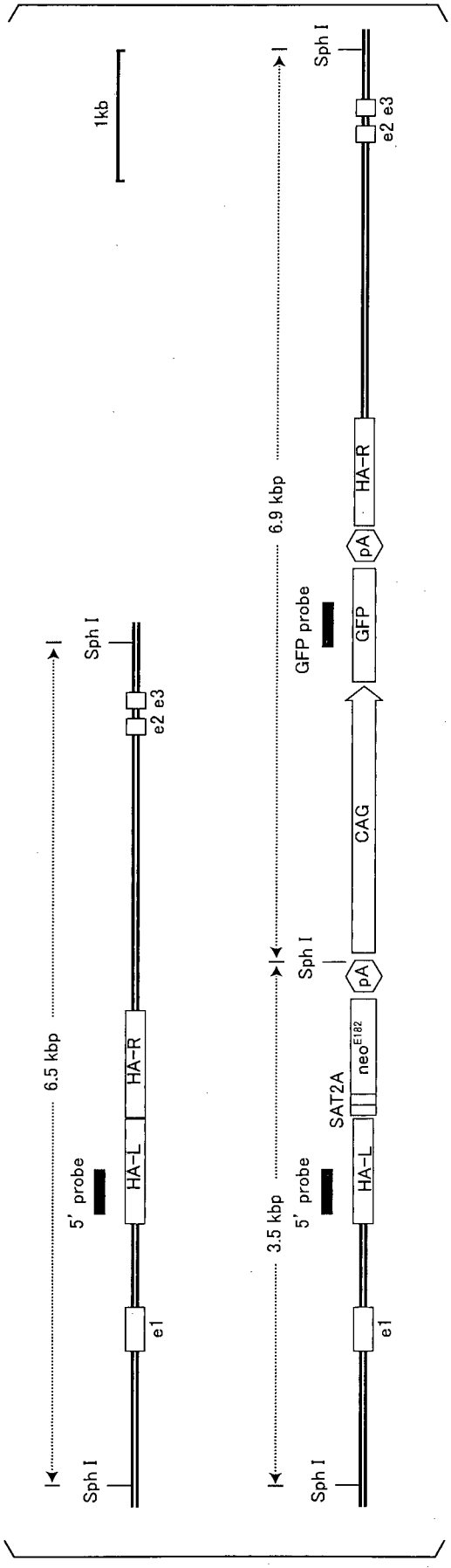
1kb
Sph I
e2 e3
HA-R
pA
GFP
GFP probe
CAG
pA
SAT2A
neo^E182
HA-L
5' probe
e1
Sph I
6.9 kbp
3.5 kbp
6.5 kbp
Sph I
e2 e3
HA-R
HA-L
5' probe
e1
Sph I

FIG. 8B

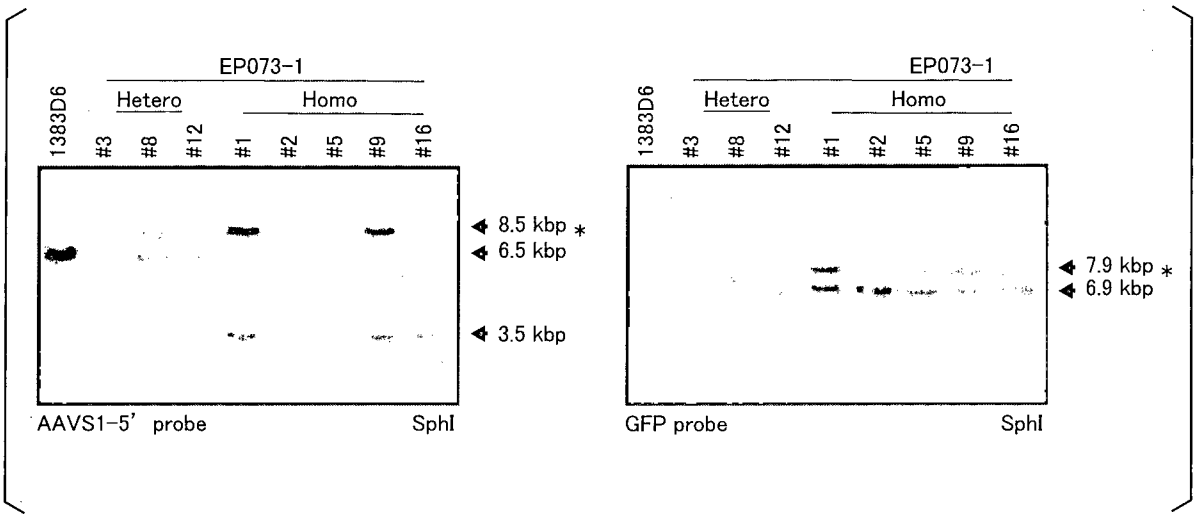
EP073-1
Hetero
Homo
1383D6
#3
#8
#12
#1
#2
#5
#9
#16
8.5 kbp *
6.5 kbp
3.5 kbp
AAVS1-5' probe
SphI
EP073-1
Hetero
Homo
1383D6
#3
#8
#12
#1
#2
#5
#9
#16
7.9 kbp *
6.9 kbp
GFP probe
SphI

FIG. 8C

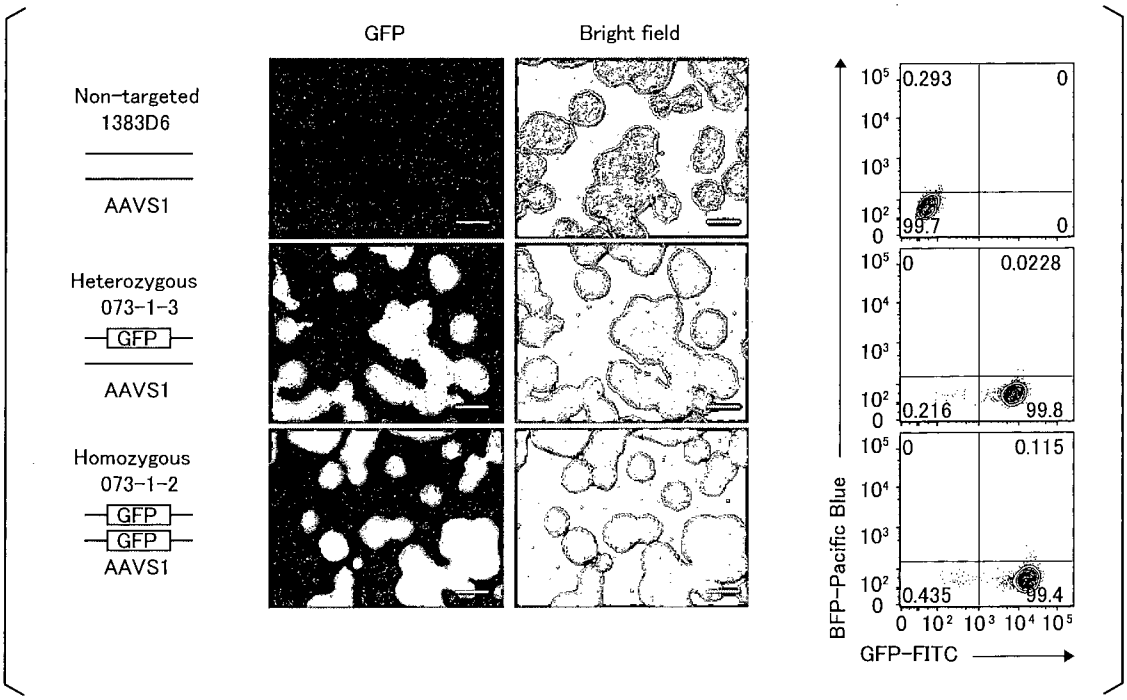
GFP
Bright field
Non-targeted
1383D6
AAVS1
Heterozygous
073-1-3
GFP
AAVS1
Homozygous
073-1-2
GFP
GFP
AAVS1
0.293
0
99.7
0
0
0.0228
0.216
99.8
0
0.115
0.435
99.4
BFP-Pacific Blue
GFP-FITC

FIG. 9A

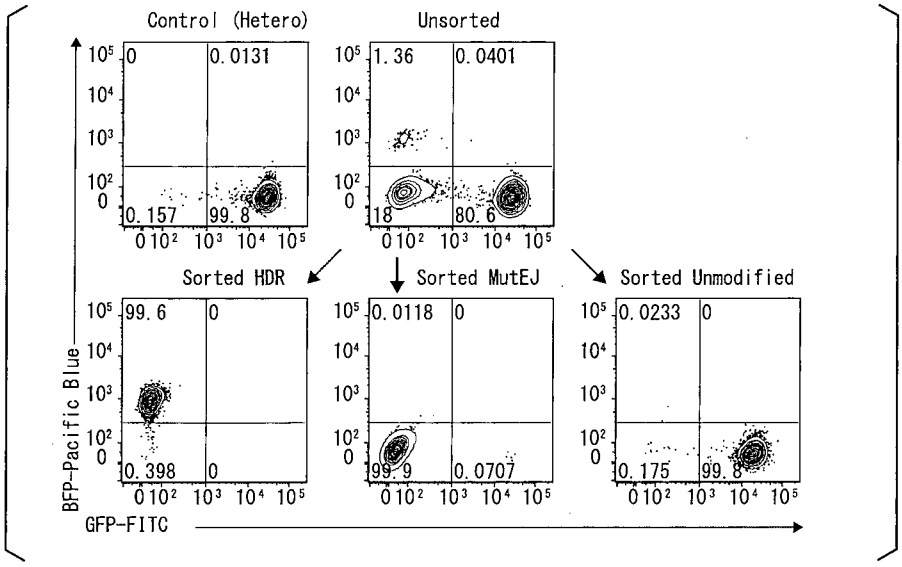
Control (Hetero)
Unsorted
0
0.0131
0.157
99.8
1.36
0.0401
18
80.6
Sorted HDR
Sorted MutEJ
Sorted Unmodified
99.6
0
0.398
0
0.0118
0
99.9
0.0707
0.0233
0
0.175
99.8
BFP-Pacific Blue
GFP-FITC

FIG. 9B

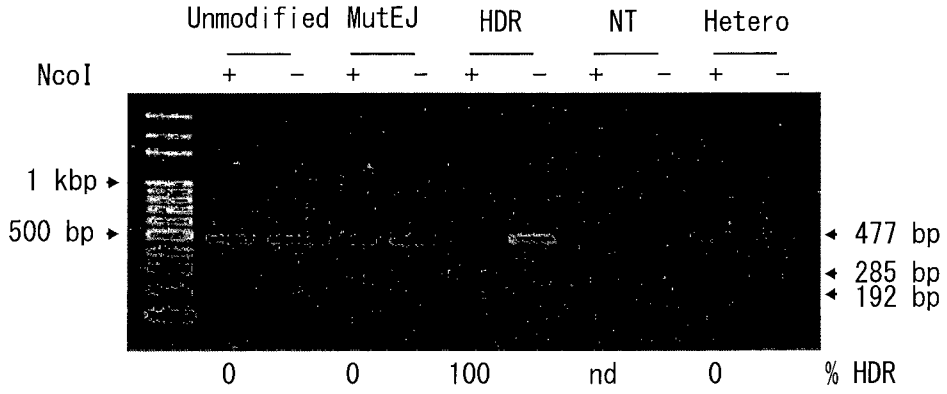
Unmodified
MutEJ
HDR
NT
Hetero
NcoI
+ − + − + − + − + −
1 kbp
500 bp
477 bp
285 bp
192 bp
0 0 100 nd 0 % HDR

FIG. 9C

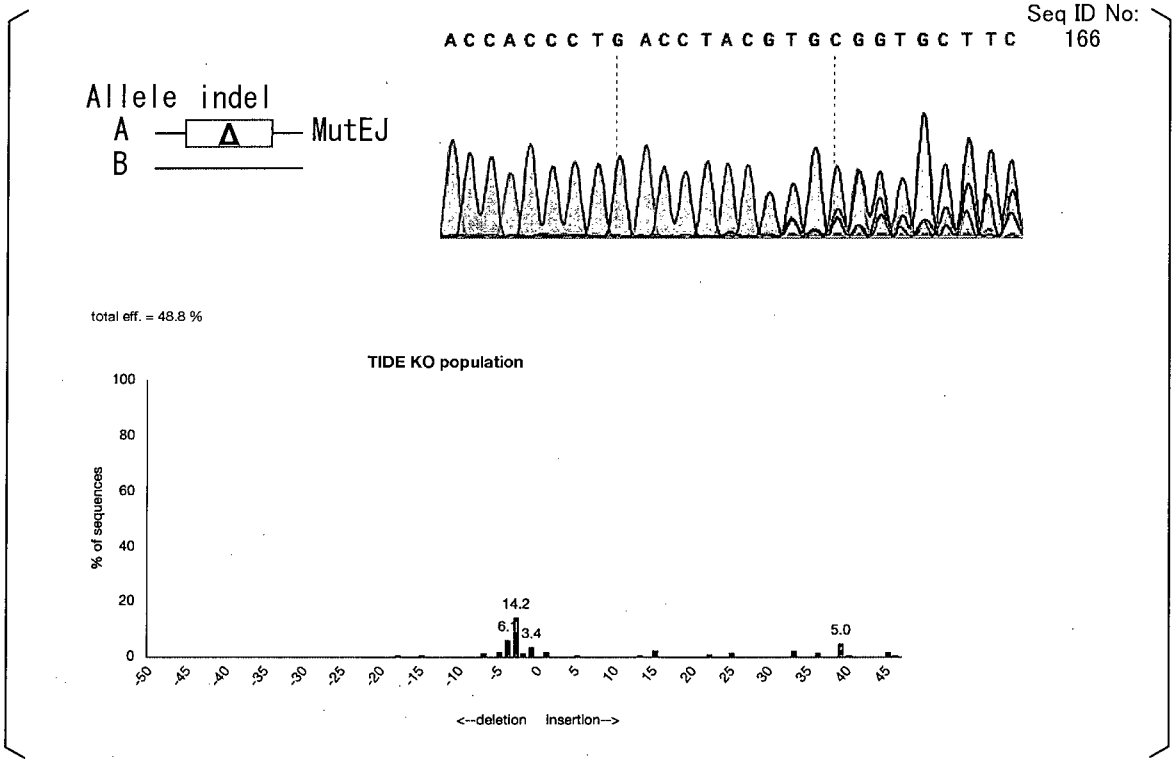
Seq ID No: 166
A C C A C C C T G A C C T A C G T G C G G T G C T T C
Allele indel
A
B
MutEJ
total eff. = 48.8 %
TIDE KO population
% of sequences
100
80
60
40
20
0
14.2
6.1
3.4
5.0
-50 -45 -40 -35 -30 -25 -20 -15 -10 -5 0 5 10 15 20 25 30 35 40 45
<--deletion insertion-->

FIG. 10A

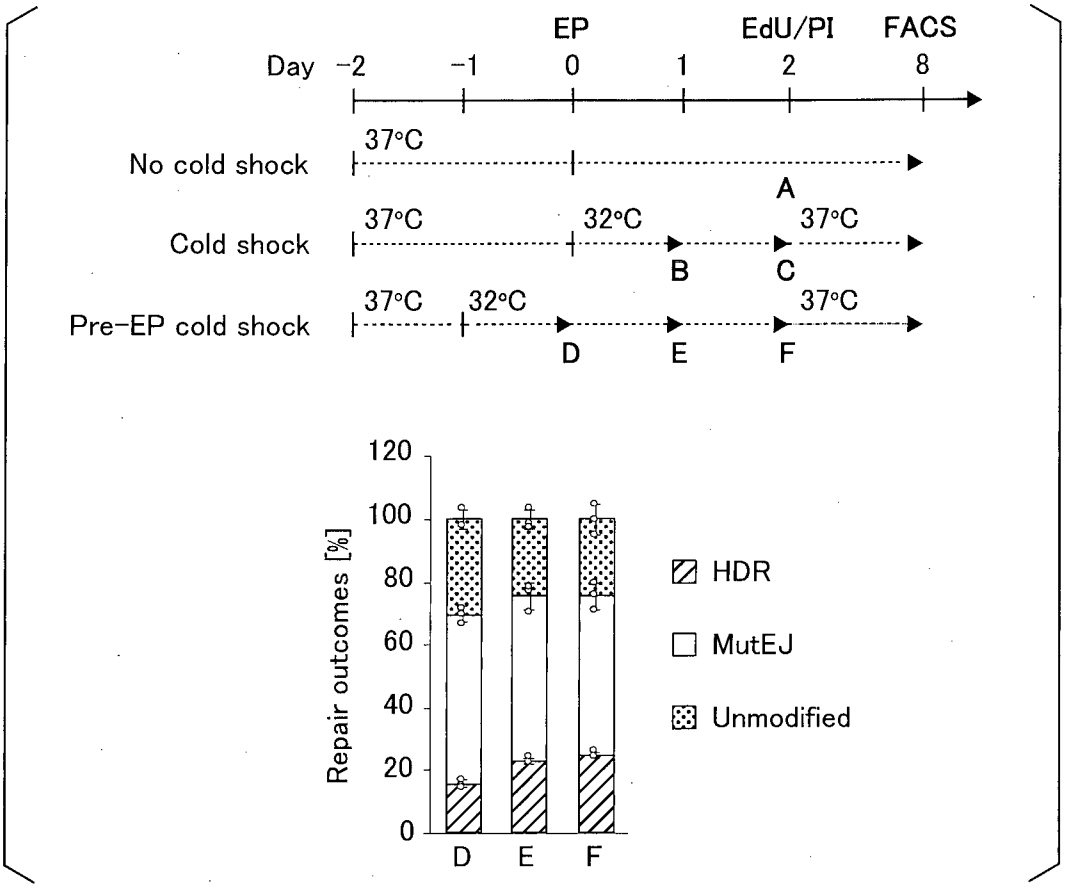

FIG. 10B

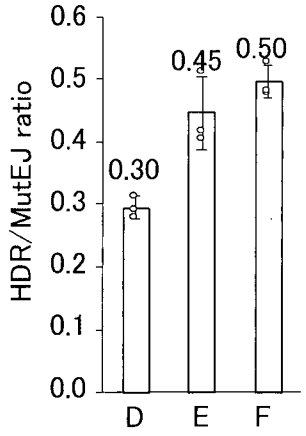

FIG. 10C

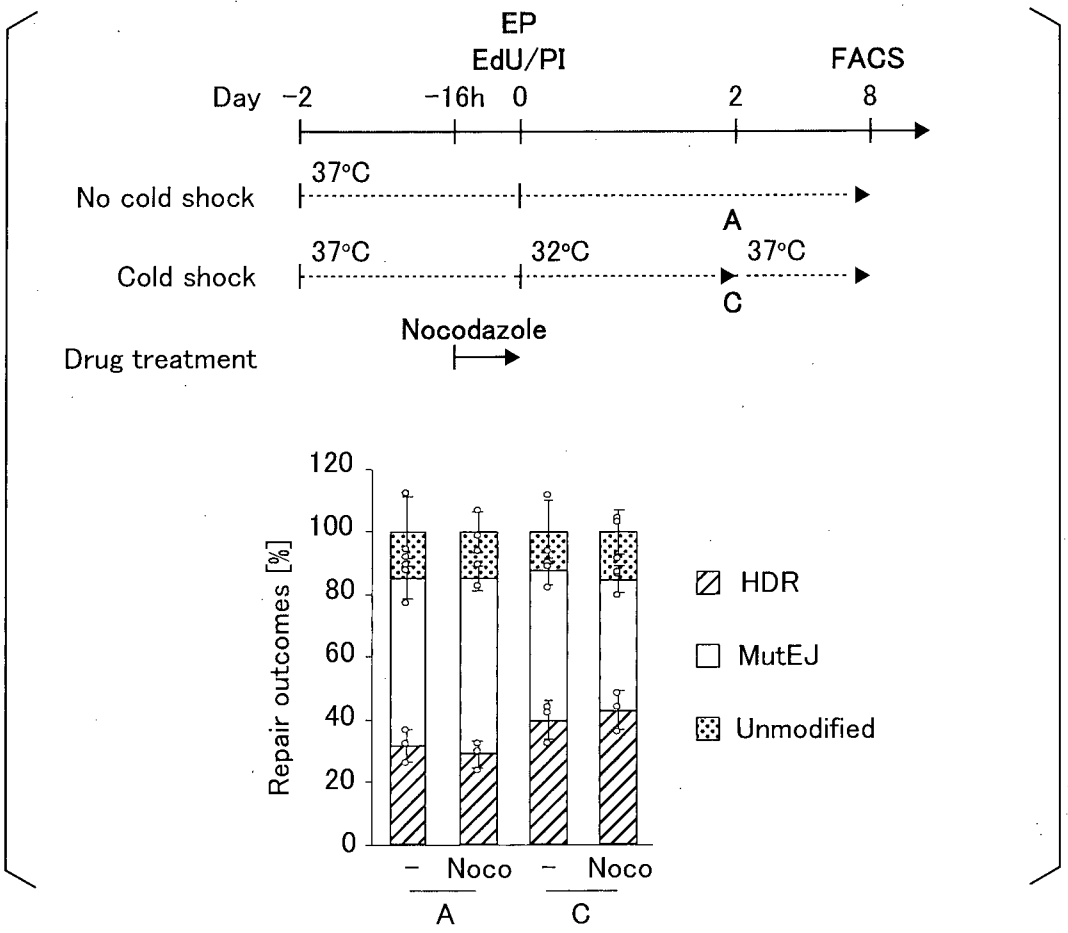

FIG. 10D

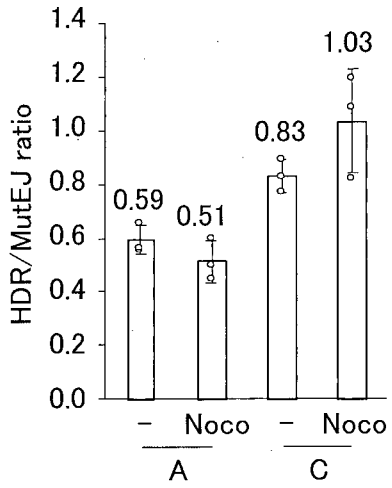

FIG. 10E

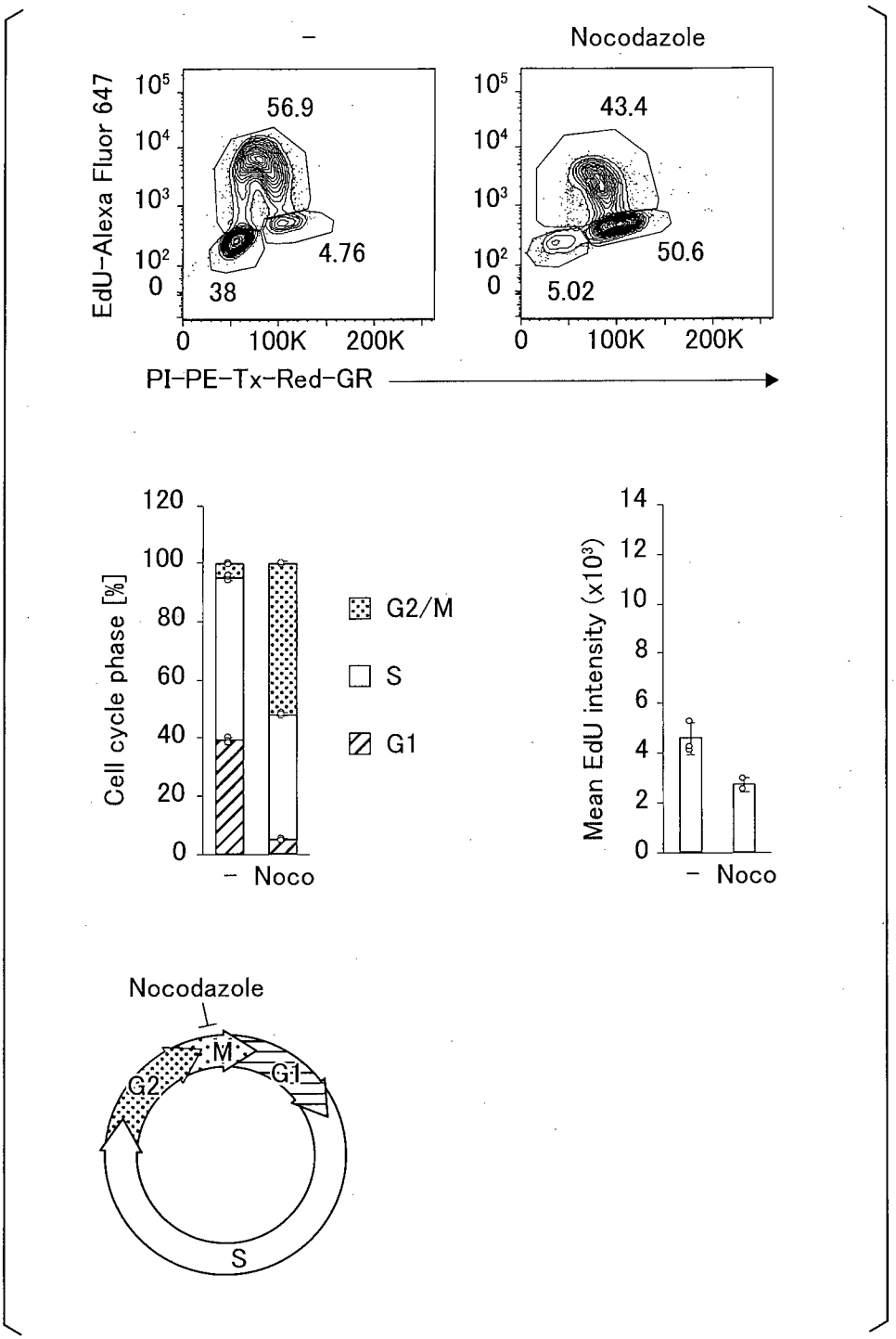
−
Nocodazole
EdU-Alexa Fluor 647
PI-PE-Tx-Red-GR
56.9
4.76
38
43.4
50.6
5.02
Cell cycle phase [%]
G2/M
S
G1
− Noco
Mean EdU intensity (x10³)
Nocodazole
M
G1
G2
S

FIG. 10F

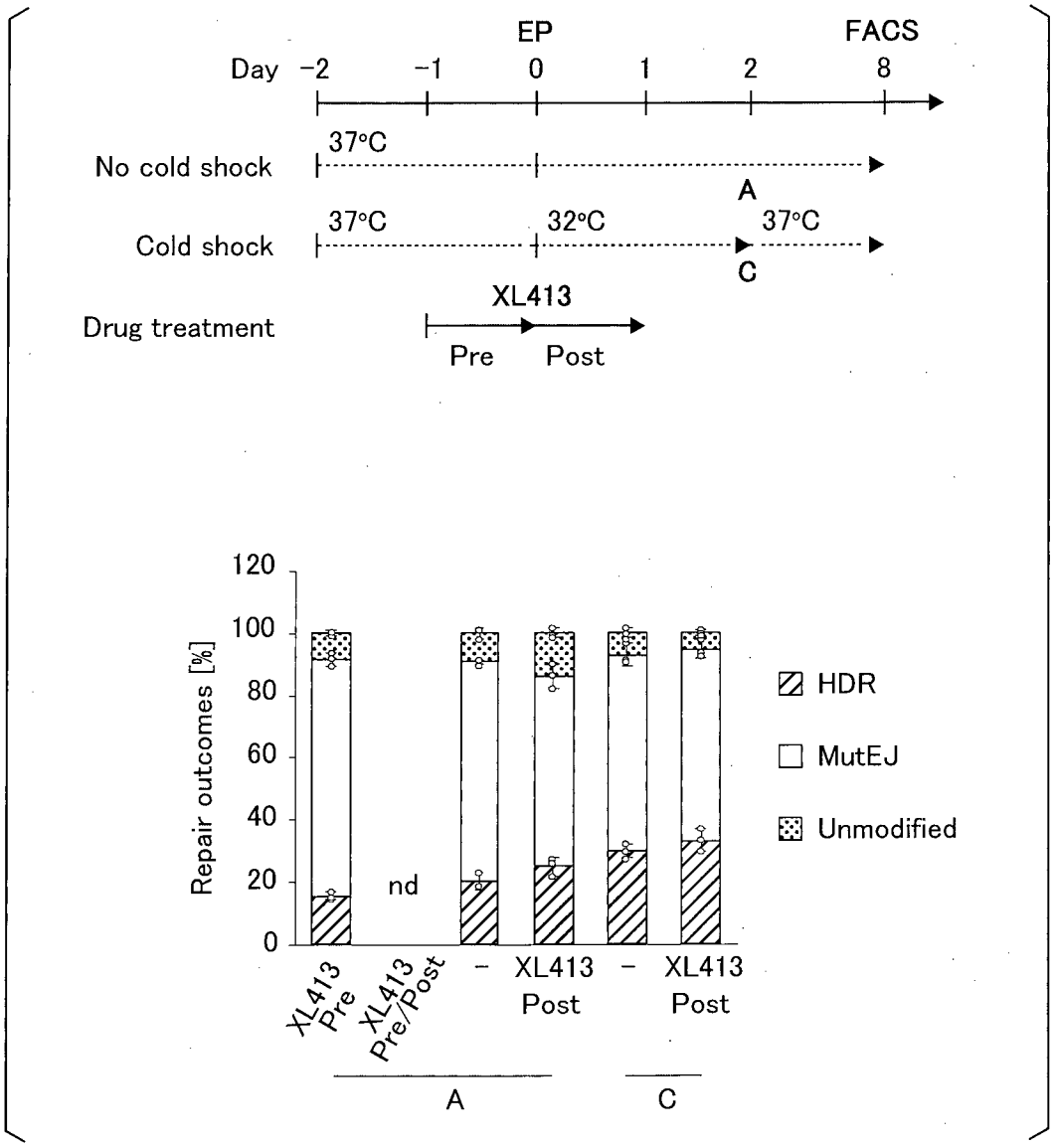
EP
FACS
Day -2 -1 0 1 2 8
No cold shock
37°C
A
Cold shock
37°C
32°C
37°C
C
Drug treatment
XL413
Pre
Post
Repair outcomes [%]
120
100
80
60
40
20
0
nd
HDR
MutEJ
Unmodified
XL413 Pre
XL413 Pre/Post
-
XL413 Post
-
XL413 Post
A
C

FIG. 10G

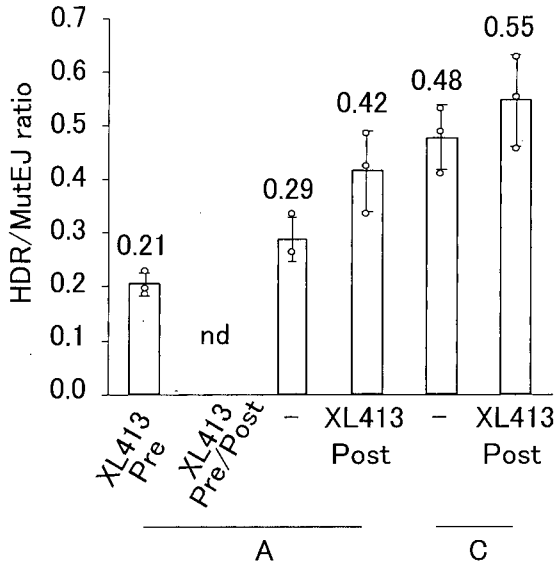

FIG. 10H

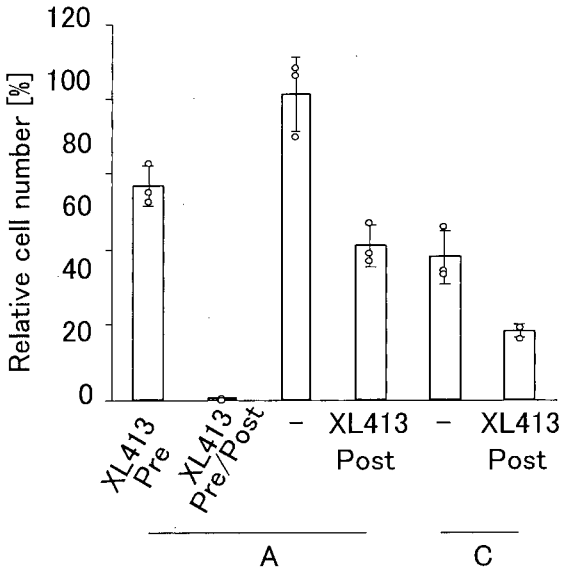

FIG. 11A

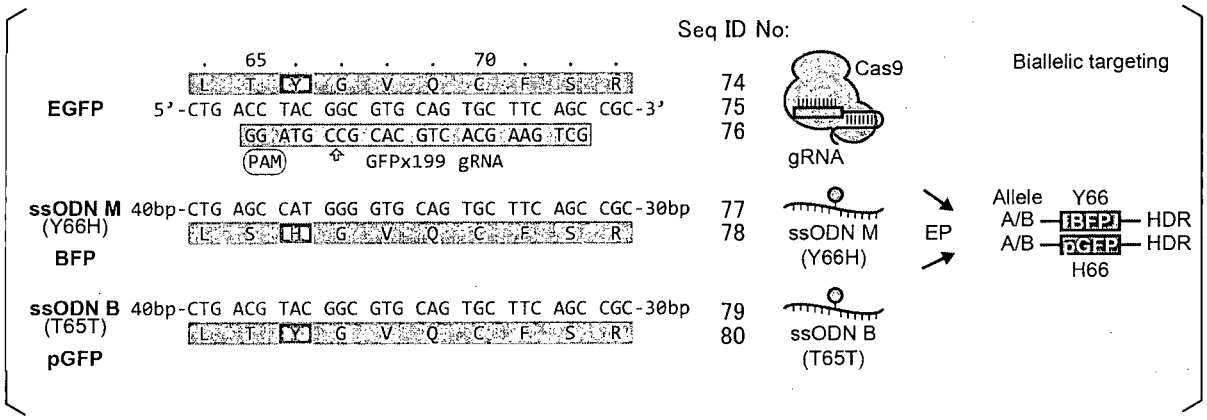
Seq ID No:
65
70
L T Y G V Q C F S R
EGFP
5'-CTG ACC TAC GGC GTG CAG TGC TTC AGC CGC-3'
GG ATG CCG CAC GTC ACG AAG TCG
PAM
GFPx199 gRNA
74
75
76
Cas9
gRNA
Biallelic targeting
ssODN M
(Y66H)
40bp-CTG AGC CAT GGG GTG CAG TGC TTC AGC CGC-30bp
L S H G V Q C F S R
BFP
77
78
ssODN M
(Y66H)
EP
Allele
Y66
A/B
BFP
HDR
A/B
pGFP
HDR
H66
ssODN B
(T65T)
40bp-CTG ACG TAC GGC GTG CAG TGC TTC AGC CGC-30bp
L T Y G V Q C F S R
pGFP
79
80
ssODN B
(T65T)

FIG. 11B

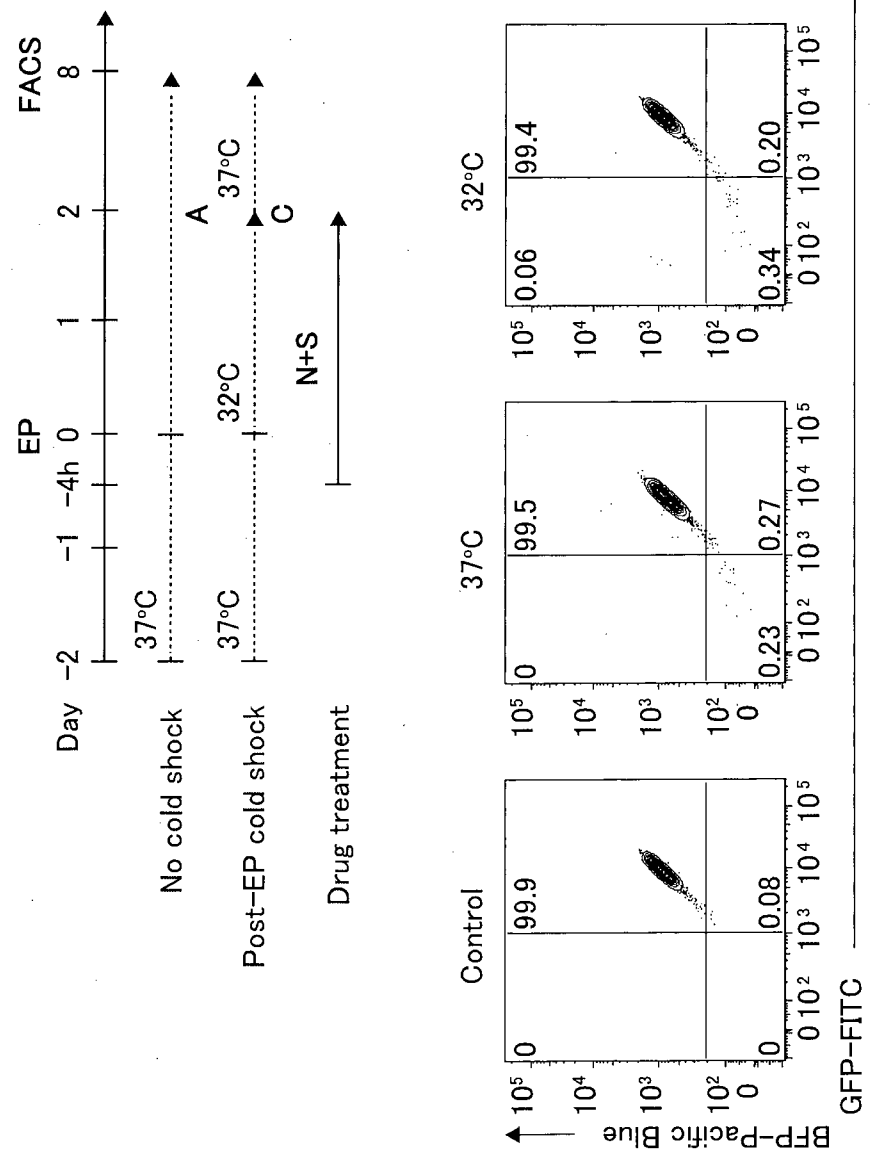
Day
−2
−1
−4h
0
1
2
8
EP
FACS
37°C
No cold shock
A
37°C
32°C
37°C
Post-EP cold shock
C
N+S
Drug treatment
Control
37°C
32°C
32°C+N+S
99.9
0.08
99.5
0.27
99.4
0.20
99.3
0.39
0.23
0.06
0.34
0.29
BFP-Pacific Blue
GFP-FITC

FIG. 11C

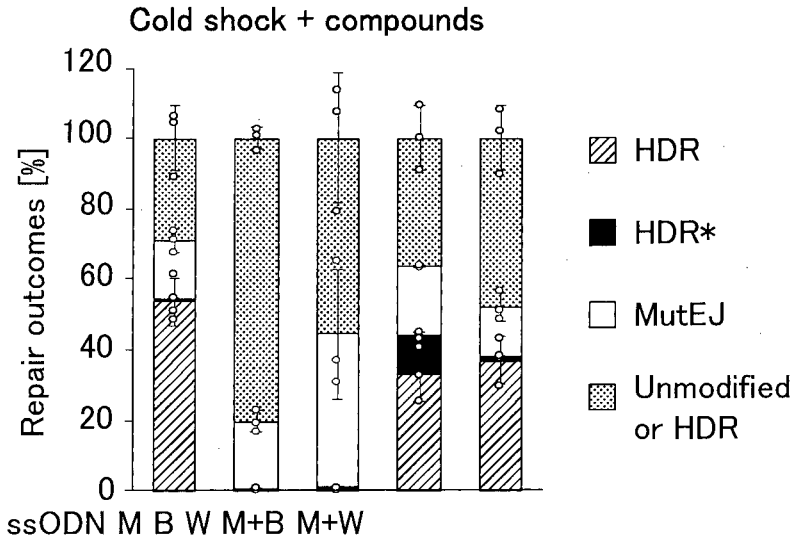
Cold shock + compounds
Repair outcomes [%]
120
100
80
60
40
20
0
ssODN M B W M+B M+W
HDR
HDR*
MutEJ
Unmodified or HDR

FIG. 11D

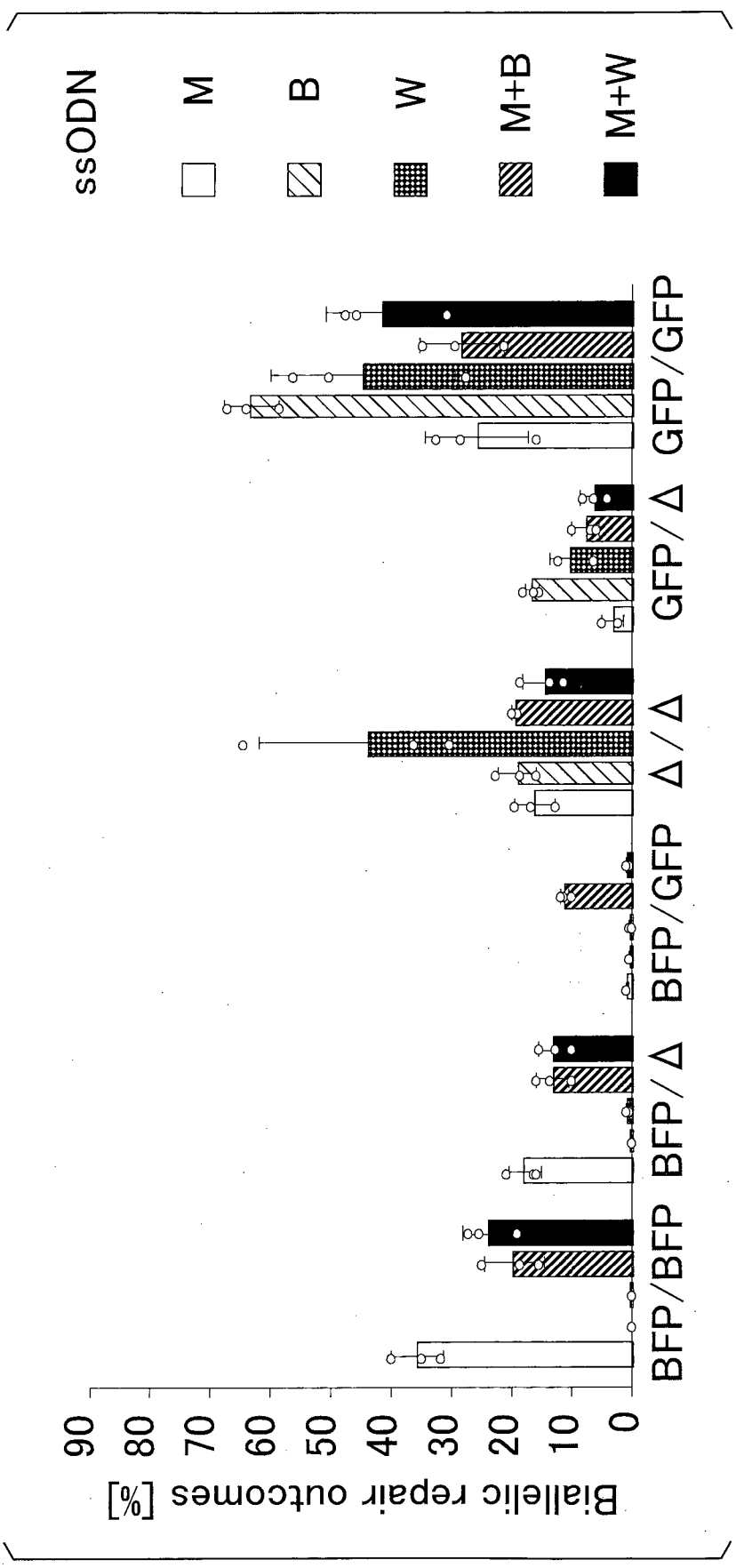
ssODN
M
B
W
M+B
M+W
Biallelic repair outcomes [%]
0
10
20
30
40
50
60
70
80
90
BFP/BFP
BFP/Δ
BFP/GFP
Δ/Δ
GFP/Δ
GFP/GFP

FIG. 11E

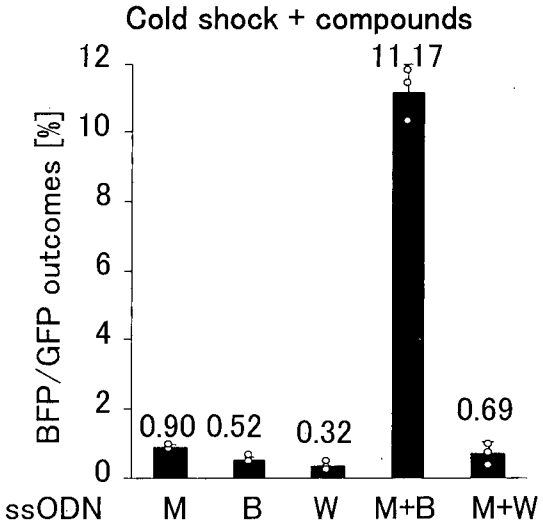

FIG. 11F

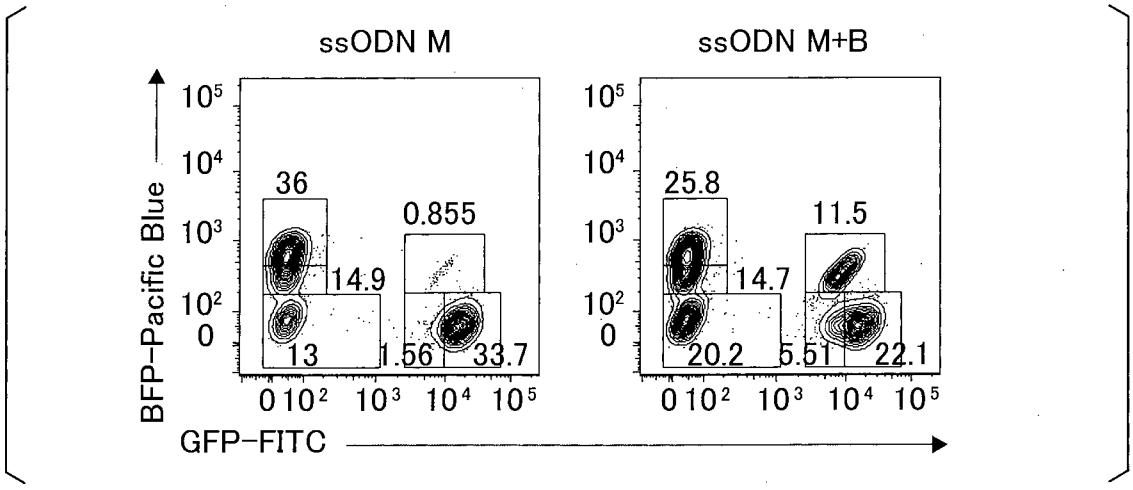

FIG. 12A

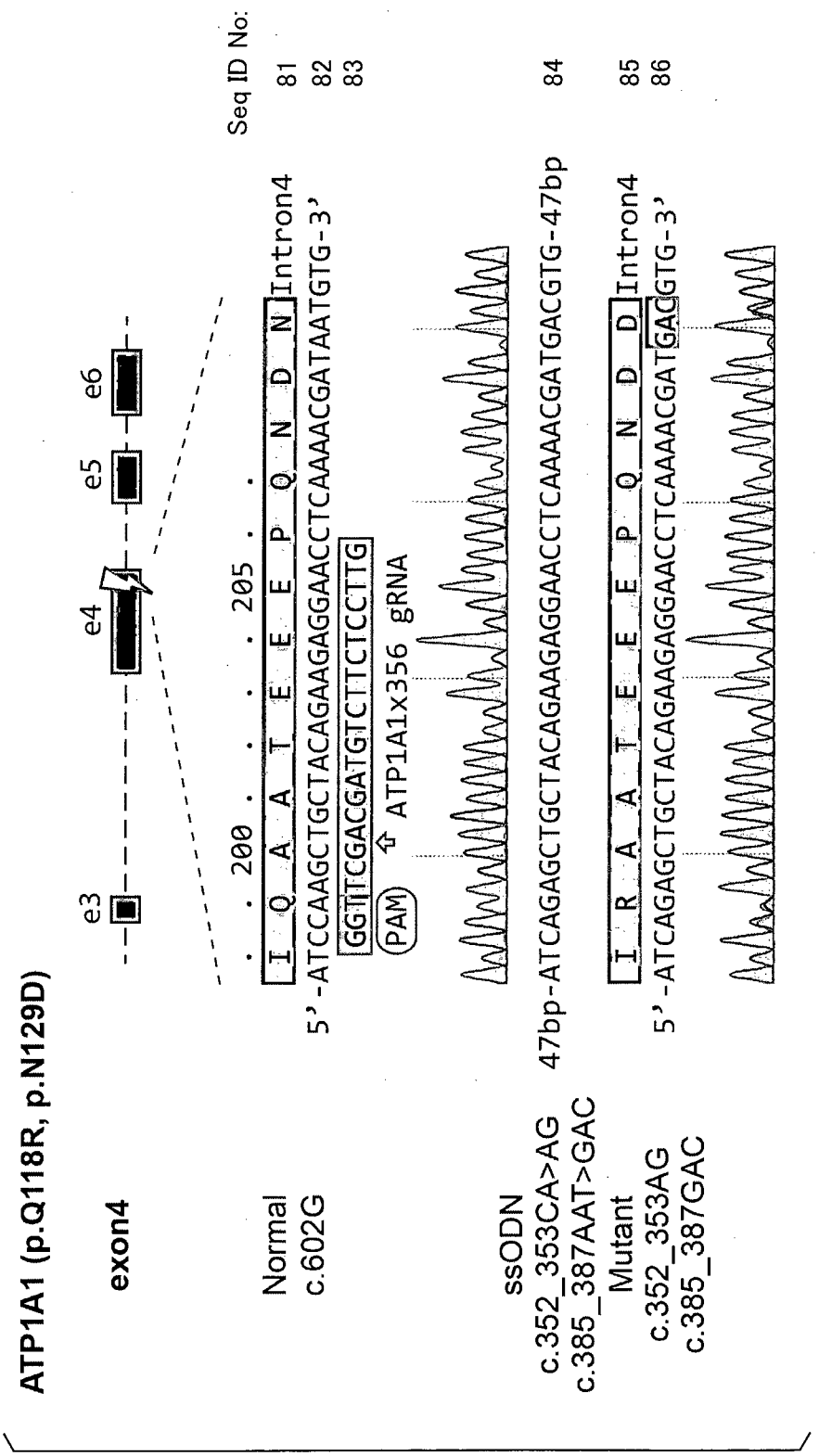
ATP1A1 (p.Q118R, p.N129D)
exon4
e3
e4
e5
e6
. . 200 . . . . . 205 . .
I Q A A T E E E P Q N D N Intron4
5'-ATCCAAGCTGCTACAGAAGAGGAACCTCAAAACGATAATGTG-3'
GGTTCGACGATGTCTTCTCCTTG
PAM
ATP1A1x356 gRNA
ssODN
c.352_353CA>AG
c.385_387AAT>GAC
47bp-ATCAGAGCTGCTACAGAAGAGGAACCTCAAAACGATGACGTG-47bp
Mutant
c.352_353AG
c.385_387GAC
I R A A T E E E P Q N D D Intron4
5'-ATCAGAGCTGCTACAGAAGAGGAACCTCAAAACGATGACGTG-3'
Seq ID No:
81
82
83
84
85
86

FIG. 12B

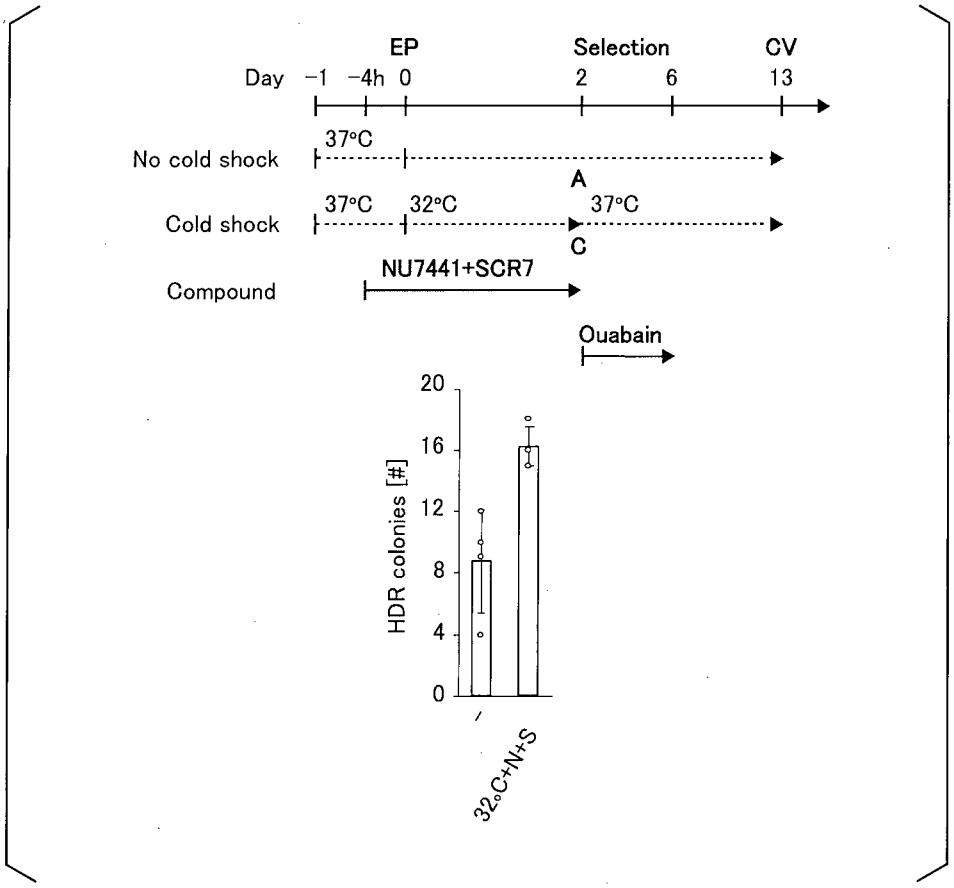
EP
Selection
CV
Day −1 −4h 0 2 6 13
No cold shock
37°C
A
Cold shock
37°C 32°C 37°C
C
Compound
NU7441+SCR7
Ouabain
HDR colonies [#]
20
16
12
8
4
0
−
32°C+N+S

FIG. 12C

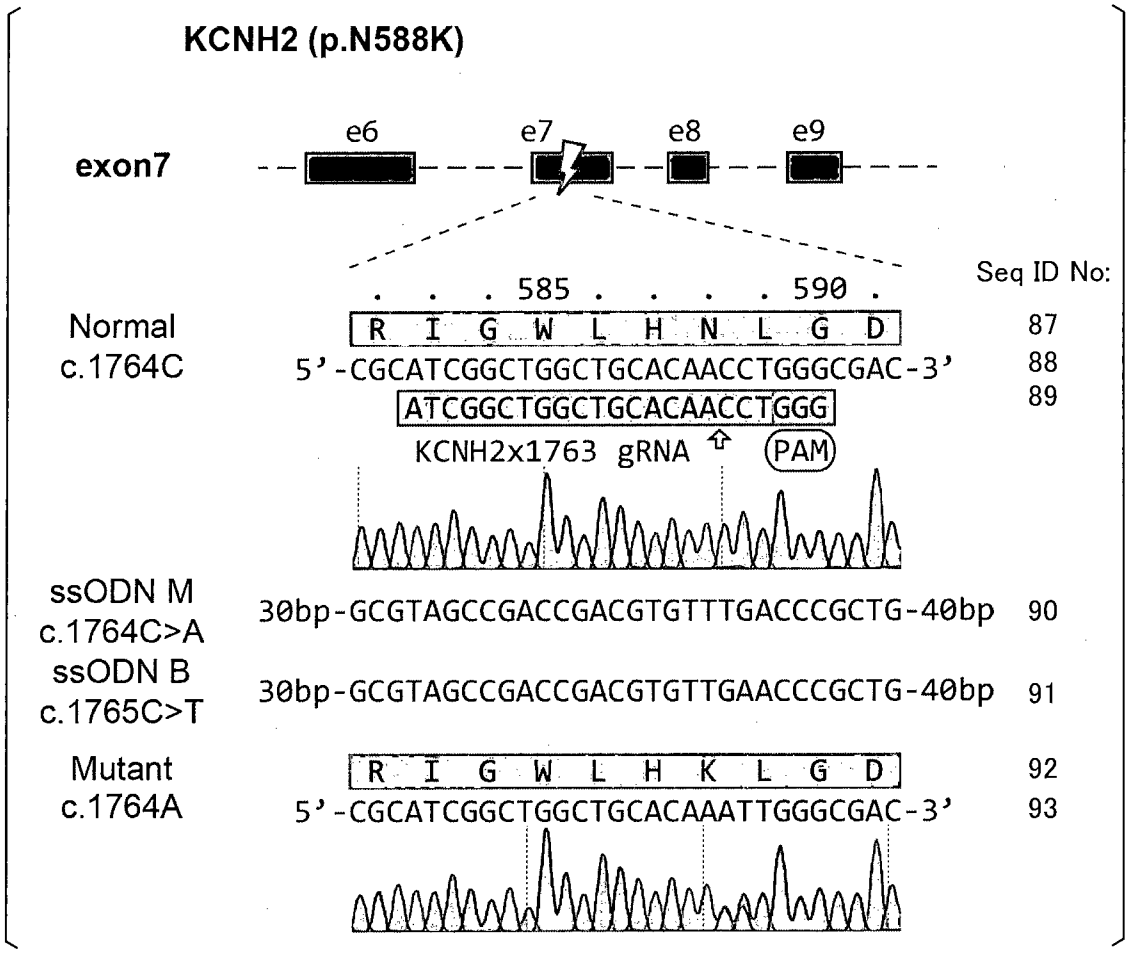
KCNH2 (p.N588K)
exon7
e6
e7
e8
e9
Seq ID No:
. . . 585 . . . . 590 .
Normal
c.1764C
R I G W L H N L G D
5'-CGCATCGGCTGGCTGCACAACCTGGGCGAC-3'
ATCGGCTGGCTGCACAACCTGGG
KCNH2x1763 gRNA
PAM
ssODN M
c.1764C>A
30bp-GCGTAGCCGACCGACGTGTTTGACCCGCTG-40bp
ssODN B
c.1765C>T
30bp-GCGTAGCCGACCGACGTGTTGAACCCGCTG-40bp
Mutant
c.1764A
R I G W L H K L G D
5'-CGCATCGGCTGGCTGCACAAATTGGGCGAC-3'
87
88
89
90
91
92
93

FIG. 12D

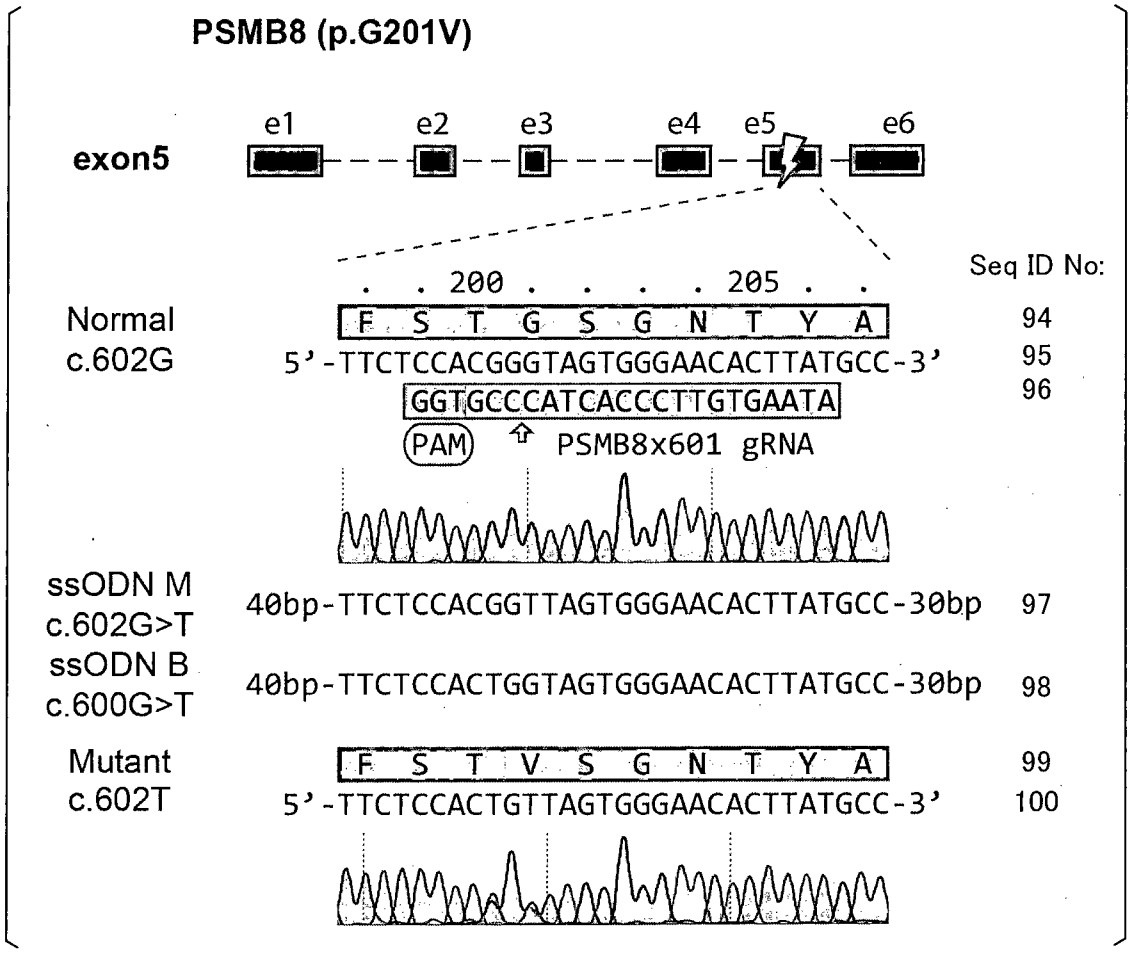
PSMB8 (p.G201V)
exon5
e1
e2
e3
e4
e5
e6
Seq ID No:
200
205
Normal
c.602G
F S T G S G N T Y A
5'-TTCTCCACGGGTAGTGGGAACACTTATGCC-3'
GGTGCCCATCACCCTTGTGAATA
PAM
PSMB8x601 gRNA
94
95
96
ssODN M
c.602G>T
40bp-TTCTCCACGGTTAGTGGGAACACTTATGCC-30bp
97
ssODN B
c.600G>T
40bp-TTCTCCACTGGTAGTGGGAACACTTATGCC-30bp
98
Mutant
c.602T
F S T V S G N T Y A
99
5'-TTCTCCACTGTTAGTGGGAACACTTATGCC-3'
100

FIG. 12E

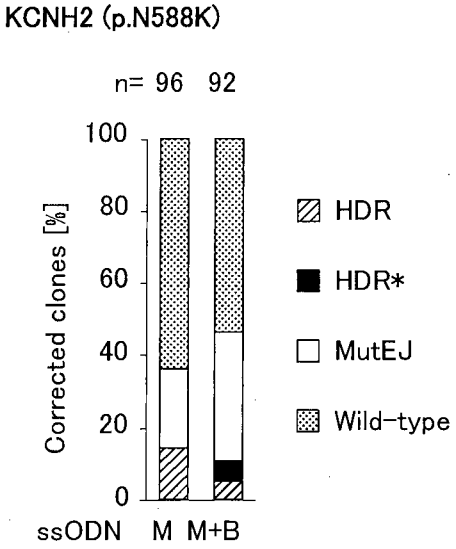

FIG. 12F

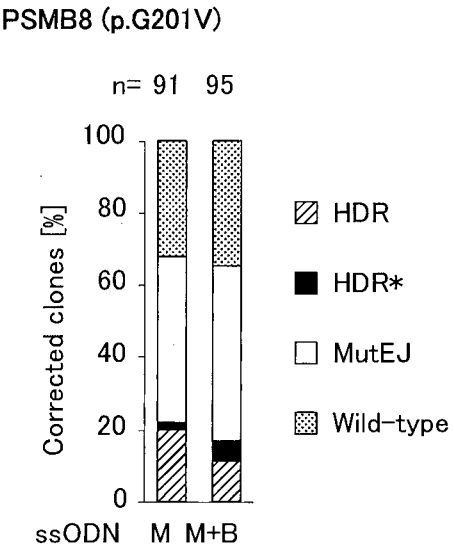

FIG. 13A

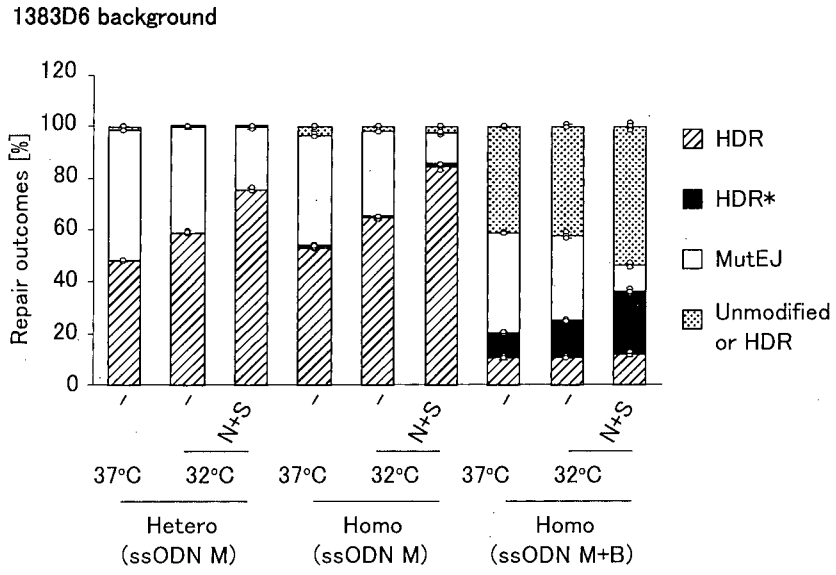

FIG. 13B

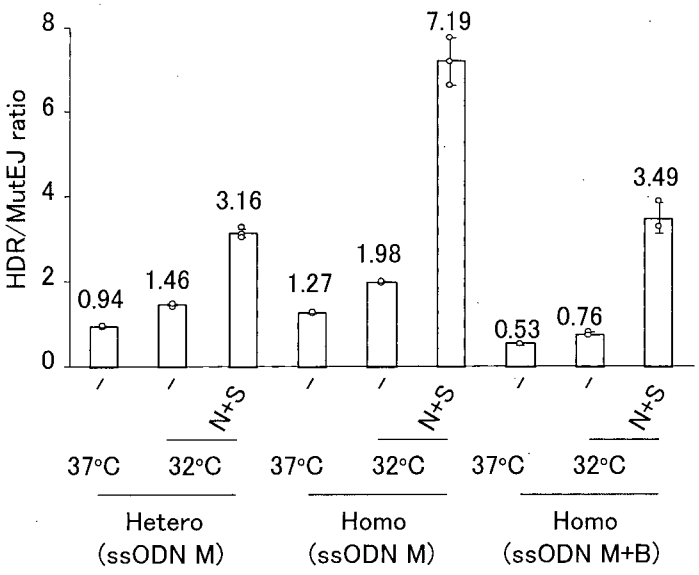

FIG. 13C

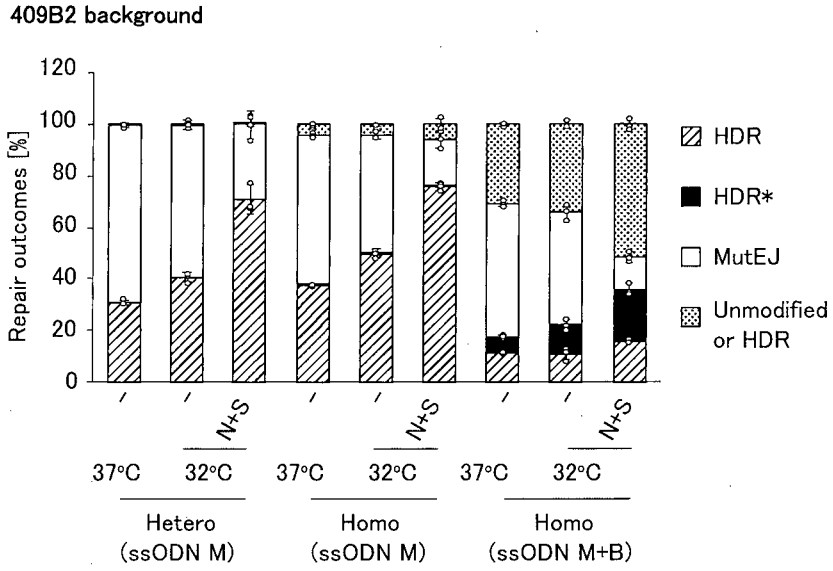

FIG. 13D

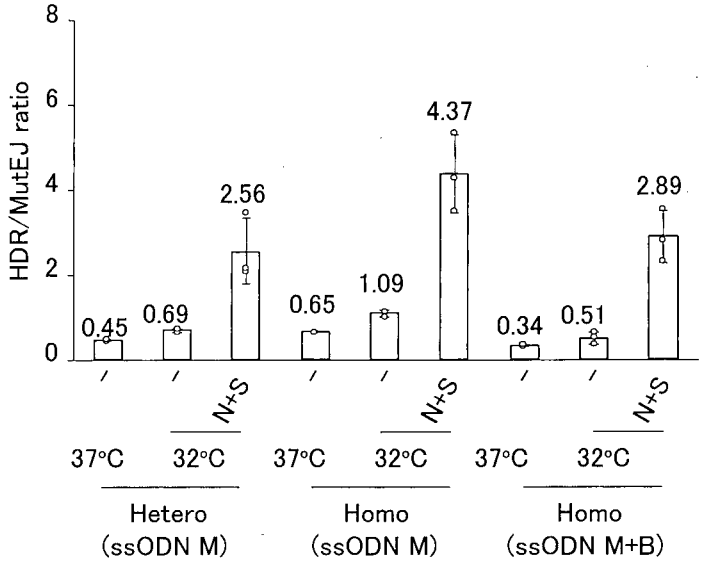

FIG. 13E

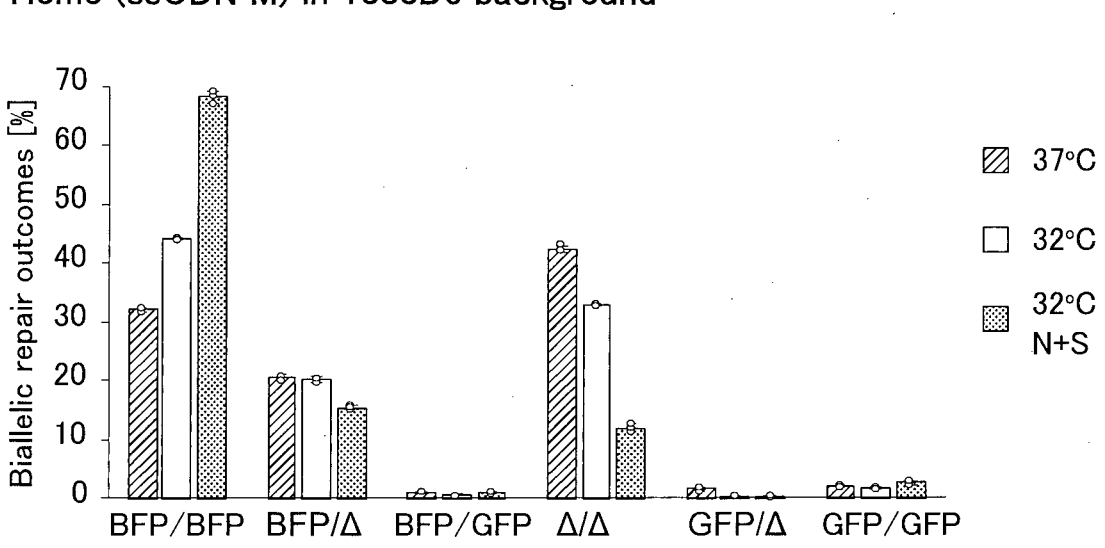

FIG. 13F

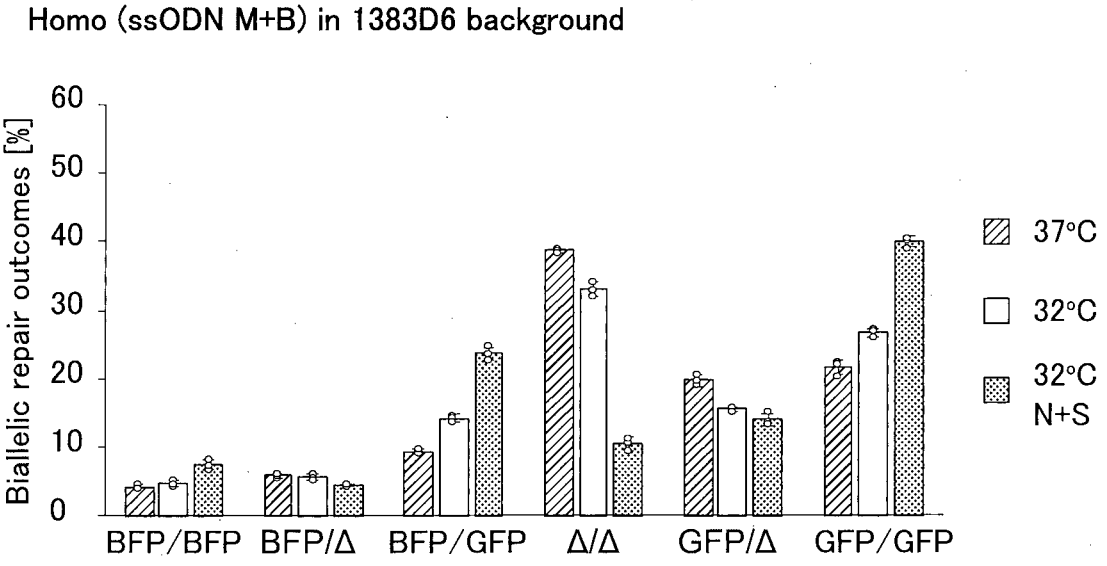

FIG. 13G

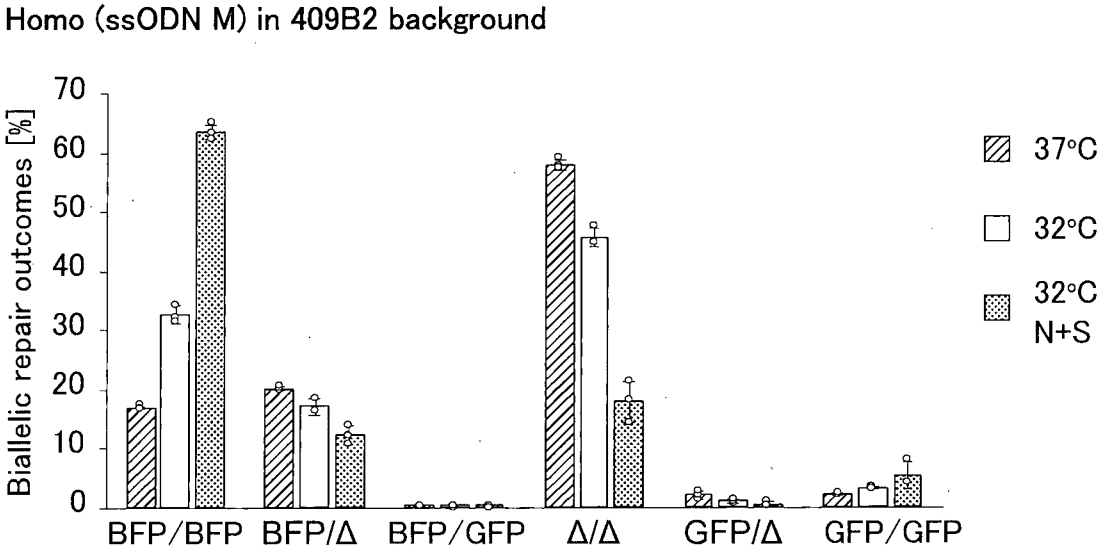

FIG. 13H

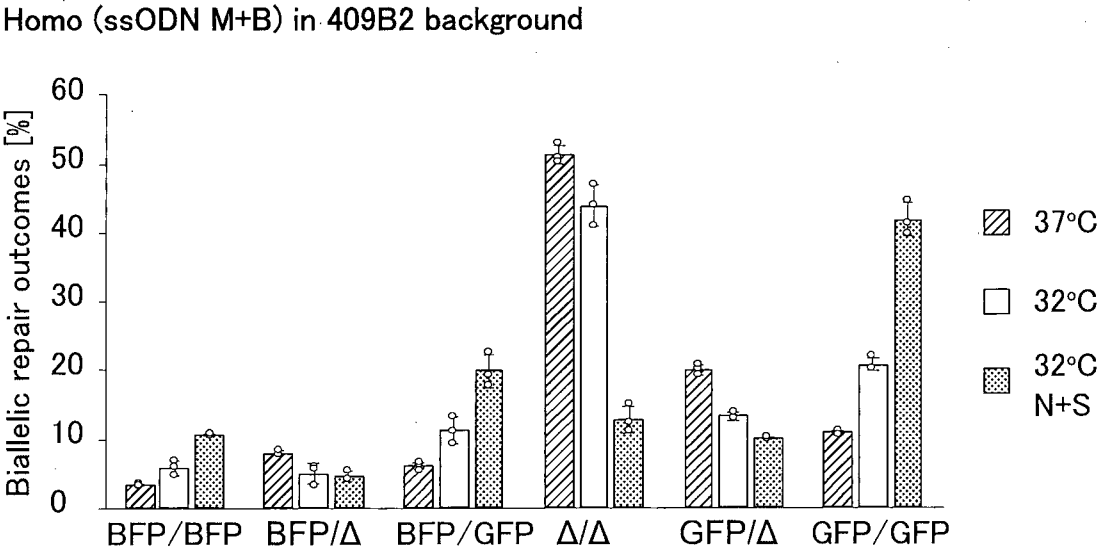

FIG. 14A

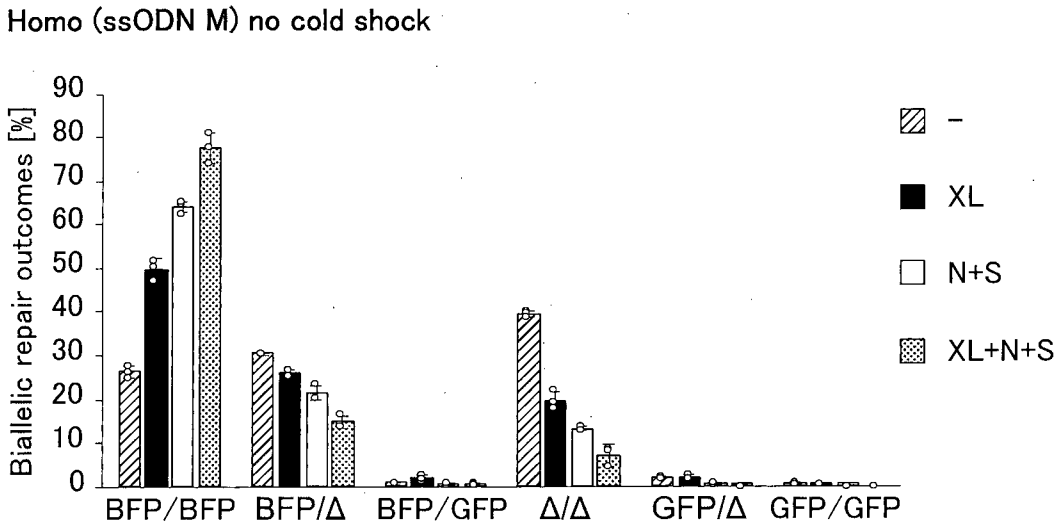

FIG. 14B

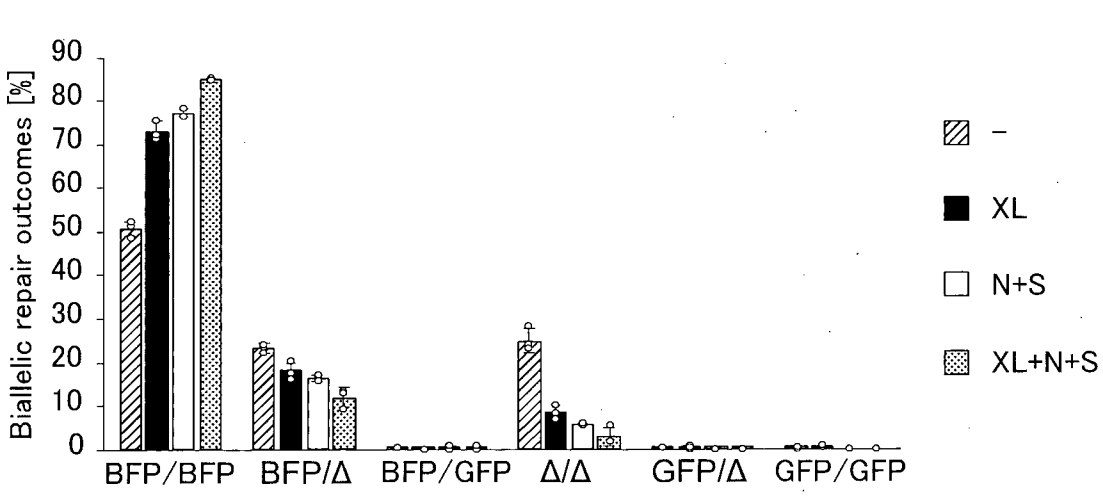

FIG. 14C

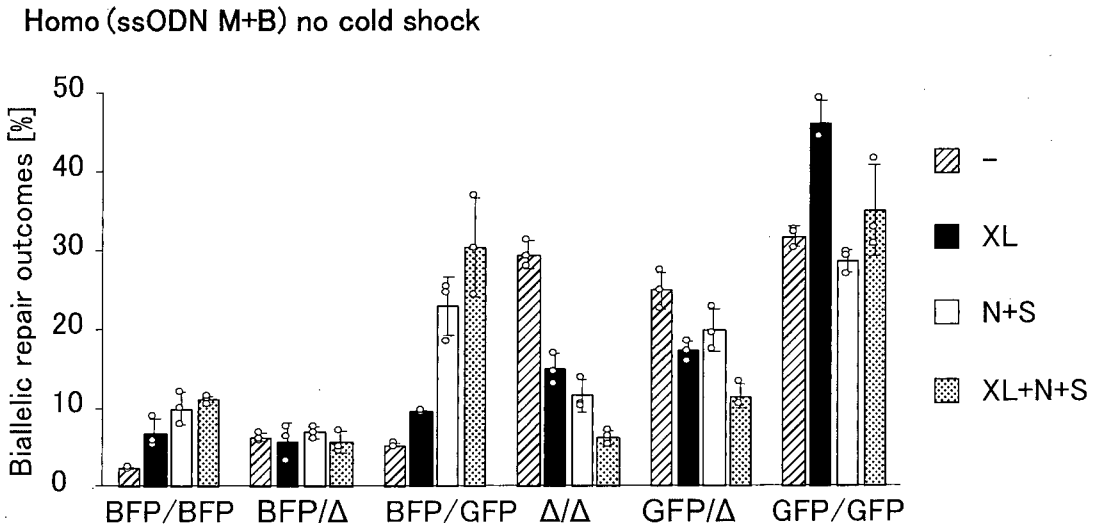

FIG. 14D

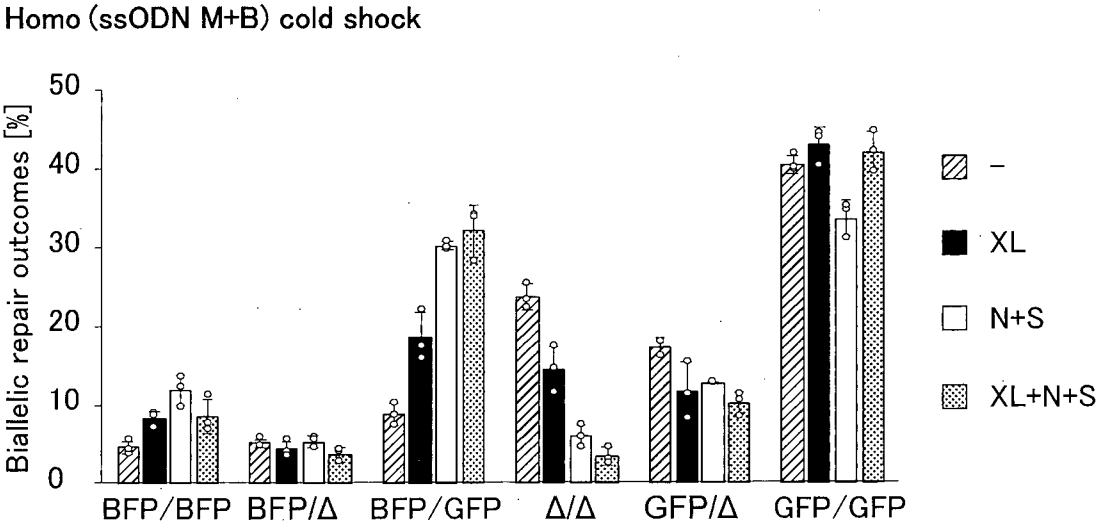

FIG. 15A

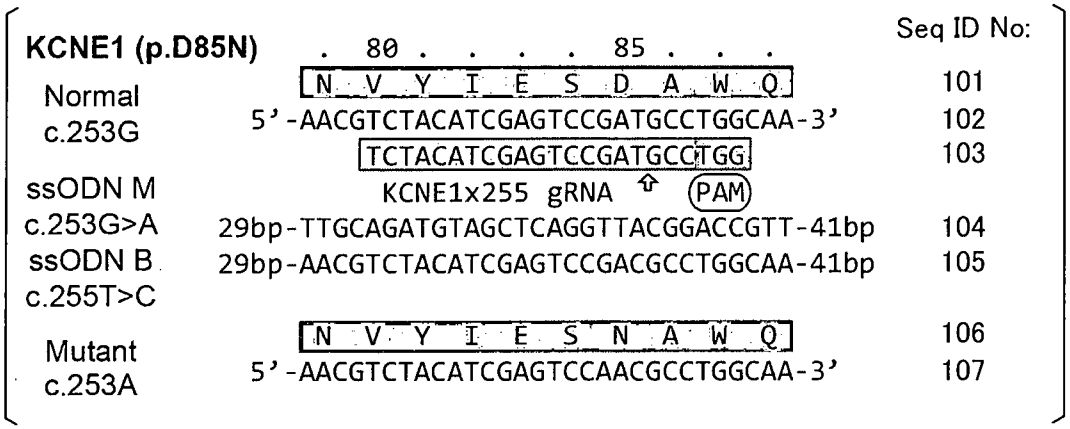

FIG. 15B

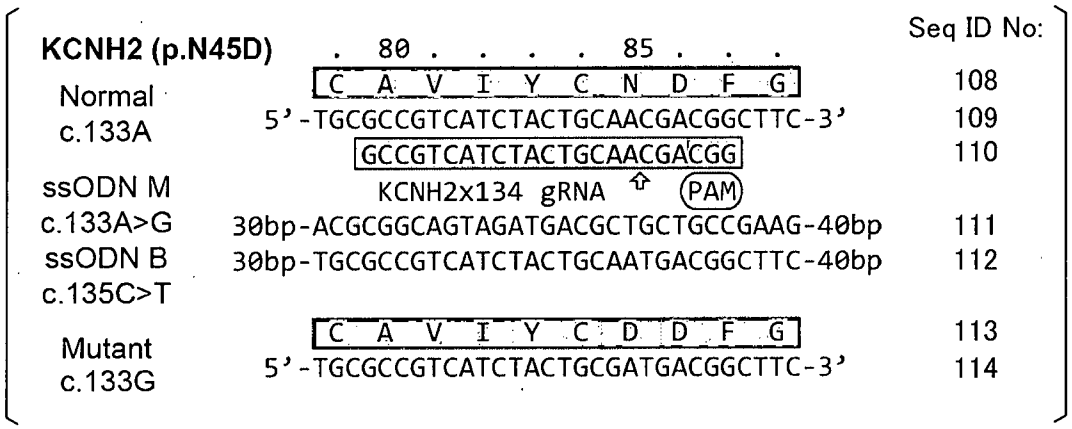

FIG. 15C

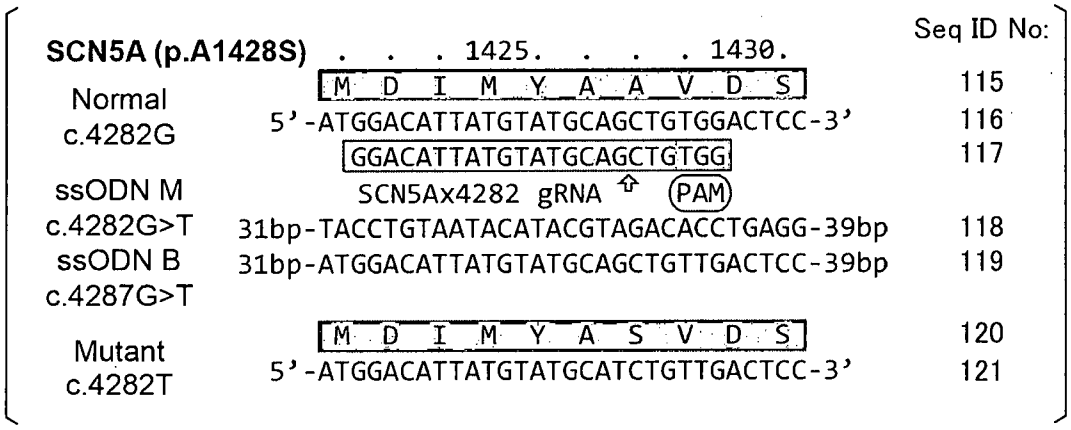

FIG. 15D

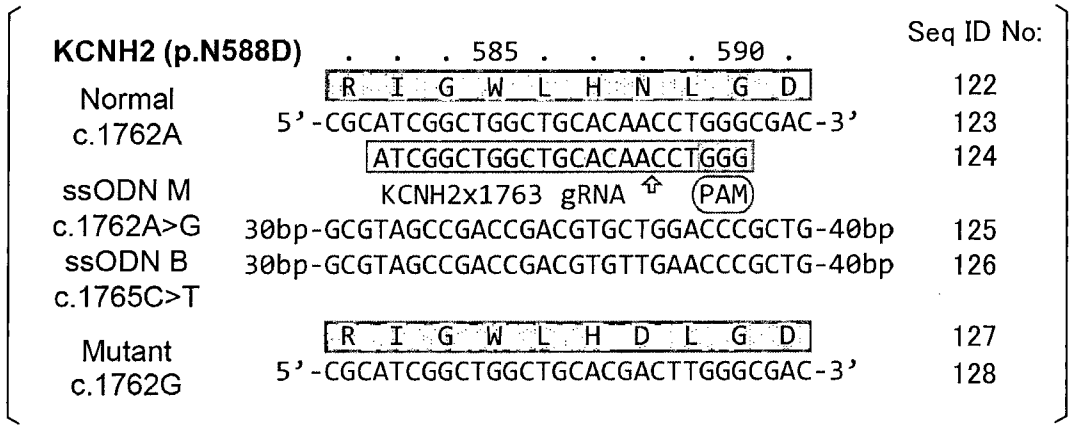

FIG. 15E

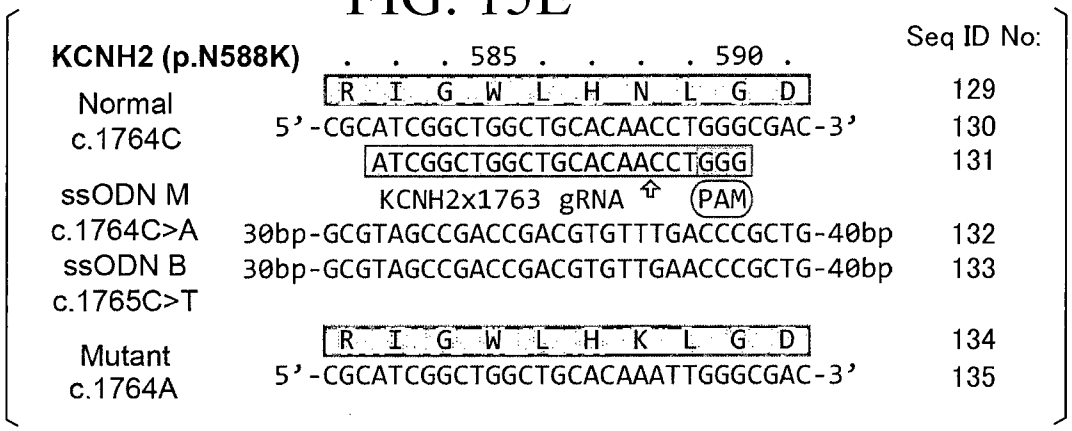

FIG. 15F

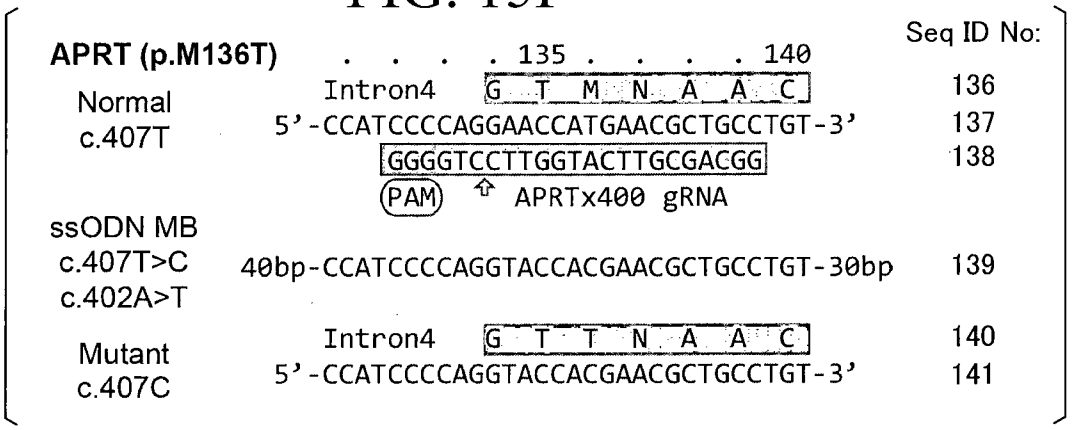

FIG. 15G

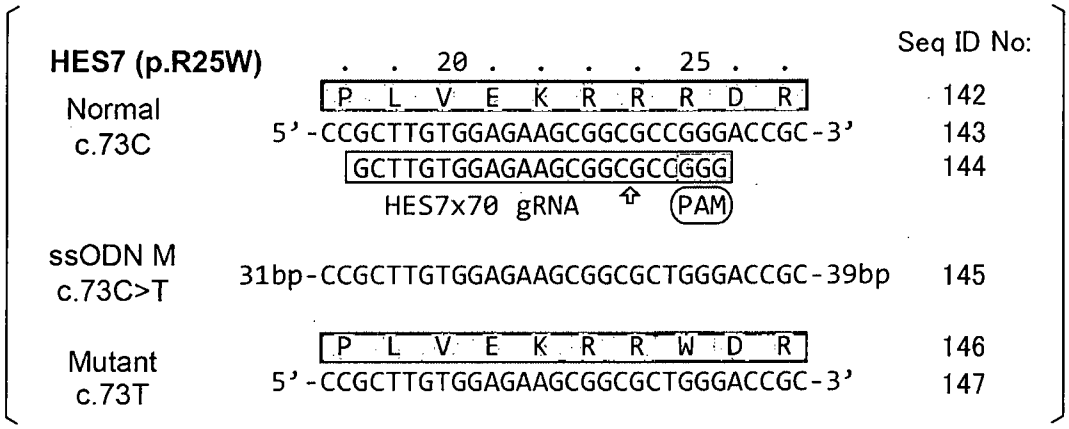

FIG. 15H

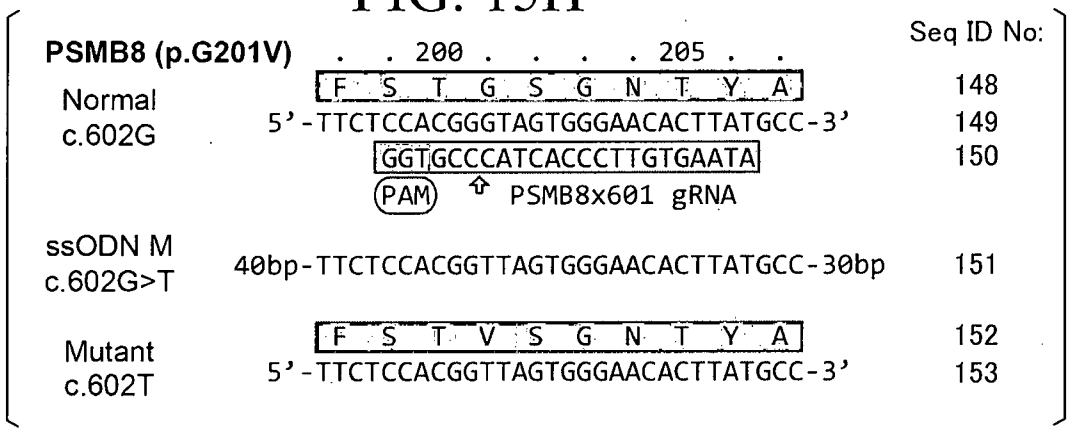

FIG. 15I

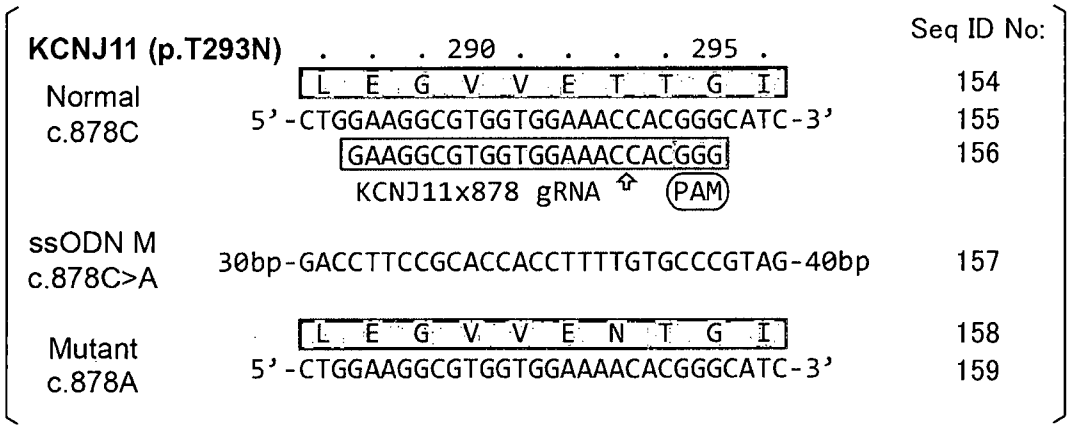

FIG. 15J

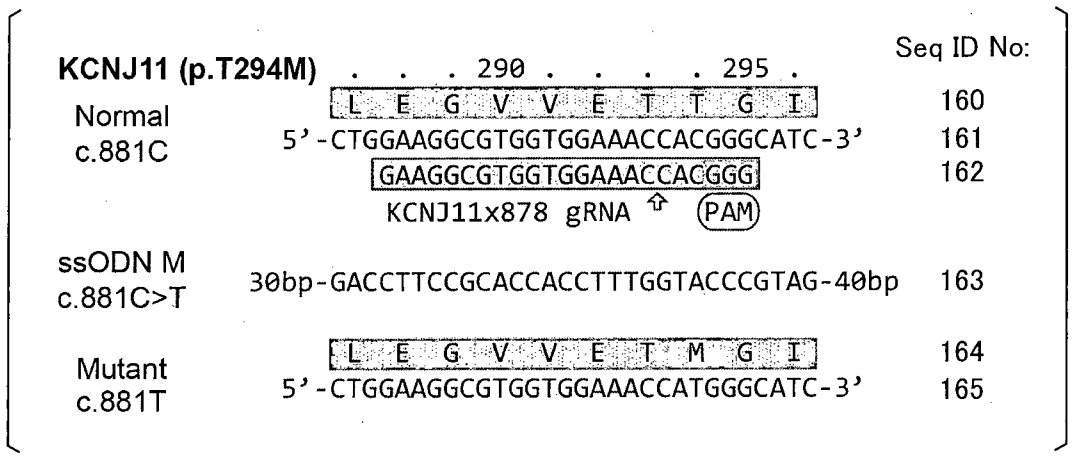
KCNJ11 (p.T294M)
. . . 290 . . . . 295 .
Seq ID No:
L E G V V E T T G I
160
Normal
c.881C
5'-CTGGAAGGCGTGGTGGAAACCACGGGCATC-3'
161
GAAGGCGTGGTGGAAACCACGGG
162
KCNJ11x878 gRNA
PAM
ssODN M
c.881C>T
30bp-GACCTTCCGCACCACCTTTGGTACCCGTAG-40bp
163
L E G V V E T M G I
164
Mutant
c.881T
5'-CTGGAAGGCGTGGTGGAAACCATGGGCATC-3'
165

INTERNATIONAL SEARCH REPORT

International application No.
PCT/JP2020/035368

A. CLASSIFICATION OF SUBJECT MATTER

C12N 15/09(2006.01)i
FI: C12N15/09 110

According to International Patent Classification (IPC) or to both national classification and IPC

B. FIELDS SEARCHED

Minimum documentation searched (classification system followed by classification symbols)

C12N15/09

Documentation searched other than minimum documentation to the extent that such documents are included in the fields searched

Published examined utility model applications of Japan 1922-1996
Published unexamined utility model applications of Japan 1971-2020
Registered utility model specifications of Japan 1996-2020
Published registered utility model applications of Japan 1994-2020

Electronic data base consulted during the international search (name of data base and, where practicable, search terms used)

JSTPlus/JMEDPlus/JST7580 (JDreamIII); MEDLINE (JDreamIII)

C. DOCUMENTS CONSIDERED TO BE RELEVANT

Category*	Citation of document, with indication, where appropriate, of the relevant passages	Relevant to claim No.
X	WO 2018/013840 A1 (VERTEX PHARMACEUTICALS INCORPORATED) 18 January 2018 (2018-01-18) Claims 1-69, Examples 1-5, Paragragh 129	1-18
X	WO 2014/130955 A1 (SANGAMO BIOSCIENCES, INC.) 28 August 2014 (2014-08-28) Claims 1-15, Examples 1-4, Paragraghs 114, 117	1-18
P, X	WIENERT, B., et al., "Timed inhibition of CDC7 increases CRISPR-Cas9 mediated templated repair.", NATURE COMMUNICATIONS, 2020.04.30, Vol.11, 2109 (p.1-15), doi: 10.1038/s41467-020-15845-1 ABSTRACT, FIGURES 1-6	1-18
P, X	MAURISSEN, T.L., et al., "Synertgistic gene editing in human iPS cells via cell cycle and DNA repair modulation.", NATURE COMMUNICATIONS, 2020.06.08, Vol.11, 2876(p.1-14), doi: 10/1038/s41467-020-16643-5 ABSTRACT, FIGURES 1-7	1-18

☐ Further documents are listed in the continuation of Box C. ☑ See patent family annex.

* Special categories of cited documents:
"A" document defining the general state of the art which is not considered to be of particular relevance
"E" earlier application or patent but published on or after the international filing date
"L" document which may throw doubts on priority claim(s) or which is cited to establish the publication date of another citation or other special reason (as specified)
"O" document referring to an oral disclosure, use, exhibition or other means
"P" document published prior to the international filing date but later than the priority date claimed
"T" later document published after the international filing date or priority date and not in conflict with the application but cited to understand the principle or theory underlying the invention
"X" document of particular relevance; the claimed invention cannot be considered novel or cannot be considered to involve an inventive step when the document is taken alone
"Y" document of particular relevance; the claimed invention cannot be considered to involve an inventive step when the document is combined with one or more other such documents, such combination being obvious to a person skilled in the art
"&" document member of the same patent family

Date of the actual completion of the international search	Date of mailing of the international search report
04 November 2020	**17 November 2020**
Name and mailing address of the ISA/JP **Japan Patent Office** **3-4-3, Kasumigaseki, Chiyoda-ku, Tokyo** **100-8915, Japan**	Authorized officer **NOMURA, Hideo 4B 4155** Telephone No. **+81-3-3581-1101 Ext. 3448**

INTERNATIONAL SEARCH REPORT

International application No.
PCT/JP2020/035368

Box No. I Nucleotide and/or amino acid sequence(s) (Continuation of item 1.c of the first sheet)

1. With regard to any nucleotide and/or amino acid sequence disclosed in the international application, the international search was carried out on the basis of a sequence listing:
   a. ☐ forming part of the international application as filed:
      ☐ in the form of an Annex C/ST.25 text file.
      ☐ on paper or in the form of an image file.
   b. ☑ furnished together with the international application under PCT Rule 13*ter*.1(a) for the purposes of international search only in the form of an Annex C/ST.25 text file.
   c. ☐ furnished subsequent to the international filing date for the purposes of international search only:
      ☐ in the form of an Annex C/ST.25 text file (Rule 13*ter*.1(a)).
      ☐ on paper or in the form of an image file (Rule 13*ter*.1(b) and Administrative Instructions, Section 713).

2. ☑ In addition, in the case that more than one version or copy of a sequence listing has been filed or furnished, the required statements that the information in the subsequent or additional copies is identical to that forming part of the application as filed or does not go beyond the application as filed, as appropriate, were furnished.

3. Additional comments:

INTERNATIONAL SEARCH REPORT
Information on patent family members

International application No.
PCT/JP2020/035368

Patent document cited in search report	Publication date (day/month/year)	Patent family member(s)	Publication date (day/month/year)
WO 2018/013840 A1	18 January 2018	JP 2019-521139 A Claims 1-69, Examples 1-5, Paragragh 99 US 2019/0225990 A1 EP 3484870 A1 CN 109863143 A	
WO 2014/130955 A1	28 August 2014	JP 2016-509063 A Claims 1-15, Examples 1-4, Paragraghs 111, 114 US 2014/0242702 A1 EP 2958996 A1	